

2-PERIODIC COMPENSATION OF DISCRETE TIME PLANTS: A 2- DEGREES-OF- FREEDOM APPROACH

This thesis is submitted in the partial fulfilment of the requirements of the degree

MASTER IN CONTROL SYSTEM ENGINEERING

Submitted by

Spandita Das

Examination Roll Number: M4CTL18006

Registration Number: 137135 of 2016–2017

Under the Guidance of

Prof. Madhubanti Maitra

and

Dr. Sayantan Chakraborty

Department of Electrical Engineering

JADAVPUR UNIVERSITY

KOLKATA–700032

May, 2018

Faculty Council of Engineering and Technology
Jadavpur University
Kolkata- 700032

Certificate

This is to certify that the thesis entitled “2-Periodic Compensation of discrete time Plants: A 2-degrees-of-freedom approach”, submitted by spandita das (examination Roll No. M4CTL18006), under the supervision and guidance of Prof. Madhubanti Maitra, Professor, Electrical Engineering Department, Jadavpur University and Dr. Sayantan Chakraborty, Assistant. Professor, Electrical Engineering Department, Jadavpur University. We are satisfied with her work, which is being presented for the partial fulfilment of the degree of Master in Control System Engineering from Jadavpur University, Kolkata-700032.

Prof. Madhubanti Maitra

Professor

Electrical Engineering Department
Jadavpur University
Kolkata – 700 032

Dr. Sayantan Chakraborty

Assistant Professor

Electrical Engineering Department
Jadavpur University
Kolkata-700 032

Prof. Subrata Paul

Head of the Department
Electrical Engineering Department
Jadavpur University
Kolkata – 700 032

Prof. Chiranjib Bhattacharjee

Dean
Faculty council of Engineering and Technology
Jadavpur University
Kolkata – 700 032

**Faculty Council of Engineering and Technology
Jadavpur University
Kolkata- 700032**

Certificate of Approval

This is to certify that the thesis entitled ‘2-Periodic Compensation of Discrete time Plants: A 2-degrees-of-freedom approach’, presented by Spandita Das (Examination Roll No. M4CTL18006, Registration No. 137135 of 2016-17) to Jadavpur University for the partial fulfilment of the Degree of Master in Control System Engineering, is hereby approved by the committee of final examination and that the student has successfully defended the thesis in the viva-voce examination.

Final examination for evaluation of thesis

Signature of Examiners

Declaration of Originality

I hereby declare that this thesis contains literature survey and original research work done by me. All the information in this document have been obtained and presented in accordance with academic rules and ethical conduct. I also declare that, as required by these rules and conduct, I have fully cited and referenced all material and results that are not original to this work.

Name : SPANDITA DAS

Examination Roll No. : M4CTL18006

Thesis Title : 2-periodic compensation of discrete time plants: A 2-degrees-of-freedom approach

Signature with Date :

ACKNOWLEDGEMENTS

I express my sincere gratitude to my supervisor, Dr. Madhubanti Maitra for her encouragement, suggestion and advices, without which it would not have been possible to complete my thesis successfully. I would like to thank Dr. Sayantan Chakraborty for being a constant source of encouragement, inspiration and for his valuable suggestions coupled with his technical expertise throughout my research work. It was a great honour for me to pursue my research under his supervision.

I would also like to thank all my co-workers Kaushik Haldar, Debnanu Nath, Anjali Shukla, Ashiqur Rahaman Molla, all the staffs of control systems laboratory for providing constant encouragement throughout my thesis work.

Last but not the least I extend my words of gratitude to my parents for personally motivating me to carry out the work smoothly.

Spandita Das
Jadavpur University
Kolkata-700032

ABSTRACT

Numerous techniques have been presented in the literature to design and analyze linear time invariant (LTI) controllers. However, compensation of a SISO, LTI plant having non-minimum phase (NMP) zeros using LTI controllers does not provide satisfactory results. The reason behind the fact is that the LTI controllers have the capability of placing the closed-loop poles but the loop-zeros remain unaltered in the closed loop transfer function resulting in poor gain margin (GM).

On the other hand, a periodic controller has the capability of placing NMP zeros at desired locations thereby improving the stability margins of the system. It has been observed that the presence of periodic variation in controller parameters yields ripple in the steady-state response to a step input. In the literature it is shown that in the discrete-time domain, these ripples can be eliminated if the loop transfer function satisfies certain necessary conditions. Otherwise, the plant needs to be augmented with the necessary LTI transfer function. However, this technique increases the plant order as well as the controller order. In this regard, it has been shown in this work that a 2-degree-of-freedom configuration of 2-periodic controller would be beneficial. In such cases it would be possible to cancel out some of the additional closed-loop poles thus improving the dynamic response of the system while retaining the loop-robustness properties as achieved using 1-DOF configuration.

CONTENTS

| | |
|---|-----|
| Abstract | v |
| List of acronyms | ix |
| List of figures | x |
| List of tables | xvi |
| Chapter 1: Introduction and Literature review | |
| 1.1 Introduction | 1 |
| 1.2 Limitations of LTI controller | 1 |
| 1.3 Periodic control | 2 |
| 1.3.1 Periodicity | 2 |
| 1.3.2 Analysis techniques of discrete-time periodic system | 3 |
| 1.4 Classification of periodic controllers | 4 |
| 1.4.1 Continuous time periodic controllers | 4 |
| 1.4.2 Discrete time periodic controllers | 5 |
| 1.5 Motivation and our contribution | 8 |
| 1.6 Thesis organisation | 8 |
| Chapter 2: 1 DOF 2-Periodic Controller Revisited | |
| 2.1 Introduction | 10 |
| 2.1.1 Analysis of discrete 2-periodic systems using Time Lifting Method | 10 |
| 2.2 Design of M-Periodic Controller | 11 |
| 2.2.1 Closed Loop Characteristic Equation | 13 |
| 2.2.2 Loop Zero Placement | 16 |
| 2.2.3 Order of the Controller | 17 |
| 2.2.4 Evaluation of Controller Parameters | 18 |

| | | |
|-------|--|----|
| 2.3 | Numerical Example of Second Order System | 22 |
| 2.4 | Ripple-Free Response | 26 |
| 2.4.1 | Numerical example | 29 |
| 2.5 | Chapter summary | 45 |

Chapter 3: 2-DOF 2-Periodic Controller

| | | |
|-------|---|----|
| 3.1 | Introduction | 46 |
| 3.2 | Design of 2-DOF 2-Periodic Controller | 46 |
| 3.2.1 | Closed Loop Characteristic Equation | 48 |
| 3.2.2 | Loop Zero Placement | 49 |
| 3.3 | Controller Synthesis Part I: Loop-Zero and Pole Placement | 50 |
| 3.3.1 | Order of the Controller | 50 |
| 3.3.2 | Evaluation of Controller Parameters | 51 |
| 3.4 | Controller Synthesis Part II: Model Matching | 54 |
| 3.4.1 | Numerical example | 57 |
| 3.5 | Ripple-Free Response | 58 |
| 3.5.1 | Numerical example | 62 |
| 3.6 | Chapter Summary | 74 |

Chapter 4: Stabilization of CIPS: A comparative study

| | | |
|-------|--|----|
| 4.1 | Introduction | 75 |
| 4.2 | Mathematical model of cart-inverted pendulum system (CIPS) | 75 |
| 4.2.1 | CIPS model in continuous-time domain | 78 |
| 4.2.2 | CIPS model in discrete-time domain | 79 |
| 4.3 | Control Techniques for Cart-Inverted Pendulum System | 80 |
| 4.3.1 | State-feedback Controller design | 80 |

| | |
|---|-----|
| 4.3.2 Two-loop Control Structure design | 81 |
| 4.3.3 Design of a 2-periodic Controller | 87 |
| 4.3.3.1 Design of a 1-DOF 2-periodic Controller | 87 |
| 4.3.3.2 Design of a 2-DOF 2-periodic Controller | 99 |
| 4.4 Chapter Summary | 106 |

Chapter 5: Conclusion

| | |
|---------------------------------|-----|
| 5.1 Contributions of the thesis | 107 |
| 5.2 Scope of future work | 107 |
| References | 108 |

List of abbreviations

- GM : Gain Margin
PM : Phase Margin
LTI : Linear Time-Invariant
LDTI : Linear Discrete-Time-Invariant
NMP : Non-Minimum-Phase
SISO : Single Input Single Output
LHS : Left Hand Side
RHS : Right Hand Side
DOF : Degrees-of-Freedom
ZOH : Zero Order Hold
CIPS : Cart-inverted Pendulum System
LQR : Linear Quadratic Regulator

List of figures

| | | |
|-------------|--|-----------|
| 1.1 | 2-periodic signal | 3 |
| 1.2 | 2-DOF continuous time periodic controller circuit | 5 |
| 1.3 | 1-DOF control topology | 6 |
| 1.4 | 2-periodic discrete time controller (1 DOF) | 6 |
| 1.5 | 2-DOF control topology | 7 |
| 1.6 | 2-periodic discrete time controller (2 DOF) | 7 |
| 2.1 | 1-degree-of-freedom periodic controller with plant | 12 |
| 2.2 | Root locus for system of example 2.3.1 compensated by dead-beat 2-periodic controller | 23 |
| 2.3 | Dead beat response of the plant with 1DOF 2-periodic controller for conditions $Q_0^+ = Q_1^-$ and $Q_0^+ = -Q_1^+$ | 25 |
| 2.4 | Dead beat response of the plant with 1DOF 2-periodic controller for conditions $Q_0^+ = -Q_1^-$ and $Q_0^+ = Q_1^+$ | 25 |
| 2.5 | Root locus of the system of (2.63) with $\beta = 0.9$ | 30 |
| 2.6 | Plot of gain margin with location of β | 31 |
| 2.7 | Response using augmentation $\frac{z}{(z-1)}$ with β for conditions $Q_0^+ = Q_1^-$ and $Q_0^+ = Q_1^+$ with pole-zero cancellation at $z^2 = 0$ | 32 |
| 2.8 | Response using augmentation $\frac{z}{(z-1)}$ with β for conditions $Q_0^+ - Q_1^+$ and $Q_0^+ = -Q_1^-$ with pole-zero cancellation at $z^2 = 0$ | 32 |
| 2.9 | Variation of settling time and maximum peak overshoot with β for condition $Q_0^+ = Q_1^-$ and $Q_0^+ = Q_1^+$ (with pole-zero cancellation at $z^2 = 0$) | 32 |
| 2.10 | Variation of settling time and maximum peak overshoot with β for condition $Q_0^+ = -Q_1^-$ and $Q_0^+ = -Q_1^+$ (with pole-zero cancellation at $z^2 = 0$) | 33 |
| 2.11 | Variation of settling time and maximum peak overshoot with β for condition $Q_0^+ = Q_1^-$ and $Q_0^+ = Q_1^+$ (with pole-zero cancellation at $z^2 = 0.1$) | 33 |
| 2.12 | Variation of settling time and maximum peak overshoot with β for condition $Q_0^+ = -Q_1^-$ and $Q_0^+ = -Q_1^+$ (with pole-zero cancellation at $z^2 = 0.1$) | 34 |
| 2.13 | Variation of settling time and maximum peak overshoot with β for condition $Q_0^+ = Q_1^-$ and $Q_0^+ = Q_1^+$ (with pole-zero cancellation at $z^2 = 0.2$) | 34 |
| 2.14 | Variation of settling time and maximum peak overshoot with β for condition $Q_0^+ = -Q_1^-$ and $Q_0^+ = -Q_1^+$ (with pole-zero cancellation at $z^2 = 0.2$) | 35 |

| | | |
|-------------|---|-----------|
| 2.15 | Root locus of the system of (2.64) with $\alpha = 0.3$ | 36 |
| 2.16 | Plot of gain margin with location of α | 36 |
| 2.17 | Response using augmentation $\frac{(z-1)}{z}$ with $\alpha = 0.2$ for conditions $Q_0^+ = Q_1^-$ and $Q_0^+ = Q_1^+$ with pole-zero cancellation at $z^2 = 0$ | 37 |
| 2.18 | Response using augmentation $\frac{(z-1)}{z}$ with $\alpha = 0.2$ for conditions $Q_0^+ = -Q_1^+$ and $Q_0^+ = -Q_1^-$ with pole-zero cancellation at $z^2 = 0$ | 38 |
| 2.19 | Change in settling time with variation of α for conditions $Q_0^+ = Q_1^-$ and $Q_0^+ = -Q_1^-$ with pole-zero cancellation at $z^2 = 0$ | 38 |
| 2.20 | Change in settling time with variation of α for conditions $Q_0^+ = Q_1^-$ and $Q_0^+ = -Q_1^-$ with pole-zero cancellation at $z^2 = 0.5$ | 39 |
| 2.21 | Change in settling time with variation of α for conditions $Q_0^+ = Q_1^-$ and $Q_0^+ = -Q_1^-$ with pole-zero cancellation at $z^2 = 0.75$ | 39 |
| 2.22 | Response using augmentation $\frac{(z+1)}{(z-1)}$ with $\beta = 0.85$ for conditions $Q_0^+ = Q_1^-$ and $Q_0^+ = Q_1^+$ with pole-zero cancellation at $z^2 = 0.5$ | 41 |
| 2.23 | Response using augmentation $\frac{(z+1)}{(z-1)}$ with $\beta = 0.85$ for conditions $Q_0^+ = -Q_1^+$ and $Q_0^+ = -Q_1^-$ with pole-zero cancellation at $z^2 = 0.5$ | 42 |
| 2.24 | Variation of settling time and maximum peak overshoot with β for condition $Q_0^+ = Q_1^-$ and $Q_0^+ = Q_1^+$ with pole-zero cancellation at $z^2 = 0$ | 42 |
| 2.25 | Variation of settling time and maximum peak overshoot with β for condition $Q_0^+ = -Q_1^-$ and $Q_0^+ = -Q_1^+$ with pole-zero cancellation at $z^2 = 0$ | 43 |
| 2.26 | Variation of settling time and maximum peak overshoot with β for condition $Q_0^+ = Q_1^-$ and $Q_0^+ = Q_1^+$ with pole-zero cancellation at $z^2 = 0.5$ | 43 |
| 2.27 | Variation of settling time and maximum peak overshoot with β for condition $Q_0^+ = -Q_1^-$ and $Q_0^+ = -Q_1^+$ with pole-zero cancellation at $z^2 = 0.5$ | 44 |
| 2.28 | Variation of settling time and maximum peak overshoot with β for condition $Q_0^+ = Q_1^-$ and $Q_0^+ = Q_1^+$ with pole-zero cancellation at $z^2 = 0.75$ | 44 |
| 2.29 | Variation of settling time and maximum peak overshoot with β for condition $Q_0^+ = -Q_1^-$ and $Q_0^+ = -Q_1^+$ with pole-zero cancellation at $z^2 = 0.75$ | 45 |
| 3.1 | 2-DOF periodic controller | 47 |
| 3.2 | 2-DOF LTI controller configuration | 47 |
| 3.3 | Root locus of the system of (2.52) | 57 |

| | | |
|-------------|--|-----------|
| 3.4 | Response of the plant with 2 DOF 2-periodic controller for conditions $Q_0^+ = Q_1^-$ and $Q_0^+ = -Q_1^+$ | 58 |
| 3.5 | Root locus of the system of (3.34) with $\alpha = 0.3$ | 63 |
| 3.6 | Plot of gain margin with location of α | 63 |
| 3.7 | Response using augmentation $\frac{z}{(z-1)}$ with $\alpha = 0.2$ for conditions $Q_0^+ = Q_1^-$ and $Q_0^+ = Q_1^+$ with pole-zero cancellation at $z^2 = 0$ | 64 |
| 3.8 | Response using augmentation $\frac{z}{(z-1)}$ with $\alpha = 0.2$ for conditions $Q_0^+ = -Q_1^+$ and $Q_0^+ = -Q_1^-$ with pole-zero cancellation at $z^2 = 0$ | 65 |
| 3.9 | Variation of settling time and maximum peak undershoot with α for condition $Q_0^+ = Q_1^-$ and $Q_0^+ = Q_1^+$ with pole-zero cancellation at $z^2 = 0$ | 65 |
| 3.10 | Variation of settling time and maximum peak undershoot with α for condition $Q_0^+ = -Q_1^-$ and $Q_0^+ = -Q_1^+$ with pole-zero cancellation at $z^2 = 0$ | 66 |
| 3.11 | Variation of settling time and maximum peak undershoot with α for condition $Q_0^+ = Q_1^-$ and $Q_0^+ = Q_1^+$ with pole-zero cancellation at $z^2 = 0.5$ | 66 |
| 3.12 | Variation of settling time and maximum peak undershoot with α for condition $Q_0^+ = -Q_1^-$ and $Q_0^+ = -Q_1^+$ with pole-zero cancellation at $z^2 = 0.5$ | 67 |
| 3.13 | Variation of settling time and maximum peak undershoot with α for condition $Q_0^+ = Q_1^-$ and $Q_0^+ = Q_1^+$ with pole-zero cancellation at $z^2 = 0.75$ | 67 |
| 3.14 | Variation of settling time and maximum peak undershoot with α for condition $Q_0^+ = -Q_1^-$ and $Q_0^+ = -Q_1^+$ with pole-zero cancellation at $z^2 = 0.75$ | 68 |
| 3.15 | Root locus of the system of (3.70) with $\beta = 0.9$ | 69 |
| 3.16 | Plot of gain margin with location of β | 69 |
| 3.17 | Response using augmentation $\frac{(z+1)}{(z-1)}$ with $\beta = 0.9$ for conditions $Q_0^+ = Q_1^-$ and $Q_0^+ = Q_1^+$ with pole-zero cancellation at $z^2 = 0.5$ | 70 |
| 3.18 | Response using augmentation $\frac{(z+1)}{(z-1)}$ with $\beta = 0.9$ for conditions $Q_0^+ = -Q_1^+$ and $Q_0^+ = -Q_1^-$ with pole-zero cancellation at $z^2 = 0.5$ | 71 |
| 3.19 | Variation of settling time and maximum peak undershoot with β for condition $Q_0^+ = Q_1^-$ and $Q_0^+ = Q_1^+$ with pole-zero cancellation at $z^2 = 0$ | 71 |
| 3.20 | Variation of settling time and maximum peak undershoot with β for condition $Q_0^+ = -Q_1^-$ and $Q_0^+ = -Q_1^+$ with pole-zero cancellation at $z^2 = 0$ | 72 |

| | | |
|-------------|--|-----------|
| 3.21 | Variation of settling time and maximum peak undershoot with β for condition $Q_0^+ = Q_1^-$ and $Q_0^+ = Q_1^+$ with pole-zero cancellation at $z^2 = 0.5$ | 72 |
| 3.22 | Variation of settling time and maximum peak undershoot with β for condition $Q_0^+ = -Q_1^-$ and $Q_0^+ = -Q_1^+$ with pole-zero cancellation at $z^2 = 0.5$ | 73 |
| 4.1 | Cart-inverted pendulum system | 75 |
| 4.2 | Free body diagram of cart | 76 |
| 4.3 | Free body diagram of pendulum | 76 |
| 4.4 | State-feedback controller | 80 |
| 4.5 | Response of the optimized system showing pendulum angle and cart position | 81 |
| 4.6 | 2-loop control structure for cart-inverted pendulum system | 82 |
| 4.7 | Root locus of inner loop | 83 |
| 4.8 | Root locus of outer loop using controller H_2 of case 1.1 | 83 |
| 4.9 | Response of pendulum angle for case 1.1 using $k = k_\theta = k_x = 1$ | 84 |
| 4.10 | Response of cart position for case 1.1 using $k = k_\theta = k_x = 1$ | 84 |
| 4.11 | Root locus of inner loop | 85 |
| 4.12 | Root locus of outer loop using controller H_2 of case 2.1 | 85 |
| 4.13 | Response of pendulum angle for case 2.1 using $k = k_\theta = k_x = 1$ | 86 |
| 4.14 | Response of cart position for case 2.1 using $k = k_\theta = k_x = 1$ | 86 |
| 4.15 | 1-DOF 2-periodic controller in outer loop for cart-inverted pendulum system | 87 |
| 4.16 | Root locus of the system of (4.30) with $\beta = 0.5$ | 89 |
| 4.17 | Root locus of the system of (4.30) with $\beta = 0.6$ | 89 |
| 4.18 | Root locus of the system of (4.30) with $\beta = 0.8$ | 89 |
| 4.19 | Response of pendulum angle using 1-DOF periodic controller using case 1.1 for condition $Q_0^+ = Q_1^-$ | 90 |
| 4.20 | Response of cart position using 1-DOF periodic controller using case 1.1 for condition $Q_0^+ = Q_1^-$ | 91 |
| 4.21 | Response of pendulum angle using 1-DOF periodic controller using case 1.1 for condition $Q_0^+ = -Q_1^-$ | 91 |
| 4.22 | Response of cart position using 1-DOF periodic controller using case 1.1 for condition $Q_0^+ = -Q_1^-$ | 92 |
| 4.23 | Response of pendulum angle using 1-DOF periodic controller using case 1.2 for condition $Q_0^+ = Q_1^-$ | 93 |
| 4.24 | Response of cart position using 1-DOF periodic controller using case 1.2 for condition $Q_0^+ = Q_1^-$ | 93 |

| | | |
|-------------|--|------------|
| 4.25 | Response of pendulum angle using 1-DOF periodic controller using case 1.2 for condition $Q_0^+ = -Q_1^-$ | 94 |
| 4.26 | Response of cart position using 1-DOF periodic controller using case 1.2 for condition $Q_0^+ = -Q_1^-$ | 94 |
| 4.27 | Response of pendulum angle using 1-DOF periodic controller using case 1.2 for condition $Q_0^+ = Q_1^-$ | 95 |
| 4.28 | Response of cart position using 1-DOF periodic controller using case 1.2 for condition $Q_0^+ = Q_1^-$ | 96 |
| 4.29 | Response of pendulum angle using 1-DOF periodic controller using case 1.2 for condition $Q_0^+ = -Q_1^-$ | 96 |
| 4.30 | Response of cart position using 1-DOF periodic controller using case 1.2 for condition $Q_0^+ = -Q_1^-$ | 96 |
| 4.31 | Response of pendulum angle using 1-DOF periodic controller using case 1.2 for condition $Q_0^+ = Q_1^-$ | 98 |
| 4.32 | Response of cart position using 1-DOF periodic controller using case 1.2 for condition $Q_0^+ = Q_1^-$ | 98 |
| 4.33 | Response of pendulum angle using 1-DOF periodic controller using case 1.2 for condition $Q_0^+ = -Q_1^-$ | 98 |
| 4.34 | Response of cart position using 1-DOF periodic controller using case 1.2 for condition $Q_0^+ = -Q_1^-$ | 99 |
| 4.35 | Compensation of cart-inverted pendulum system by 2-DOF 2-periodic controller in outer loop | 99 |
| 4.36 | Response of pendulum angle using 2-DOF periodic controller using case 1.1 for conditions $Q_0^+ = Q_1^-$ and $Q_0^+ = Q_1^+$ | 100 |
| 4.37 | Response of cart position using 2-DOF periodic controller using case 1.1 for conditions $Q_0^+ = Q_1^-$ and $Q_0^+ = Q_1^+$ | 100 |
| 4.38 | Response of pendulum angle using 2-DOF periodic controller using case 1.1 for conditions $Q_0^+ = -Q_1^-$ and $Q_0^+ = -Q_1^+$ | 100 |
| 4.39 | Response of cart position using 2-DOF periodic controller using case 1.1 for conditions $Q_0^+ = -Q_1^-$ and $Q_0^+ = -Q_1^+$ | 101 |
| 4.40 | Response of pendulum angle using 2-DOF periodic controller using case 1.2 for conditions $Q_0^+ = Q_1^-$ and $Q_0^+ = Q_1^+$ | 101 |
| 4.41 | Response of cart position using 2-DOF periodic controller using case 1.2 for conditions $Q_0^+ = Q_1^-$ and $Q_0^+ = Q_1^+$ | 101 |

| | | |
|-------------|--|------------|
| 4.42 | Response of pendulum angle using 2-DOF periodic controller using case 1.2 for conditions $Q_0^+ = -Q_1^-$ and $Q_0^+ = -Q_1^+$ | 102 |
| 4.43 | Response of cart position using 2-DOF periodic controller using case 1.2 for conditions $Q_0^+ = -Q_1^-$ and $Q_0^+ = -Q_1^+$ | 102 |
| 4.44 | Response of pendulum angle using 2-DOF periodic controller using case 2.1 for conditions $Q_0^+ = Q_1^-$ and $Q_0^+ = Q_1^+$ | 102 |
| 4.45 | Response of cart position using 2-DOF periodic controller using case 2.1 for conditions $Q_0^+ = Q_1^-$ and $Q_0^+ = Q_1^+$ | 103 |
| 4.46 | Response of pendulum angle using 2-DOF periodic controller using case 2.1 for conditions $Q_0^+ = -Q_1^-$ and $Q_0^+ = -Q_1^+$ | 103 |
| 4.47 | Response of cart position using 2-DOF periodic controller using case 2.1 for conditions $Q_0^+ = -Q_1^-$ and $Q_0^+ = -Q_1^+$ | 103 |
| 4.48 | Response of pendulum angle using 2-DOF periodic controller using case 2.2 for conditions $Q_0^+ = Q_1^-$ and $Q_0^+ = Q_1^+$ | 104 |
| 4.49 | Response of cart position using 2-DOF periodic controller using case 2.2 for conditions $Q_0^+ = Q_1^-$ and $Q_0^+ = Q_1^+$ | 104 |
| 4.50 | Response of pendulum angle using 2-DOF periodic controller using case 2.2 for conditions $Q_0^+ = -Q_1^-$ and $Q_0^+ = -Q_1^+$ | 104 |
| 4.51 | Response of cart position using 2-DOF periodic controller using case 2.2 for conditions $Q_0^+ = -Q_1^-$ and $Q_0^+ = -Q_1^+$ | 104 |

List of tables

| | | |
|------------|--|------------|
| 2.1 | Variation of settling time and maximum peak undershoot with β for condition $Q_0^+ = Q_1^-$ and $Q_0^+ = -Q_1^-$ with pole-zero cancellation at $z^2 = 0.5$ | 31 |
| 2.2 | Variation of settling time and maximum peak undershoot with α for condition $Q_0^+ = Q_1^-$ and $Q_0^+ = -Q_1^-$ with pole-zero cancellation at $z^2 = 0.5$ | 37 |
| 2.3 | Variation of settling time and maximum peak undershoot with β for condition $Q_0^+ = Q_1^-$ and $Q_0^+ = -Q_1^-$ with pole-zero cancellation at $z^2 = 0.5$ | 41 |
| 3.1 | Variation of settling time and maximum peak undershoot with α for condition $Q_0^+ = Q_1^-$ and $Q_0^+ = -Q_1^-$ with pole-zero cancellation at $z^2 = 0$ | 64 |
| 3.2 | Variation of settling time and maximum peak undershoot with β for condition $Q_0^+ = Q_1^-$ and $Q_0^+ = -Q_1^-$ with pole-zero cancellation at $z^2 = 0$ | 70 |
| 3.3 | Comparison of settling time variation with 1-DOF and 2-DOF configuration with augmentation $\frac{z+1}{z}$ for conditions $Q_0^+ = Q_1^-$ and $Q_0^+ = -Q_1^-$ | 73 |
| 3.4 | Comparison of settling time variation with 1-DOF and 2-DOF configuration with augmentation $\frac{z+1}{z-1}$ for conditions $Q_0^+ = Q_1^-$ and $Q_0^+ = -Q_1^-$ | 74 |
| 4.1 | Inverted pendulum system parameters | 78 |
| 4.2 | Variation of settling time with choice of the inner and the outer loop LDTI controller | 86 |
| 4.3 | Comparison of performance of 1-DOF and 2-DOF 2-periodic controller for 2 different systems | 105 |

CHAPTER 1

Introduction and Literature review

1.1 Introduction

The primary objective of control engineers is to achieve desired output from any plant. To get this from a Single-Input-Single-Output (SISO), Linear-Time-Invariant (LTI) plant we, the control engineers, need to design a controller which can satisfy the following basic requirements.

- i. **Stability:** Stability is the first and foremost concern of the control engineers. If a plant is unstable, we cannot do anything with that plant. So, we have to ensure that a plant or a compensated one is stable. For that, basic control theory states that, all the poles of the compensated system should lie on the left half of s-plane for continuous time systems or within the unit circle on z-plane for discrete time systems.
- ii. **Pole placement:** The controller, if required, should be capable of placing closed loop poles at desired locations in s and/or z-plane.
- iii. **Robustness:** The compensated system should be able to take care of model uncertainties and parameter uncertainties.
- iv. **Disturbance rejection:** The compensated system should be capable of rejecting noise or external disturbances.

Depending on the control challenges several linear/non-linear or time-invariant/time-varying controllers have been developed [1-3, 7, 11-15]. To name a few, P, PI, PD, PID, LQR, Lead, Lag, Lead-Lag (compensator) etc. are popularly used in industrial applications.

1.2 Limitations of LTI controller

Linear time invariant (LTI) controllers are considered to be the simplest controller and have wide industrial applications. In the literature there are wide variety of techniques available to design LTI controllers [1-3, 7, 11-15]. However, it is found that they have several limitations [16, 17].

- i. **Zero placement:** LTI controller has the capability of placing poles but it cannot place zeros. If any right half plane zero occurs at open loop transfer function then after compensation by LTI controller, it remains unaltered in closed loop transfer function.

For example, let the plant transfer function be $k \frac{b(z)}{a(z)}$ and the controller transfer function be

$\frac{p(z)}{q(z)}$. With unity feedback the closed loop transfer function becomes $\frac{kb(z)p(z)}{a(z)q(z)+kb(z)p(z)}$

So, from the closed loop transfer function it is clear that open loop zeros remain unaltered. [1-3]. The only way to handle zeros (using LTI controller) is pole-zero cancellation. However, if non-minimum phase (NMP) zeros are present in the system LTI control design renders several hindrances.

- ii. **Gain margin:** The gain margin (GM) compensation of NMP systems does not provide satisfactory result. As the root locus starts from open-loop poles and terminates at loop-zeros, presence of an NMP zero will force at least a branch of root locus to enter into the right half of s-plane (for continuous time systems) or to move out of the unit circle (in z-plane for discrete time systems). Consequently, the system may remain stable for small values of loop gain. Clearly, the LTI controller cannot provide stability for higher values of loop gain and thus reduces the stability margins. If unstable poles and zeros come closer to each other, gain margin decreases significantly and in the worst case tends to 1. [22,23]

In the literature it has been shown that above limitations can be overcome by using time-varying controllers as they have the capability of placing loop-zeros. [8, 18]

1.3 Periodic control

Periodic Controller is a special type of linear controller, which has the gains/coefficients that vary periodically with time. So, it can be said that periodic control is a linear time varying control.

Several attempts have been made in the literature to overcome the limitations of LTI controller using time-varying control technique. We reiterate that periodic controllers perform better than LTI controllers by virtue of its loop zero placement capability [8, 18].

1.3.1 Periodicity

If the gains of a periodic system have periodicity M then it is called as M-periodic system.

For example, a 2-periodic signal (shown in Fig. 1.1) has periodicity 2. The gain is same (e) for all the even instants and in the odd instants the gain is o .

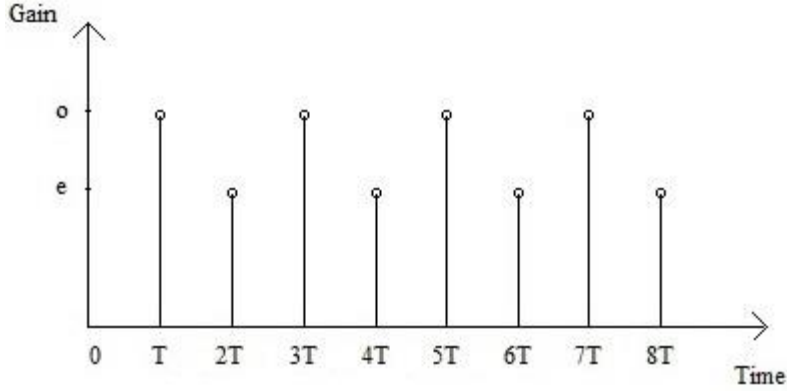


Fig. 1.1: 2-periodic signal

1.3.2 Analysis techniques of discrete-time periodic system

The analytical tools that have been developed so far, are based on reformulation of the closed-loop periodic control system to a class of time-invariant systems. The reformulation techniques as discussed in [46] are as follows,

- i. **Time-lifted reformulation:** The time-lifted reformulation is a classical method. The idea of this technique is to split the time axis into M parts for a M -periodic system and considering each part as an individual LTI system, i.e. an m -input n -output M -periodic system is represented by an $m \times M$ -input $n \times M$ -output LTI system. Then a system transfer matrix is formed combining all the M parts and the system is analysed as a MIMO LTI system.
- ii. **Frequency-lifted Reformulation:** In this technique each of the input and the output signals of an M -periodic system are expressed with the help of discrete Fourier transformation having the fundamental and $(M-1)$ higher harmonic components. Then a time-invariant transfer matrix is generated from aforesaid expressions.
- iii. **Cyclic Reformulation:** In this technique one sample is picked up per period for an M -periodic signal and represented them as an $M \times 1$ vector. The positions of the samples in

the vector are shifted with consecutive sample times and after completion of each period an $M \times M$ transfer matrix is formed.

- iv. **Floquet theory:** It is a characteristic equation based approach. Floquet theory provides the solution of ordinary differential equations with periodic coefficients. This technique is applied to the difference equation of discrete periodic system to obtain the characteristic equation.

Periodic controllers can be realized in both continuous time domain [27, 30, 35] and discrete time domain [9, 10, 20-22, 31-33]. In some cases, continuous time periodic controller becomes difficult to implement practically [32]. In this aspect discrete time periodic controllers provide advantage over continuous time periodic controllers.

1.4 Classification of periodic controllers

1.4.1 Continuous time periodic controllers

Continuous time periodic control was conceived from the pioneering work by Lee *et al* [18]. It was observed that the controller proposed by them was capable of placing zeros at desired location by varying the values of the controller parameters. However, significant ripples of order 1 i.e. $O(1)$ was present in the output response, along with $O(\omega^r)$ oscillations (where, ω is the frequency of parameter variation and r is the relative order of the plant) in the controller output i.e. the plant input. As a consequence, the performance of overall control system was found to be poor. Hence, 2-degree-of-freedom (DOF) controller configuration (shown in figure 1.3.1) was further considered to alleviate the problem stated above [27, 30].

Figure 1.2 shows schematic of a continuous time periodic controller along with the plant. Unlike LTI controllers, periodic terms $\alpha(\omega t)$ and $\beta(\omega t)$ (with periodicity 2π) multiplied by high frequency (ω) terms are added to the gains of periodic controller.

Here, n is the order of the plant, r is the relative order or the number of zeros of the plant. Order of the controller is taken as $m \geq n$ [27, 30].

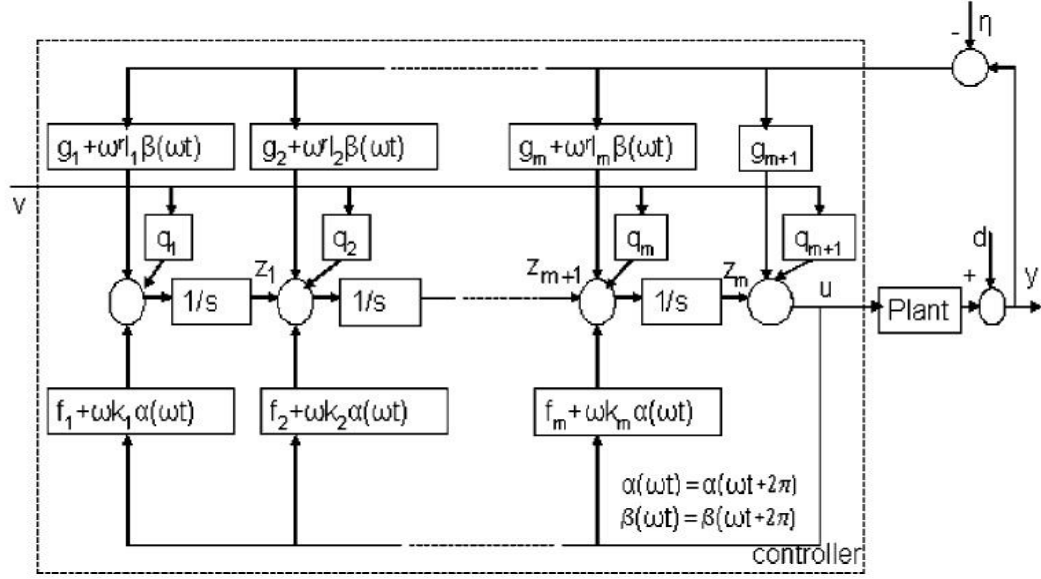


Figure 1.2: 2-DOF continuous time periodic controller circuit (taken from [27])

Here, v : the reference input, d : disturbance signal/input, η : noise signal, y : the system output and k_i, f_i, l_i, g_i, q_i are constant gains and ω is the frequency of parameter variation.

Averaging principle was used as a tool to synthesize the periodic controller in [27]. It was found that oscillations of $O(1)$ was present at controller output, which was much smaller than the oscillation of $O(\omega^r)$, which was present in the design of [18]. The oscillation in system output was also reduced to $O(\frac{1}{\omega^r})$ from $O(1)$. By making the frequency (ω) significantly high, order of oscillation at the output i.e. $O(\frac{1}{\omega^r})$ can be made insignificant.

The continuous time periodic controller has been used to compensate practical systems [35-39, 41, 42]. In [35] continuous time periodic controller is applied to compensate a cart inverted pendulum system. It has been shown that periodic controller gives better result than LQR controller when used to compensate a system with non-minimum phase zero. However, the design of [35] was not practically implementable as the magnitude of signals at some intermediate points of the controller were of $O(\omega^r)$, which is very high (as ω is very high). In [38] the authors have carried out a comparison between sliding mode control (SMC) and periodic control and shown that periodic control gives better stability margins.

1.4.2 Discrete time periodic controller

Like continuous-time periodic controllers, discrete time periodic controllers are also capable of relocating the loop-zeros and thus improving loop robustness and gain margin of the system.

Numerous researches have been carried out on discrete time periodic control [9, 10, 20-22, 31-33]. Several techniques to synthesize discrete time periodic controller have been shown in the literature including the modified z-transform method [4], lifting technique [19, 20], Floquet theory [3, 21]. Compensation of a SISO LTI plants using 2-periodic controller have been shown in [28, 32-34].

There are two configurations of discrete time periodic controller: 1-DOF and 2-DOF configuration. 1-DOF periodic controllers have the capability to place poles and loop zeros at desired locations [31-33]. A 2-periodic controller has been designed with controller order $m \geq n$ (where n is the plant order) in [33]. The controller was capable of placing poles and loop zeros at desired locations and improving stability margins. Unfortunately, there was considerable amount of ripple present in output. Figure 1.3 shows the 1-DOF control topology.

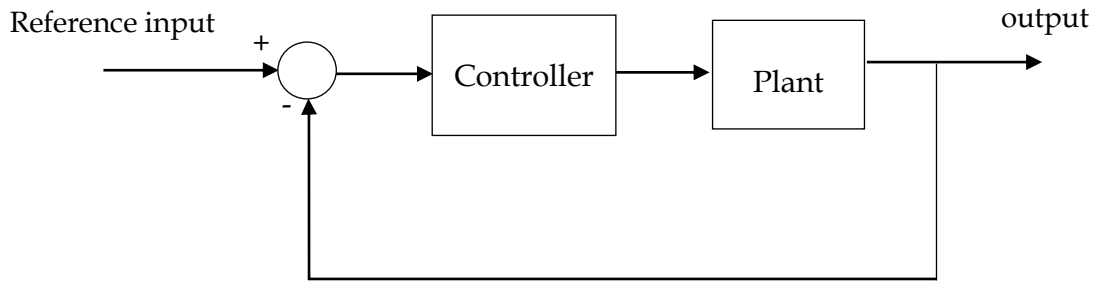


Figure 1.3: 1-DOF control topology

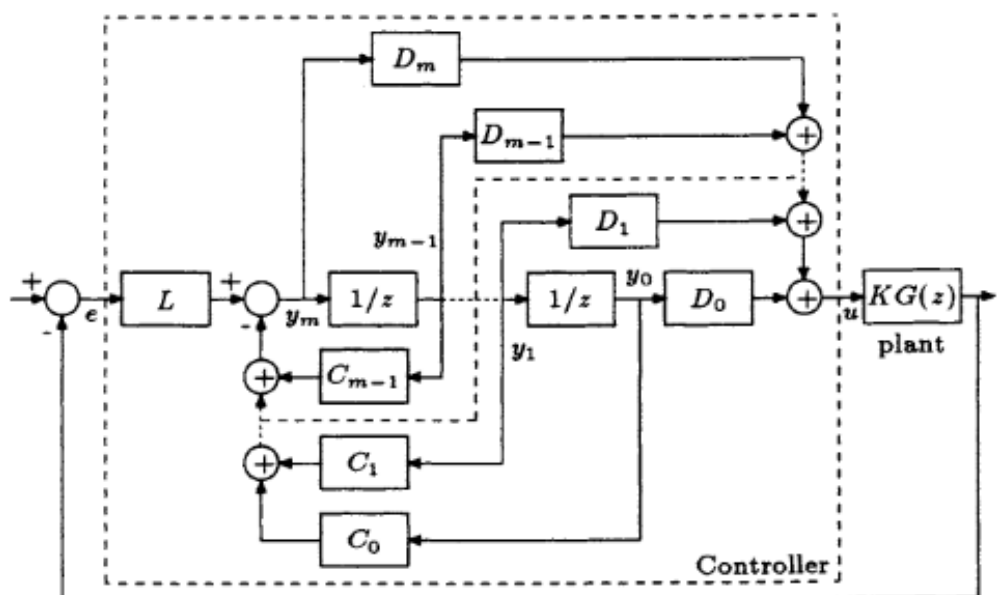


Figure 1.4: 2-periodic discrete time controller (1 DOF) [33]

Figure 1.4 shows the 1-DOF configuration of 2-periodic discrete time controller [33]. It has been observed that the presence of periodic variation in controller parameters creates ripple in the steady-state response to a step input [31,33]. In the literature it is shown that in the discrete-time domain, these ripples can be eliminated if the loop transfer function contains a zero at -1 or a pole at 1 [31]. If the plant does not contain any such term, then it should be multiplied by an augmentation transfer function containing any of such terms to get ripple free response [31].

2-DOF control topology is shown in figure 1.4. It contains feedback and feedforward controllers which were not present in 1-DOF topology. This modification reduces the controller order, however, its loop-compensation capability remains same as 1-DOF controller.

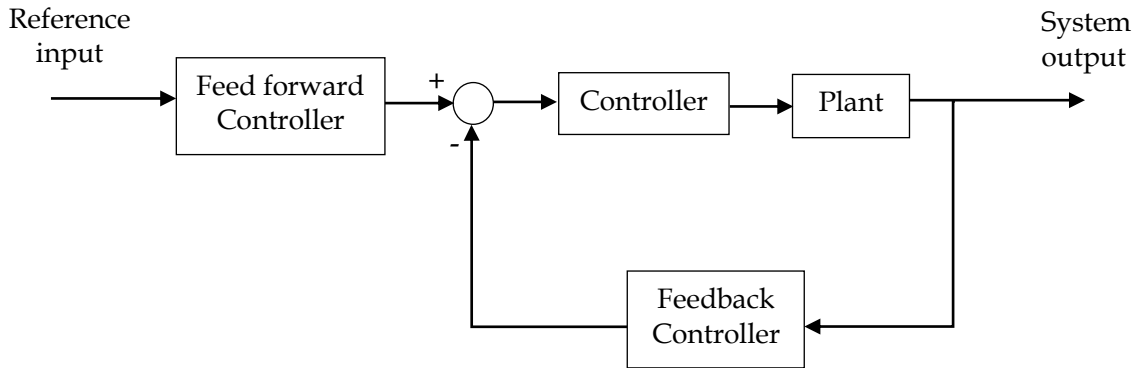


Figure 1.5: 2-DOF control topology

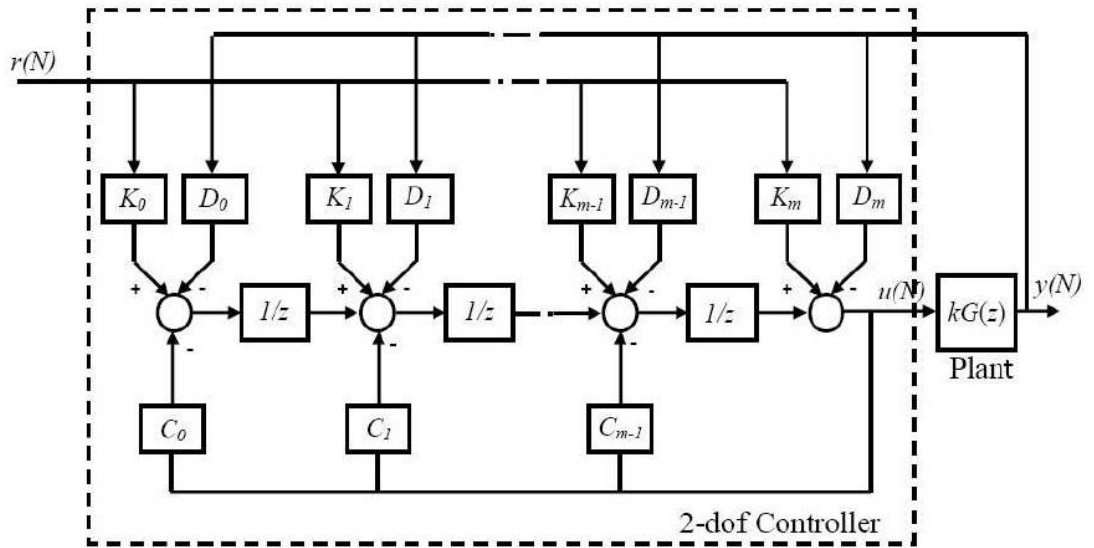


Figure 1.6: 2-periodic discrete time controller (2 DOF) [34]

Figure 1.6 shows schematic diagram of a 2-DOF 2-periodic discrete time controller (taken from [34]). In [34] the controller was designed using $m \geq n$ (where n is the plant order and m is the

controller order). Authors have shown that the presence of feedforward gain K_i results in cancellation of a few poles and thus reduction of the order of the overall system. Controller synthesis have been done using a two stage algorithm. Output ripples have been avoided by multiplying the input with a periodic gain.

1.5 Motivation and our contribution

It is well known that the LTI plants containing unstable poles along with NMP zeros result in poor stability margins when compensated using LTI controllers. On the other hand, it has been observed that the periodic controllers are capable of overcoming the shortcomings of LTI controllers. However, output response of periodic controllers inherently contains significant ripples that persist even at the steady-state. Fortunately, in case of continuous-time plants such ripple problems have been taken care of by using a 2–DOF configuration [30]. Subsequently for discrete-time periodic controllers a set of conditions have also been derived for ensuring ripple-free steady-state response [31,34].

The contributions of the thesis are as follows:

- This work intends to revisit the problem of compensating LDTI plants by using 2-periodic controllers with both 1-DOF and 2-DOF configurations.
- The main contribution of the work is to establish the additional benefit reaped from a 2–DOF configuration and to show how the same can be utilized to improve the system performance. It is important to note that such freedom comes in the form of additional feed-forward gains that can be used to tune the system response. A synthetic example is considered to illustrate the fact.
- Finally, the 2-DOF 2-periodic controller is employed on a real-time system, a cart-inverted pendulum system, with greater benefits as compared to LTI as well as 1-DOF 2-periodic controller.

1.6 Thesis organisation

The thesis is organised as follows:

- Chapter 1 introduces the basic control objectives and the concept of periodic control. It points out the limitations of LTI controllers and discusses how periodic controllers can overcome them.

- Chapter 2 reviews the compensation of LDTI plants by 1-DOF 2-periodic controllers. In this regard the chapter presents the controller synthesis for a synthetic LDTI plant with several iterations of control designs and a comparative study of the results is carried out.
- A 2-DOF 2-periodic controller configuration is studied in Chapter 3. The controller synthesis is carried out for the same plant as in Chapter 2 with several iterations of control designs. The results are compared with that of 1-DOF configuration presented in Chapter 2 to illustrate the benefits of the 2-DOF approach.
- In Chapter 4 the cart-inverted pendulum system (CIPS) is considered as a real-time example. Conventional LDTI controllers and 2-periodic controllers with both 1-DOF and 2-DOF configurations are used to stabilize the CIPS. A comparison of results is presented for the purpose of performance evaluation of the controllers employed.
- Chapter 5 concludes the contributions of the thesis and points out the scope of future work.

CHAPTER 2

1-DOF 2-Periodic Controller: Revisited

2.1 Introduction

It is seen from the preceding chapter that periodic controllers, unlike the LDTI counterparts, are capable of relocating the loop-zeros at desired locations. Consequently, periodic control provides better gain margin in respect of compensation of NMP plants.

This chapter aims to review the capabilities of 1-DOF 2-periodic controllers in respect of providing superior GM compensation to LDTI, NMP plants. Further this chapter proposes an enhancement to the existing 1-DOF, 2-periodic control scheme and illustrates the same via numerical example.

2.1.1 Analysis of discrete 2-periodic systems using Time Lifting Method

For discrete time-varying plants, system dynamics is expressed using a difference equation with coefficients varying periodically with time. These systems may be analysed using either time-lifted reformulation, cyclic reformulation, frequency-lifted reformulation method or Floquet theory approach. In this thesis analysis of SISO, causal, discrete-time 2-periodic systems has been carried out using the time-domain lifting method as discussed next.

In time-domain lifting technique, a SISO M-periodic system is represented as M-input M-output LDTI system and produces a $M \times M$ transfer matrix (i.e., MIMO representation).

In a 2-periodic system, coefficients of all the even instants are same and odd instants are same. So, a SISO 2-periodic map g can be lifted to a 2-input 2-output time invariant representation and thus making the lifted system expressed as even and odd LDTI systems.

Let, $e(0), e(1), e(2), \dots$ be the input sequence and $u(0), u(1), u(2), \dots$ be the corresponding output sequence. Now, lifting the system to even and odd instants inputs and outputs one gets

$$E_e(z^2) = \sum_{i=0}^{\infty} z^{-2i} e(2i)$$
$$z^{-1} E_o(z^2) = \sum_{i=0}^{\infty} z^{-2i} e(2i + 1) \quad (2.1)$$

$$U_e(z^2) = \sum_{i=0}^{\infty} z^{-2i} u(2i)$$

$$z^{-1}U_o(z^2) = \sum_{i=0}^{\infty} z^{-2i} u(2i+1) \quad (2.2)$$

So, the even and odd instant input and output sequences can be written as,

$$E(z^2) = E_e(z^2) + z^{-1}E_o(z^2)$$

$$U(z^2) = U_e(z^2) + z^{-1}U_o(z^2) \quad (2.3)$$

where,

$E(z^2)$ is the z-transform of complete instant input sequence

$E_e(z^2)$ is the z-transform of even instant input sequence

$E_o(z^2)$ is the z-transform of odd instant input sequence

and $U(z^2)$ is the z-transform of complete instant output sequence

$U_e(z^2)$ is the z-transform of even instant output sequence

$U_o(z^2)$ is the z-transform of odd instant output sequence

Now, the overall system can be expressed as,

$$\begin{bmatrix} U_e(z^2) \\ z^{-1}U_o(z^2) \end{bmatrix} = \bar{G}(z^2) \begin{bmatrix} E_e(z^2) \\ z^{-1}E_o(z^2) \end{bmatrix}$$

with, $\bar{G}(z^2) = \begin{bmatrix} G_{11}(z^2) & z^{-1}G_{12}(z^2) \\ z^{-1}G_{21}(z^2) & G_{22}(z^2) \end{bmatrix} \quad (2.4)$

where, all G_{ij} (for $i, j = 1, 2$) are LDTI transfer functions in z^2 .

$\bar{G}(z^2)$ is the lifted transfer matrix which satisfies causality condition that $\bar{G}(\infty)$ is lower triangular.

2.2 Design of M-Periodic Controller

Let us consider a SISO, LDTI, n^{th} order plant $G(z) = k \frac{b(z)}{a(z)}$

where, $a(z) = z^n + a_{n-1}z^{n-1} + \dots + a_1z + a_0$

$$b(z) = z^r + b_{r-1}z^{r-1} + \dots + b_1z + b_0 \text{ with } r < n \quad (2.5)$$

Considering a m^{th} order M-periodic controller with maximum degrees of freedom (Fig 2.2.1) with

$$C_i(N) = C_i(N + M) = \sum_{k=0}^{M-1} \alpha^{kN} c_{ik} \quad (2.6)$$

For $i = 1, 2, \dots, (m - 1)$

$$D_i(N) = D_i(N + M) = \sum_{k=0}^{M-1} \alpha^{kN} d_{ik} \quad (2.7)$$

For $i = 1, 2, \dots, m$

$$\alpha := e^{j2\pi/M}$$

The overall controller transfer function can be written as

$$C(z, N) = [D_m(N)z^m + D_{m-1}(N)z^{m-1} + \dots + D_1(N)z + D_0(N)] \\ [z^m + C_{m-1}(N)z^{m-1} + \dots + C_1(N)z + C(N)]^{-1} \quad (2.8)$$

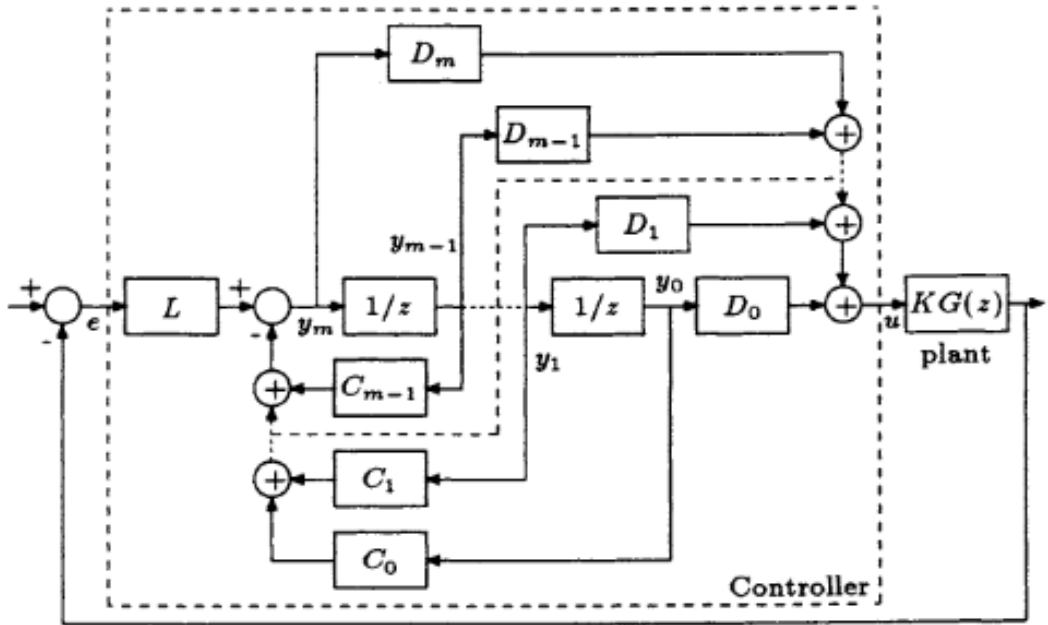


Fig. 2.1: 1-degree-of-freedom periodic controller with plant

The equation may also be written as

$$C(z, N) = [Q_0(z) + Q_1(z)\alpha^N + \dots + Q_{(M-1)}(z)\alpha^{(M-1)N}] \\ [P_0(z) + P_1(z)\alpha^N + \dots + P(z)\alpha^{(M-1)N}]^{-1} \quad (2.9)$$

where,

$$P_0 = z^m + c_{m-1,0}z^{m-1} + \dots + c_{1,0}z + c_{0,0}$$

$$P_i = c_{m-1,i}z^{m-1} + \dots + c_{1,i}z + c_{0,i}, \quad i = 0, 1, \dots, (M-1) \quad (2.10)$$

$$Q_i = d_{m,i}z^m + d_{m-1,i}z^{m-1} + \dots + d_{0,i}, \quad i = 1, 2, \dots, (M-1) \quad (2.11)$$

For a 2-periodic system, $M = 2$, $\alpha = -1$ and the controller transfer function becomes

$$C(z, N) = [Q_0(z) + (-1)^N Q_1(z)][P_0(z) + (-1)^N P_1(z)]^{-1} = [Q(z)][P(z)]^{-1}$$

where,

$$\begin{aligned} Q(z) &= (d_{m,0}z^m + d_{m-1,0}z^{m-1} + \cdots + d_{1,0}z + d_{0,0}) + \\ &\quad (-1)^N(d_{m,1}z^m + d_{m-1,1}z^{m-1} + \cdots + d_{1,1}z + d_{0,1}) \end{aligned} \quad (2.12)$$

$$\begin{aligned} P(z) &= (z^m + c_{m-1,0}z^{m-1} + \cdots + c_{1,0}z + c_{0,0}) + \\ &\quad (-1)^N(c_{m-1,1}z^{m-1} + \cdots + c_{1,1}z + c_{0,1}) \end{aligned} \quad (2.13)$$

2.2.1 Closed Loop Characteristic Equation

Let, for any polynomial $f(z)$, $f^+ = f(z)$ and $f^- = f(-z)$

Time domain lifting theory is applied to the controller and the plant. The transfer matrix of the polynomial $Q(z)$ becomes

$$\bar{Q}(z^2) = \begin{bmatrix} Q_{11}(z^2) & z^{-1}Q_{12}(z^2) \\ zQ_{21}(z^2) & Q_{22}(z^2) \end{bmatrix} \quad (2.14)$$

$$\begin{aligned} \text{where } Q_{11} &= Q_0^+ + Q_0^- + Q_1^+ + Q_1^- \\ Q_{12} &= Q_0^+ - Q_0^- + Q_1^+ - Q_1^- \\ Q_{21} &= Q_0^+ - Q_0^- - Q_1^+ + Q_1^- \\ Q_{22} &= Q_0^+ + Q_0^- - Q_1^+ - Q_1^- \end{aligned} \quad (2.15)$$

The lifted transfer matrix of the polynomial $P(z)$,

$$\bar{P}(z^2) = \frac{1}{2} \begin{bmatrix} P_{11}(z^2) & z^{-1}P_{12}(z^2) \\ zP_{21}(z^2) & P_{22}(z^2) \end{bmatrix} \quad (2.16)$$

$$\begin{aligned} \text{where } P_{11} &= P_0^+ + P_0^- + P_1^+ + P_1^- \\ P_{12} &= P_0^+ - P_0^- + P_1^+ - P_1^- \\ P_{21} &= P_0^+ - P_0^- - P_1^+ + P_1^- \\ P_{22} &= P_0^+ + P_0^- - P_1^+ - P_1^- \end{aligned} \quad (2.17)$$

As we know, controller transfer function is $C(z, N) = [Q(z)][P(z)]^{-1}$

So, from (2.14) and (2.16),

$$\bar{C}(z^2) = \frac{1}{\Delta_c} \begin{bmatrix} C_{11}(z^2) & z^{-1}C_{12}(z^2) \\ zC_{21}(z^2) & C_{22}(z^2) \end{bmatrix} \quad (2.18)$$

where,

$$\Delta_c = 2(P_0^+P_0^- - P_1^+P_1^-) \quad (2.19)$$

$$C_{11} = Q_0^+P_0^- + Q_0^-P_0^+ - Q_0^+P_1^- - Q_0^-P_1^+ + Q_1^+P_0^- + Q_1^-P_0^+ - Q_1^+P_1^- - Q_1^-P_1^+$$

$$C_{12} = Q_0^+P_0^- - Q_0^-P_0^+ + Q_0^+P_1^- - Q_0^-P_1^+ + Q_1^+P_0^- - Q_1^-P_0^+ + Q_1^+P_1^- - Q_1^-P_1^+$$

$$C_{21} = Q_0^+P_0^- - Q_0^-P_0^+ - Q_0^+P_1^- + Q_0^-P_1^+ - Q_1^+P_0^- + Q_1^-P_0^+ + Q_1^+P_1^- - Q_1^-P_1^+$$

$$C_{22} = Q_0^+P_0^- + Q_0^-P_0^+ + Q_0^+P_1^- + Q_0^-P_1^+ - Q_1^+P_0^- - Q_1^-P_0^+ - Q_1^+P_1^- - Q_1^-P_1^+ \quad (2.20)$$

Now, the lifted transfer matrix of the plant is

$$\bar{G}(z^2) = \frac{1}{\Delta_c} \begin{bmatrix} G_{11}(z^2) & z^{-1}G_{12}(z^2) \\ zG_{21}(z^2) & G_{22}(z^2) \end{bmatrix} \quad (2.21)$$

$$\text{where, } \Delta_c = \frac{1}{2a^+a^-} \quad (2.22)$$

$$\begin{aligned} G_{11} &= G_{22} = b^+a^- + b^-a^+ \\ G_{12} &= G_{21} = b^+a^- - b^-a^+ \end{aligned} \quad (2.23)$$

The characteristic equation of the overall system (i.e. including the 2-periodic controller and the plant) is given by

$$\Delta = \det[I + K\bar{G}\bar{C}] \quad (2.24)$$

Substituting the values of 2×2 transfer matrices of \bar{G} and \bar{C} from equation (2.18) and (2.21) to the characteristic equation of (2.24), we get,

$$\begin{aligned} \Delta = a^+a^-(&P_0^+P_0^- - P_1^+P_1^-) + K [b^+a^-(Q_0^+P_0^- - Q_1^-P_1^+) + b^-a^+(Q_0^-P_0^+ - Q_1^+P_1^-)] \\ &+ K^2b^+b^-(Q_0^+Q_0^- - Q_1^+Q_1^-) = 0 \end{aligned} \quad (2.25)$$

Now, consider the special cases of 2-periodic controller with controllable canonical form (CCF) and make any one of the choices $Q_0^\pm = \pm Q_1^\pm$ which omits the K^2 -term of equation (2.2.10). It is to be noted that the choices yield controllers that are either even or odd input (or output) controller. Each of these controllers are discussed below.

- i. **Even output controller:** When the controller output becomes zero at the odd instants, it is called even output controller. The condition for even output controller is $Q_0^+ = Q_1^+$. Considering an additional condition $Q_0^+ = (-1)^m Q_0^-$, where, m is order of the controller.

The controller transfer matrix becomes

$$\bar{C}(z^2) = \frac{1}{\Delta_c} \begin{bmatrix} C_{11}(z^2) & z^{-1}C_{12}(z^2) \\ 0 & 0 \end{bmatrix} \quad (2.26)$$

where, $\Delta_c = 2(P_0^+P_0^- - P_1^+P_1^-)$

Case I: when m is even

$$\text{So,} \quad Q_0^+ = Q_0^-$$

$$Q_1^+ = Q_1^-$$

When m is even, for an even output controller C_{11} and C_{12} becomes,

$$C_{11} = 2Q_0^+(P_0^- + P_0^+ - P_1^- - P_1^+)$$

$$C_{12} = 2Q_0^+(P_0^- - P_0^+ + P_1^- - P_1^+)$$

Case II: when m is odd

$$\text{So,} \quad Q_0^+ = -Q_0^-$$

$$Q_1^+ = -Q_1^-$$

When m is odd, for an even output controller C_{11} and C_{12} becomes,

$$C_{11} = 2Q_0^+(P_0^- - P_0^+ - P_1^- + P_1^+)$$

$$C_{12} = 2Q_0^+(P_0^- + P_0^+ + P_1^- + P_1^+)$$

- ii. **Odd output controller:** When the controller output becomes zero at the even instants, then it is called odd output controller. The condition for even output controller is $Q_0^+ = -Q_1^+$.

Considering additional condition $Q_0^+ = (-1)^m Q_0^-$

The controller transfer matrix becomes

$$\bar{C}(z^2) = \frac{1}{\Delta_c} \begin{bmatrix} 0 & 0 \\ zC_{21}(z^2) & C_{22}(z^2) \end{bmatrix} \quad (2.27)$$

Where, $\Delta_c = 2(P_0^+P_0^- - P_1^+P_1^-)$

Case I: When m is even

$$\text{So,} \quad Q_0^+ = Q_0^-$$

$$Q_1^+ = Q_1^-$$

When m is even, for an odd output controller C_{21} and C_{22} becomes,

$$C_{21} = 2Q_0^+(P_0^- - P_0^+ - P_1^- + P_1^+)$$

$$C_{22} = 2Q_0^+(P_0^- + P_0^+ + P_1^- + P_1^+)$$

Case II: When m is odd

$$\begin{aligned} \text{So, } Q_0^+ &= -Q_0^- \\ Q_1^+ &= -Q_1^- \end{aligned}$$

When m is odd, for an odd output controller C_{21} and C_{22} becomes,

$$\begin{aligned} C_{21} &= 2Q_0^+(P_0^- + P_0^+ - P_1^- - P_1^+) \\ C_{22} &= 2Q_0^+(P_0^- - P_0^+ + P_1^- - P_1^+) \end{aligned}$$

- iii. **Even input controller:** When the controller rejects odd instant inputs, then it is called even input controller. The condition for even output controller is $Q_0^+ = Q_1^-$.

The controller transfer matrix becomes

$$\bar{C}(z^2) = \frac{1}{\Delta_c} \begin{bmatrix} C_{11}(z^2) & 0 \\ zC_{21}(z^2) & 0 \end{bmatrix} \quad (2.28)$$

$$\begin{aligned} \text{where, } \Delta_c &= 2(P_0^+P_0^- - P_1^+P_1^-) \\ C_{11} &= (Q_0^+ + Q_1^+)(P_0^- - P_1^- + P_0^+ - P_1^+) \\ C_{21} &= (Q_0^+ - Q_1^+)(P_0^- - P_1^- + P_0^+ - P_1^+) \end{aligned}$$

- iv. **Odd input controller:** When the controller rejects even instant inputs, then it is called odd input controller. The condition for even output controller is $Q_0^+ = -Q_1^-$.

The controller transfer matrix becomes

$$\bar{C}(z^2) = \frac{1}{\Delta_c} \begin{bmatrix} 0 & z^{-1}C_{12}(z^2) \\ 0 & C_{22}(z^2) \end{bmatrix} \quad (2.29)$$

$$\begin{aligned} \text{where, } \Delta_c &= 2(P_0^+P_0^- - P_1^+P_1^-) \\ C_{12} &= (Q_0^+ + Q_1^+)(P_0^- + P_1^- + P_0^+ + P_1^+) \\ C_{22} &= (Q_0^+ - Q_1^+)(P_0^- + P_1^- + P_0^+ + P_1^+) \end{aligned}$$

2.2.2 Loop Zero Placement

From the characteristic equation of (2.25), the plant zeros are the co-efficient of K^2 term. Due to the presence of term, loop-zeros cannot be placed arbitrarily. But coefficient of K term does not contain such term and roots of this coefficient can be assigned to the required places.

Therefore, if coefficient of K^2 term is made equal to zero then coefficient of K term would determine the locations of loop-zeros. Consequently, achieving the loop-zero placement. To make the K^2 term equal to zero, the following four conditions are used,

- i. $Q_0^+ = Q_1^-$
- ii. $Q_0^+ = -Q_1^-$
- iii. $Q_0^+ = Q_1^+$
- iv. $Q_0^+ = -Q_1^+$

The equation (2.25) now becomes,

$$\Delta = a^+ a^- (P_0^+ P_0^- - P_1^+ P_1^-) + K [b^+ a^- (Q_0^+ P_0^- - Q_1^- P_1^+) + b^- a^+ (Q_0^- P_0^+ - Q_1^+ P_1^-)] \quad (2.30)$$

The above equation can be written as,

$$\hat{A}(z^2) \hat{P}(z^2) + \hat{Z}(z^2) = \hat{\Delta}(z^2) = \check{\Delta}(z^2) \check{D}(z^2) = 0 \quad (2.31)$$

Where,

$$\begin{aligned} \hat{A}(z^2) &= \text{Plant poles} = a^+ a^- \\ &= a_0 + a_2 z^2 + \dots + (-1)^n z^{2n} \end{aligned} \quad (2.32)$$

$$\begin{aligned} \hat{P}(z^2) &= \text{Controller poles} = (P_0^+ P_0^- - P_1^+ P_1^-) \\ &= \hat{p}_0 + \hat{p}_2 z^2 + \dots + (-1)^m z^{2m} \end{aligned} \quad (2.33)$$

$$\begin{aligned} \hat{Z}(z^2) &= \text{Zero polynomial of the overall system} \\ &= K [b^+ a^- (Q_0^+ P_0^- - Q_1^- P_1^+) + b^- a^+ (Q_0^- P_0^+ - Q_1^+ P_1^-)] \\ &= r_0 + r_2 z^2 + \dots + r_{2\theta} z^{2\theta} \end{aligned} \quad (2.34)$$

$\check{\Delta}(z^2)$ = Desired closed loop poles

$\check{D}(z^2)$ = Additional closed loop poles

From the above equations it can be noted that the controller pole polynomial and the loop-zero polynomial both are assignable. So, by adjusting the parameters of zero polynomial, zero placement can be achieved.

2.2.3 Order of the Controller

It can be observed from (2.31), the degree of polynomials $\hat{A}(z^2)$ and $\hat{P}(z^2)$ are $2n$ and $2m$ respectively. The degree of the polynomial $\hat{Z}(z^2)$ can be defined as,

$$\theta = m + \vartheta$$

with $\vartheta = n - I^+ \left\{ \frac{(n-r)}{2} \right\}$ (2.35)

where,

I^+ is the ceiling operator,

θ is the total number of assignable loop-zeros,

ϑ is the assignable plant zeros which depends upon the relative order of the plant.

From (2.12), (2.13) and (2.33), the total number of assignable coefficients is $(2m + m)$ to place m controller poles and $(m + \vartheta)$ loop zeros. The order of the controller is defined by,

$$m \geq \vartheta = n - I^+ \left\{ \frac{(n-r)}{2} \right\} \quad (2.36)$$

2.2.4 Evaluation of Controller Parameters

Controller parameters are evaluated by solving the characteristic equation. The controller is synthesized using approach of [3]. It is a two-stage method. In stage-I, an intermediate polynomial is obtained and in stage-II, controller parameters are calculated from the intermediate polynomial.

Stage I:

Let,

$$\begin{aligned} \hat{B}(z) &= b^+ a^- = [\hat{b}_0 + \hat{b}_2 z^2 + \dots + \hat{b}_{2\varphi_1} z^{2\varphi_1}] + z[\hat{b}_1 + \hat{b}_3 z^2 + \dots + \hat{b}_{2\varphi_2+1} z^{2\varphi_2}] \\ &= \hat{B}_e(z^2) + z\hat{B}_d(z^2) \end{aligned} \quad (2.37)$$

With $\varphi_1 = I^- \left\{ \frac{n+r}{2} \right\}$ and $\varphi_2 = I^- \left\{ \frac{n+r-1}{2} \right\}$

$$\begin{aligned} \hat{L}(z) &= (Q_0^+ P_0^- - Q_1^- P_1^+) \\ &= [\hat{l}_0 + \hat{l}_2 z^2 + \dots + \hat{l}_{2m} z^{2m}] + z[\hat{l}_1 + \hat{l}_3 z^2 + \dots + \hat{l}_{2m-1} z^{2(m-1)}] \\ &= \hat{L}_e(z^2) + z\hat{L}_d(z^2) \end{aligned} \quad (2.38)$$

From (2.37), (2.38) we obtain,

$$\begin{aligned} \hat{Z}(z^2) &= \hat{B}^+ \hat{L}^+ + \hat{B}^- \hat{L}^- = 2\hat{B}_e(z^2)\hat{L}_e(z^2) + 2z^2\hat{B}_d(z^2)\hat{L}_d(z^2) \\ &= r_0 + r_2 z^2 + \dots + r_{2\theta} z^{2\theta} \end{aligned} \quad (2.39)$$

Now, using (2.37), (2.38) and (2.39) the Sylvester matrix like equation is obtained below,

$$\begin{bmatrix} r_0 \\ r_2 \\ r_4 \\ \vdots \\ r_{2\theta} \end{bmatrix} = \begin{bmatrix} \hat{b}_0 & \dots & 0 & 0 & \dots & 0 \\ \hat{b}_2 & \dots & 0 & \hat{b}_1 & \dots & 0 \\ \hat{b}_4 & \dots & 0 & \hat{b}_3 & \dots & 0 \\ \vdots & \ddots & \vdots & \vdots & \ddots & \vdots \\ 0 & \dots & \hat{b}_{2\varphi_1} & 0 & \dots & \hat{b}_{2\varphi_2+1} \end{bmatrix} \begin{bmatrix} \hat{l}_0 \\ \vdots \\ \hat{l}_{2m} \\ \hat{l}_1 \\ \vdots \\ \hat{l}_{2m-1} \end{bmatrix} \quad (2.40)$$

Now, from (2.39) we can say that (2.40) will be a consistent set of equations if the following conditions are satisfied [44]:

- If the plant has a pole-zero cancelation at p then the effective loop transfer function would have the same at p^2 , signifying that the loop-zero polynomial must have a root at p^2 . (Clearly, for internal stability, the plant should not have any unstable pole-zero cancelation at p , when $|p| < 1$)
- If the plant denominator has an even factor $(z^2 + c)$, then also the loop transfer function would have a pole-zero cancelation at $-c$, and so the loop-zero polynomial must contain the same factor. (Again, for internal stability, $|c| < 1$ must be satisfied.)
- If the plant numerator has an even factor $(z^2 + c)$, then the loop-zero polynomial must also contain the same.

Equation (2.40) is solved using matrix inversion method and the $\hat{L}(z)$ polynomial is obtained.

But the matrix \bar{B} may become singular for the following cases:

- i. If the plant has pole(s) or zero(s) at origin.
- ii. If the plant has a pole-zero cancelation at origin.
- iii. If the denominator and numerator contains only even factors.

All these cases will lead to some all-zero identities, which will make (2.40) an undeterminable but consistent set of linear equations.

Assume rank of $\bar{B} = \text{rank of } [\bar{B} \mid \bar{r}]$; then the equation (2.40) becomes consistent and the polynomial $\hat{L}(z)$ can be obtained.

Stage II:

Polynomial $\hat{L}(z)$ which is obtained in stage-I, now, will be divided into two parts for all four conditions $Q_0^\pm = \pm Q_1^\pm$ and will be suitably assigned to pole polynomials to calculate the controller parameters.

Condition I: $Q_0^+ = Q_1^-$

From (2.38) we get,

$$\hat{L}(z) = Q_0^-(P_0^+ - P_1^-)$$

Then, to find Q_0^- and $(P_0^+ - P_1^-)$, polynomial $\hat{L}(z)$ is divided into two parts such that

- i. Both the halves are real polynomials (i.e., a complex root and its conjugate should be present in the same half).
- ii. At least one of the halves has no even factor.

If the factor that satisfies the 2nd condition is, in addition, monic, then the same can be chosen as $(P_0^+ - P_1^-)$ and the rest would be Q_0^- . Values of $d_{i,0}$ and $d_{i,1}$ (for $i = 0, 1, \dots, m$) can be directly obtained from Q_0^- and Q_1^+ . Calculations for finding $c_{i,0}$ and $c_{i,1}$ (for $i = 0, 1, \dots, m-1$) are shown below.

Let,

$$(P_0^+ - P_1^-) = \Gamma(z) = \gamma_0 + \gamma_1 z + \dots + \gamma_m z^m \quad (2.41)$$

From (2.13) and (2.41) it is obtained,

$$(P_0^+ \Gamma^- - P_1^- \Gamma^+) = \hat{P}(z^2) + \Gamma^+ \Gamma^- \quad (2.42)$$

Now, comparing both sides of the equation (2.42), we get,

$$\begin{bmatrix} \gamma_0 & 0 & 0 & 0 & \cdots & 0 & 0 \\ \gamma_2 & -\gamma_1 & \gamma_0 & 0 & \cdots & 0 & 0 \\ \gamma_4 & -\gamma_3 & \gamma_2 & -\gamma_1 & \cdots & 0 & 0 \\ \vdots & \vdots & \vdots & \vdots & \ddots & \vdots & \vdots \\ 0 & 0 & 0 & 0 & \cdots & (-1)^{m-1} \gamma_{m-1} & (-1)^m \gamma_{m-2} \\ 0 & 0 & 0 & 0 & \cdots & 0 & (-1)^m \gamma_m \end{bmatrix} = \begin{bmatrix} C_{0,0} \\ C_{1,0} \\ C_{2,0} \\ \vdots \\ C_{(m-1),0} \\ 1 \end{bmatrix} = \begin{bmatrix} \hat{p}_0 + \gamma_0^2 \\ \hat{p}_2 + 2\gamma_0\gamma_2 - \gamma_1^2 \\ \hat{p}_4 + \gamma_0\gamma_4 - 2\gamma_1\gamma_3 + \gamma_2^2 \\ \vdots \\ \hat{p}_{2(m-1)} + 2(-1)^m \gamma_m \gamma_{m-2} - (-1)^{(m-1)} \gamma_{m-1}^2 \\ (-1)^m + (-1)^m \gamma_m^2 \end{bmatrix} \quad (2.43)$$

The coefficients of P_0 i.e. $C_{0,0}, C_{1,0}, C_{2,0}, \dots, C_{(m-1),0}$ can be obtained by solving equation (2.43). Using these values, coefficients of P_1 i.e. $C_{0,1}, C_{1,1}, C_{2,1}, \dots, C_{(m-1),1}$ can be calculated from the following equation,

$$C_{i,1} = (-1)^i (C_{i,0} - \gamma_0) \quad \text{with } i = 0, 1, \dots, (m-1) \quad (2.44)$$

Condition II: $Q_0^+ = -Q_1^-$

From (2.38) we get,

$$\hat{L}(z) = Q_0^-(P_0^+ + P_1^-)$$

Now, procedures shown for condition can be followed. But equation for obtaining coefficients of P_1 from coefficients of P_0 will change and become as follows.

$$C_{i,1} = (-1)^i(\gamma_0 - C_{i,0}) \quad \text{with } i = 0, 1, \dots, (m-1) \quad (2.45)$$

Condition III: $Q_0^+ = Q_1^+$

In order to extract the factor Q_0 from $\hat{L}(z)$, the following condition must be considered.

$$Q_i^+ = (-1)^m Q_i^- \quad \text{with } i = 0, 1$$

m is the controller order.

From (2.38) we get,

$$\hat{L}(z) = Q_0^-(P_0^+ - (-1)^m P_1^-)$$

Now, procedures shown for condition can be followed. But equation for obtaining coefficients of P_1 from coefficients of P_0 will change and become as follows.

Condition IV: $Q_0^+ = -Q_1^+$

In order to extract the factor Q_0 from $\hat{L}(z)$, the following condition must be considered.

$$Q_i^+ = (-1)^m Q_i^- \quad \text{with } i = 0, 1$$

m is the controller order.

From (2.38) we get,

$$\hat{L}(z) = Q_0^-(P_0^+ + (-1)^m P_1^-)$$

Now, procedures shown for condition can be followed. But equation for obtaining coefficients of P_1 from coefficients of P_0 will change and become as follows.

2.3 Numerical Example: Second Order System

Example 2.3.1:

Consider a second order non-minimum phase plant

$$G(z) = \frac{(z - 1.2)}{(z - 0.5)(z - 1.5)}$$

with sampling time 1 sec.

The dead-beat response of the system can be obtained by placing all the closed loop poles at origin. Consider a 2-periodic controller of the form of Fig. 2.1, of order $m = 1$. The compensated system will have 3 closed loop poles and 2 loop zeros.

Besides placing all these poles at origin, the loop zeros are relocated to improve the loop robustness. One of the loop-zeros and the controller pole are chosen to be at origin and thus ensuring that the controller pole remains at origin even in closed loop. Then the other loop-zero would have to be placed at 0.225 such that the two plant poles also end up at the origin when the loop is closed. The loop gain is found to be 2.5.

The time-lifted representation of $G(z)$ is,

$$\tilde{G}(z^2) = \frac{1}{(z^2 - 2.25)(z^2 - 0.25)} \begin{bmatrix} (0.8z^2 - 0.9) & (z^2 - 1.65) \\ z^2(z^2 - 1.65) & (0.8z^2 - 0.9) \end{bmatrix}$$

and $\hat{A}(z^2) = (z^2 - 2.25)(z^2 - 0.25)$

$$\hat{P}(z^2) = -z^2$$

$$\hat{Z}(z^2) = -2.5 z^2(z^2 - 0.225)$$

$$\hat{\Delta}(z^2) = (z^2)^2$$

$$\check{D}(z^2) = -z^2$$

The corresponding Root Locus is shown in Fig. 2.2 The gain margin of the 2-periodic compensated system is 2.7413.

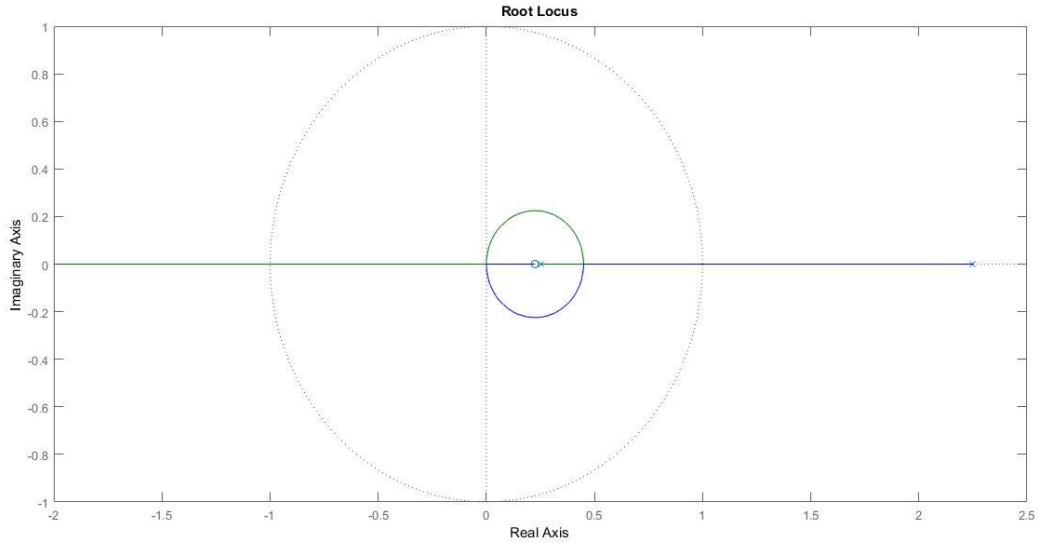


Fig. 2.2: Root locus for the system of Example 2.3.1 compensated by dead-beat 2-periodic controller

The controller parameters can be evaluated using technique discussed in Section 2.2.4.

Condition I: $\mathbf{Q}_0^+ = \mathbf{Q}_1^-$

For this condition, controller parameters are found to be

$$d_{0,0} = d_{0,1} = 0$$

$$d_{1,0} = -d_{1,1} = 4.2411$$

$$c_{0,0} = -c_{0,1} = 0.2527$$

The controller polynomials $Q(z)$ and $P(z)$ are calculated from equations (2.12) and (2.13). The corresponding time-lifted representations are,

$$\bar{P}(z^2) = \begin{bmatrix} -0.0001 & 0 \\ z^2 & 0.5053 \end{bmatrix}$$

$$\text{and } \bar{Q}(z^2) = \begin{bmatrix} 0 & 8.4822 \\ 0 & 0 \end{bmatrix}$$

So, the controller transfer matrix is

$$\bar{C}(z^2) = \frac{1}{0.00005053} \begin{bmatrix} 8.4822z^2 & 0.00084822 \\ 0 & 0 \end{bmatrix}$$

Condition II: $\mathbf{Q}_0^+ = -\mathbf{Q}_1^-$

For this condition, controller parameters are found to be

$$d_{0,0} = d_{0,1} = 0$$

$$d_{1,0} = d_{1,1} = 4.2411$$

$$c_{0,0} = c_{0,1} = 0.2527$$

The controller polynomials $Q(z)$ and $P(z)$ are calculated from equations (2.12) and (2.13). The corresponding time-lifted representations are,

$$\bar{P}(z^2) = \begin{bmatrix} 0.5053 & 0 \\ z^2 & -0.0001 \end{bmatrix}$$

$$\text{And } \bar{Q}(z^2) = \begin{bmatrix} 0 & 8.4822 \\ 0 & 0 \end{bmatrix}$$

So, the controller transfer matrix is

$$\bar{C}(z^2) = \frac{1}{0.00005053} \begin{bmatrix} 8.4822z^2 & -4.2861 \\ 0 & 0 \end{bmatrix}$$

Condition III: $\mathbf{Q}_0^+ = \mathbf{Q}_1^+$

For this condition, controller parameters are found to be

$$d_{0,0} = d_{0,1} = 0$$

$$d_{1,0} = d_{1,1} = 4.2411$$

$$c_{0,0} = c_{0,1} = 0.2527$$

The controller polynomials $Q(z)$ and $P(z)$ are calculated from equations (2.12) and (2.13). The corresponding time-lifted representations are,

$$\bar{P}(z^2) = \begin{bmatrix} 0.5053 & 0 \\ z^2 & -0.0001 \end{bmatrix}$$

$$\text{and } \bar{Q}(z^2) = \begin{bmatrix} 0 & 8.4822 \\ 0 & 0 \end{bmatrix}$$

So, the controller transfer matrix is

$$\bar{C}(z^2) = \frac{1}{0.00005053} \begin{bmatrix} 8.4822z^2 & -4.2861 \\ 0 & 0 \end{bmatrix}$$

Condition IV: $\mathbf{Q}_0^+ = -\mathbf{Q}_1^+$

For this condition, controller parameters are found to be

$$d_{0,0} = d_{0,1} = 0$$

$$d_{1,0} = -d_{1,1} = 4.2411$$

$$c_{0,0} = -c_{0,1} = 0.2527$$

The controller polynomials $Q(z)$ and $P(z)$ are calculated from equations (2.12) and (2.13). The corresponding time-lifted representations are,

$$\bar{P}(z^2) = \begin{bmatrix} -0.0001 & 0 \\ z^2 & 0.5053 \end{bmatrix}$$

And $\bar{Q}(z^2) = \begin{bmatrix} 0 & 8.4822 \\ 0 & 0 \end{bmatrix}$

So, the controller transfer matrix is

$$\bar{C}(z^2) = \frac{1}{0.00005053} \begin{bmatrix} 8.4822z^2 & 0.00084822 \\ 0 & 0 \end{bmatrix}$$

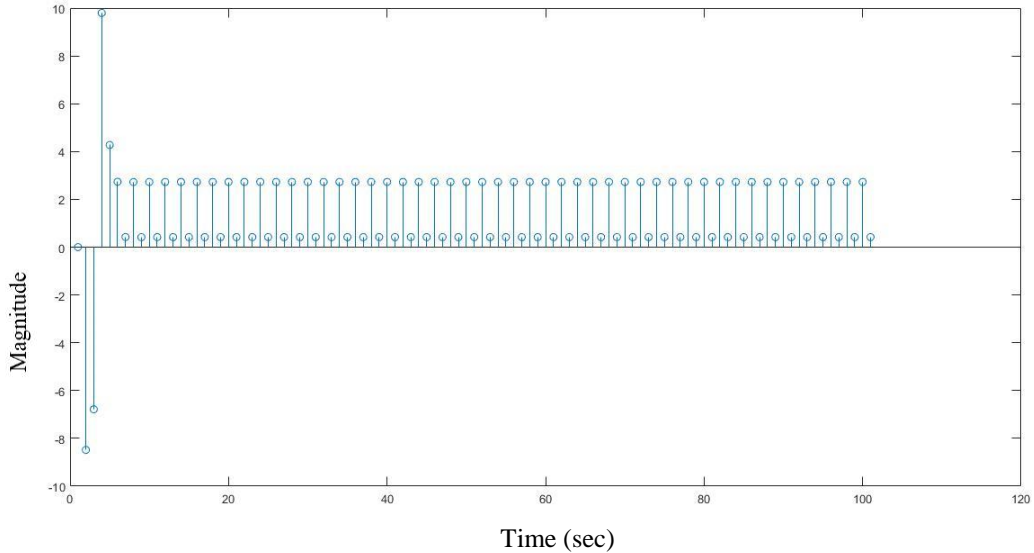


Fig. 2.3: Dead beat response of the plant with 1-DOF 2-periodic controller for conditions $Q_0^+ = Q_1^-$ and $Q_0^- = -Q_1^+$

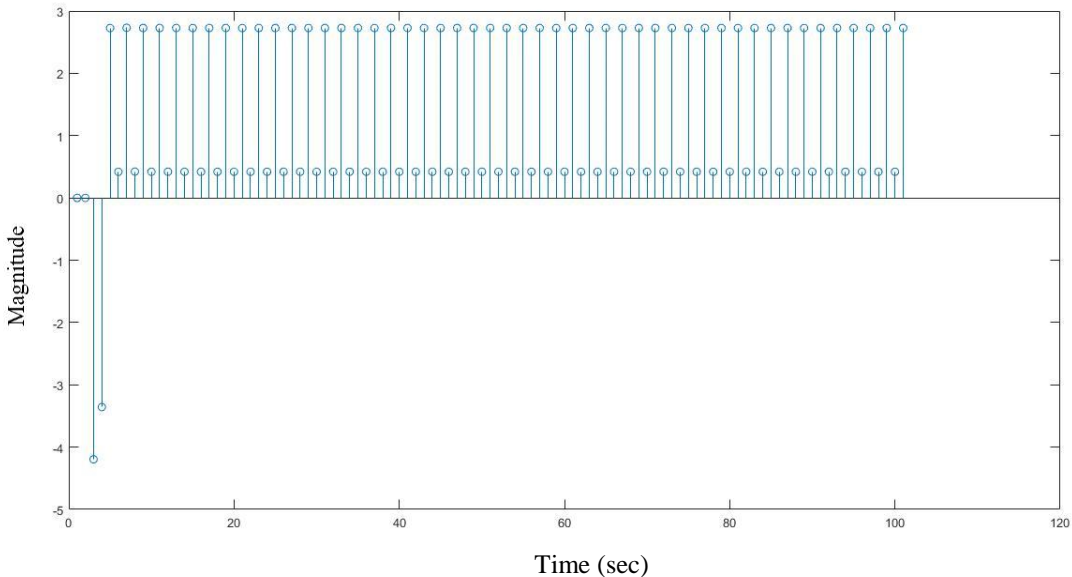


Fig. 2.4: Dead beat response of the plant with 1-DOF 2-periodic controller for conditions $Q_0^+ = -Q_1^-$ and $Q_0^- = Q_1^+$

2.4. Ripple-Free Response

In Example 2.3.1, the 2-periodic controller design for a second order plant is shown and loop-zero placement capability of that controller is also demonstrated. It is observed that a 2-periodic oscillation is present in the steady-state response, which makes the controller inconvenient. In this section, techniques of removing aforesaid 2-periodic ripple are discussed.

Theorem 1: The steady-state step-response of a 2-periodically compensated system would be ripple-free if the loop contains any of the following time-invariant component [31],

- i. Pole at -1
- ii. Zero at 1
- iii. Pole at -1 and zero at 1 both

Proof: The lifted transform domain relation between the reference input and error as

$$\begin{bmatrix} E_e(z^2) \\ E_o(z^2) \end{bmatrix} = [I + K\bar{G}\bar{C}]^{-1} \begin{bmatrix} R_e(z^2) \\ R_o(z^2) \end{bmatrix}$$

Considering a step input for which $\begin{bmatrix} R_e(z^2) \\ R_o(z^2) \end{bmatrix} = \begin{bmatrix} 1 \\ 1 \end{bmatrix} \frac{z^2}{(z^2-1)}$

$$\begin{bmatrix} E_e(z^2) \\ E_o(z^2) \end{bmatrix} = \frac{1}{\Delta} \begin{bmatrix} \Delta_c d - z^{-1}(n_1 - n_2)C_{12} + (n_1 - z^{-2}n_2)C_{22} \\ \Delta_c d - (n_1 - n_2)C_{12} + z(n_1 - z^{-2}n_2)C_{22} \end{bmatrix} \frac{z^2}{(z^2-1)} \quad (2.46)$$

where $d = a^+ a^-$

$$\Delta = \Delta_c d + (C_{11} + C_{22})n_1 + z^{-1}(C_{21} + C_{12})n_2 + b^+ b^-$$

$$n_1 = (b^+ a^- + b^- a^+)$$

$$n_2 = z(b^+ a^- - b^- a^+)$$

$$\text{So, } n_1 - n_2 = (1 - z) b^+ a^- + (1 + z) b^- a^+$$

$$n_1 - z^{-2}n_2 = z^{-1}[(z - 1) b^+ a^- + (1 + z) b^- a^+]$$

The steady state errors are calculated using the final value theorem and given by,

$$\begin{bmatrix} E_{e,ss} \\ E_{o,ss} \end{bmatrix} = \lim_{z^2 \rightarrow 1} \frac{z^2}{\Delta} \begin{bmatrix} \Delta_c d - z^{-1}(n_1 - n_2)C_{12} + (n_1 - z^{-2}n_2)C_{22} \\ \Delta_c d - (n_1 - n_2)C_{12} + z(n_1 - z^{-2}n_2)C_{22} \end{bmatrix} \quad (2.47)$$

It is clear from the above equation (2.47) that steady state ripples are introduced in even instants by the term $\{-z^{-1}(n_1 - n_2)C_{12} + (n_1 - z^{-2}n_2)C_{22}\}$ and $\{-(n_1 - n_2)C_{12} + z(n_1 - z^{-2}n_2)C_{22}\}$ in odd instants. So, to make the response ripple free, we need to make $(n_1 - n_2)$ and $(n_1 - z^{-2}n_2)$ equal to zero. This can be achieved if a $(z^2 - 1)$ term is present in $(n_1 - n_2)$ and $(n_1 - z^{-2}n_2)$, which will become zero due to the limit $(z^2 \rightarrow 1)$.

So, if the plant contains either a pole at 1 or a zero at -1 or both i.e. a denominator factor $(z - 1)$ or a numerator factor $(z + 1)$ or both, then the steady state response will not contain any ripple. If the plant does not contain any of those terms then it should be augmented by any of such factors before designing the periodic controller. The effects of the presence of the factors $\frac{z}{(z-1)}$, $\frac{(z+1)}{z}$ and $\frac{(z+1)}{(z-1)}$ in plant model is discussed next.

- i. **Pole at 1:** If the plant denominator contains a factor $(z - 1)$ then the plant transfer function can be expressed as

$$G(z) = K \frac{b(z)}{a(z)} = K \frac{b(z)}{\check{a}(z)(z-1)} = K \frac{b(z)(-1)^n \check{a}(-z)(z+1)}{\check{a}(z)(-1)^n \check{a}(-z)(z^2-1)} = \frac{\check{n}(z)(z+1)}{\check{d}(z)(z^2-1)} \quad (2.48)$$

with, $b(z)(-1)^n \check{a}(-z) = \check{n}(z)$ and $\check{a}(z)(-1)^n \check{a}(-z) = \check{d}(z)$

Now, the lifted transfer function becomes

$$G(z^2) = \frac{[\check{n}_1(z^2) + z^{-1}\check{n}_2(z^2)](z+1)}{\check{d}(z)(z^2-1)} = \frac{[\check{n}_1(z^2) + \check{n}_2(z^2)] + z^{-1}[z^2\check{n}_1(z^2) + \check{n}_2(z^2)]}{\check{d}(z)(z^2-1)} = \frac{[n_1(z^2) + z^{-1}n_2(z^2)]}{\check{d}(z)(z^2-1)} \quad (2.49)$$

with, $[\check{n}_1(z^2) + \check{n}_2(z^2)] = n_1(z^2)$ and $[z^2\check{n}_1(z^2) + \check{n}_2(z^2)] = n_2(z^2)$ (2.50)

Now, from (2.50) we get,

$$\begin{aligned} n_1 - n_2 &= -(z^2 - 1)\check{n}_1(z^2) \\ n_1 - z^{-2}n_2 &= z^{-2}(z^2 - 1)\check{n}_1(z^2) \end{aligned} \quad (2.51)$$

From (2.47) and (2.51) we get,

$$\begin{aligned} \begin{bmatrix} E_{e,ss} \\ E_{o,ss} \end{bmatrix} &= \lim_{z^2 \rightarrow 1} \frac{z^2}{\Delta} \begin{bmatrix} \Delta_c d + z^{-1}(z^2 - 1)\check{n}_1(z^2)C_{12} + z^{-2}(z^2 - 1)\check{n}_1(z^2)C_{22} \\ \Delta_c d + (z^2 - 1)\check{n}_1(z^2)C_{12} + z^{-1}(z^2 - 1)\check{n}_1(z^2)C_{22} \end{bmatrix} \\ &= \lim_{z^2 \rightarrow 1} \frac{z^2}{\Delta} \begin{bmatrix} \Delta_c d \\ \Delta_c d \end{bmatrix} \end{aligned} \quad (2.52)$$

It can be concluded from (2.52) that the presence of a pole at 1 in plant transfer function make the response ripple free.

- ii. **Zero at -1:** If the plant numerator contains a factor $(z + 1)$ then the plant transfer function can be expressed as

$$G(z) = K \frac{b(z)}{a(z)} = K \frac{\check{b}(z)(z+1)}{a(z)} = K \frac{\check{b}(z)(-1)^n a(-z)(z+1)}{a(z)(-1)^n a(-z)} = \frac{\check{n}(z)(z+1)}{\check{d}(z)} \quad (2.53)$$

with, $\check{b}(z)(-1)^n a(-z) = \check{n}(z)$ and $a(z)(-1)^n a(-z) = \check{d}(z)$

Now, the lifted transfer function becomes

$$G(z^2) = \frac{[\check{n}_1(z^2) + z^{-1}\check{n}_2(z^2)](z+1)}{\check{d}(z)(z^2-1)} = \frac{[\check{n}_1(z^2) + \check{n}_2(z^2)] + z^{-1}[z^2\check{n}_1(z^2) + \check{n}_2(z^2)]}{\check{d}(z)} = \frac{[n_1(z^2) + z^{-1}n_2(z^2)]}{\check{d}(z)} \quad (2.54)$$

with, $[\check{n}_1(z^2) + \check{n}_2(z^2)] = n_1(z^2)$ and $[z^2\check{n}_1(z^2) + \check{n}_2(z^2)] = n_2(z^2)$ (2.55)

Now, from (2.55) we get,

$$\begin{aligned} n_1 - n_2 &= -(z^2 - 1)\check{n}_1(z^2) \\ n_1 - z^{-2}n_2 &= z^{-2}(z^2 - 1)\check{n}_1(z^2) \end{aligned} \quad (2.56)$$

From (2.47) and (2.56) we get,

$$\begin{aligned} \begin{bmatrix} E_{e,ss} \\ E_{o,ss} \end{bmatrix} &= \lim_{z^2 \rightarrow 1} \frac{z^2}{\Delta} \begin{bmatrix} \Delta_c d + z^{-1}(z^2 - 1)\check{n}_1(z^2)C_{12} + z^{-2}(z^2 - 1)\check{n}_1(z^2)C_{22} \\ \Delta_c d + (z^2 - 1)\check{n}_1(z^2)C_{12} + z^{-1}(z^2 - 1)\check{n}_1(z^2)C_{22} \end{bmatrix} \\ &= \lim_{z^2 \rightarrow 1} \frac{z^2}{\Delta} \begin{bmatrix} \Delta_c d \\ \Delta_c d \end{bmatrix} \end{aligned} \quad (2.57)$$

It can be concluded from (2.57) that the presence of a zero at -1 in plant transfer function make the response ripple free.

- iii. **A Pole at 1 and a zero at -1:** As we already know, from (2.52) and (2.57), that the presence of a pole at 1 or a zero at -1 in plants transfer function makes the response ripple free. So, presence of both will also eliminate ripple in steady state response. It is proved in the following section.

The plant transfer function can be expressed as

$$G(z) = K \frac{b(z)}{a(z)} = K \frac{\check{b}(z)(z+1)}{\check{a}(z)(z-1)} = K \frac{\check{b}(z)(-1)^n \check{a}(-z)(z+1)}{\check{a}(z)(-1)^n \check{a}(-z)(z-1)} = \frac{\check{n}(z)(z+1)}{\check{d}(z)(z-1)} \quad (2.58)$$

with, $\check{b}(z)(-1)^n \check{a}(-z) = \check{n}(z)$

$$\check{a}(z)(-1)^n \check{a}(-z) = \check{d}(z)$$

Now, the lifted transfer function becomes

$$G(z^2) = \frac{[\check{n}_1(z^2) + z^{-1} \check{n}_2(z^2)](z+1)}{\check{d}(z)(z-1)} = \frac{[\check{n}_1(z^2) + \check{n}_2(z^2)] + z^{-1}[z^2 \check{n}_1(z^2) + \check{n}_2(z^2)]}{\check{d}(z)(z-1)} = \frac{[n_1(z^2) + z^{-1} n_2(z^2)]}{\check{d}(z)(z-1)} \quad (2.59)$$

with, $[\check{n}_1(z^2) + \check{n}_2(z^2)] = n_1(z^2)$ and $[z^2 \check{n}_1(z^2) + \check{n}_2(z^2)] = n_2(z^2)$ (2.60)

Now, from (2.60) we get,

$$\begin{aligned} n_1 - n_2 &= -(z^2 - 1) \check{n}_1(z^2) \\ n_1 - z^{-2} n_2 &= z^{-2}(z^2 - 1) \check{n}_1(z^2) \end{aligned} \quad (2.61)$$

From (2.47) and (2.61) we get,

$$\begin{aligned} \begin{bmatrix} E_{e,ss} \\ E_{o,ss} \end{bmatrix} &= \lim_{z^2 \rightarrow 1} \frac{z^2}{\Delta} \begin{bmatrix} \Delta_c d + z^{-1}(z^2 - 1) \check{n}_1(z^2) C_{12} + z^{-2}(z^2 - 1) \check{n}_1(z^2) C_{22} \\ \Delta_c d + (z^2 - 1) \check{n}_1(z^2) C_{12} + z^{-1}(z^2 - 1) \check{n}_1(z^2) C_{22} \end{bmatrix} \\ &= \lim_{z^2 \rightarrow 1} \frac{z^2}{\Delta} \begin{bmatrix} \Delta_c d \\ \Delta_c d \end{bmatrix} \end{aligned} \quad (2.62)$$

From the above equation (2.62) we can see that the response has become ripple free.

2.4.1 Numerical example

Example 2.4.1: Considering the plant of Example 2.3.1, it will now be compensated to obtain a ripple-free steady-state step response besides robustness.

I. With Augmentation $\frac{z}{(z-1)}$

The augmented transfer function is

$$G(z) = \frac{z(z-1.2)}{(z-0.5)(z-1)(z-1.5)}$$

From (2.37) and (2.38) the order of the 2-periodic controller is $m = 2$ and number of controller zeros is 4

$$\hat{A}(z^2) = -(z^2 - 1)(z^2 - 2.25)(z^2 - 0.25)$$

$$\hat{P}(z^2) = z^4$$

$$\hat{Z}(z^2) = k_z z^4(z^2 - 0.25)(z^2 - \beta)$$

$$\check{D}(z^2) = -z^4(z^2 - 0.25)$$

It can be noted from above that 2 pole-zero cancellations are performed at origin of z^2 -plane. These cancellations can be done at any arbitrary locations. Further, note that β is the location of the loop-zero which along with loop-gain k_z are the parameters that can be varied to obtain any desired closed loop pole as shown in the root locus of Fig. 2.5. It is important to point out that such freedom of choice of loop-zeros is not available with LTI controllers.

If the pole-zero cancellations are performed on $z^2 = 0.1$ then equations of pole, zero and desired pole polynomial of the controller will become

$$\hat{P}(z^2) = (z^2 - 0.1)^2$$

$$\hat{Z}(z^2) = k_z (z^2 - 0.1)^2(z^2 - 0.25)(z^2 - \beta)$$

$$\check{D}(z^2) = -(z^2 - 0.1)^2(z^2 - 0.25)$$

The effect of variation in the location of pole-zero cancellation on the system overall performance is discussed next.

The loop transfer function of overall system is

$$G_{loop1}(z) = \frac{(z^2 - \beta)}{(z^2 - 1)(z^2 - 2.25)} \quad (2.63)$$

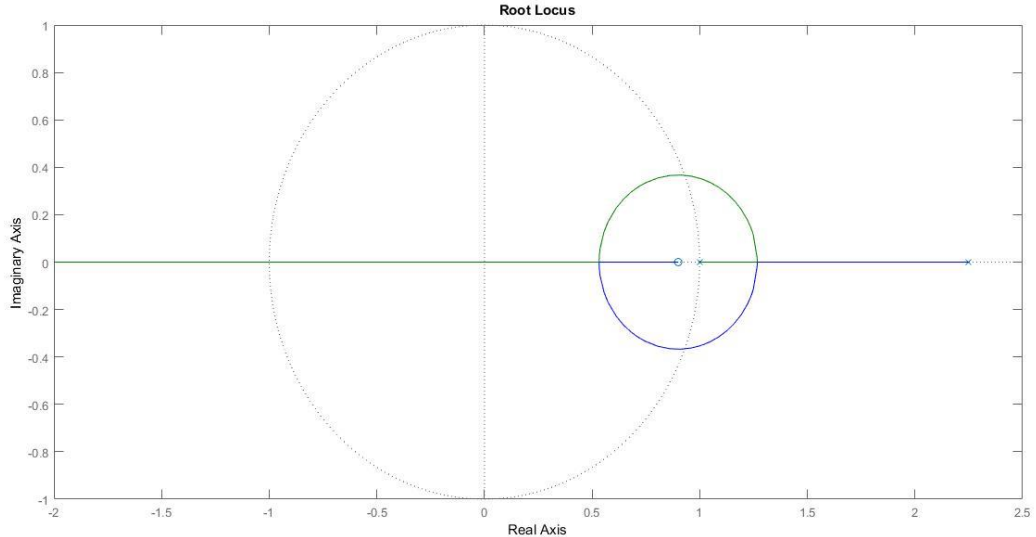


Fig. 2.5: Root locus of the system of (2.63) with $\beta = 0.9$

Gain margin of overall system is calculated for different values of β . It is seen that as β comes closer to $z^2 = 1$, the gain margin increases (shown in Fig 2.5).

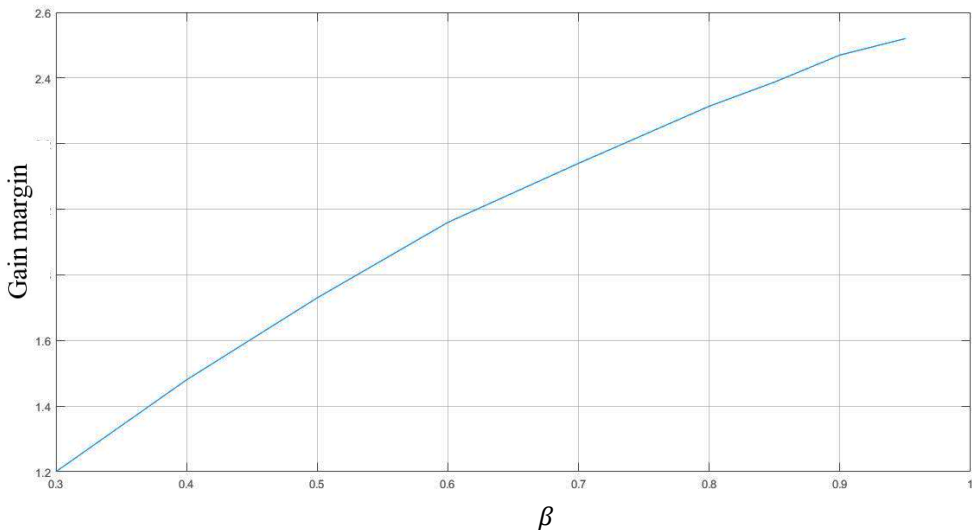


Fig. 2.6: Plot of gain margin with location of β

Now, response of the overall system i.e. $G_{loop1}(z)$ is recorded for different values of β with conditions $Q_0^+ = \pm Q_1^\pm$. Settling time and maximum peak overshoot are noted for all the conditions and a comparative study is carried out on the performance of controller for different values of β . Plots showing these comparisons for aforesaid pole-zero cancellations at $z^2 = 0, 0.1, 0.2$ are given next.

Table 2.1: Variation of settling time and maximum peak undershoot with β for condition $Q_0^+ = Q_1^-$ and $Q_0^+ = -Q_1^-$ with pole-zero cancellation at $z^2 = 0.5$

| β | Condition | Settling time (t_s) | Maximum peak undershoot ($\times 100\%$) |
|---------|------------------|-------------------------|--|
| 0.7 | $Q_0^+ = Q_1^-$ | 8 | 11.5 |
| | $Q_0^+ = -Q_1^-$ | 9 | 12 |
| 0.8 | $Q_0^+ = Q_1^-$ | 14 | 8 |
| | $Q_0^+ = -Q_1^-$ | 15 | 8.9 |
| 0.85 | $Q_0^+ = Q_1^-$ | 18 | 7 |
| | $Q_0^+ = -Q_1^-$ | 19 | 7.5 |
| 0.9 | $Q_0^+ = Q_1^-$ | 28 | 5.5 |
| | $Q_0^+ = -Q_1^-$ | 27 | 6 |
| 0.95 | $Q_0^+ = Q_1^-$ | 52 | 4 |
| | $Q_0^+ = -Q_1^-$ | 53 | 4.05 |

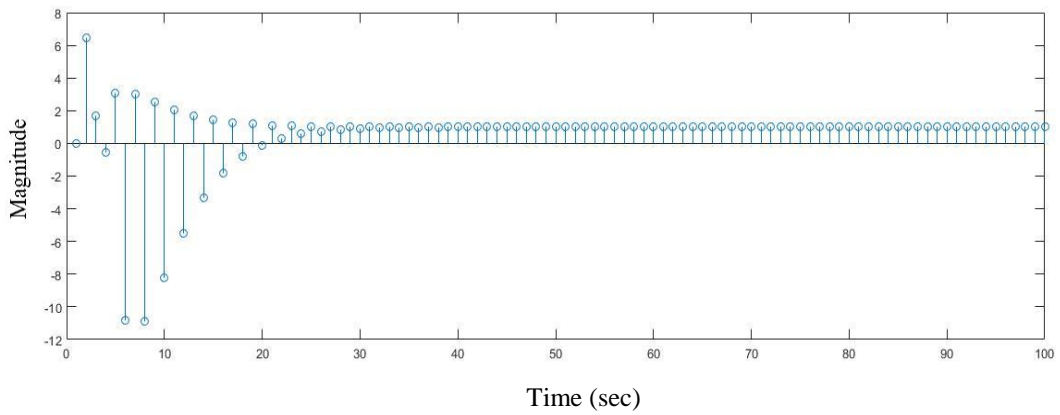


Fig. 2.7: Response using augmentation $\frac{z}{(z-1)}$ with β for conditions $Q_0^+ = Q_1^-$ and $Q_0^+ = Q_1^+$ with pole-zero cancellation at $z^2 = 0$

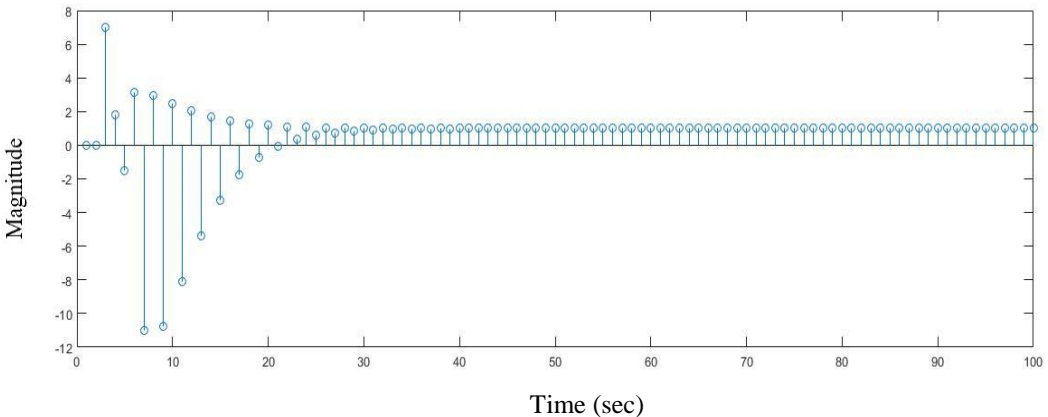


Fig. 2.8: Response using augmentation $\frac{z}{(z-1)}$ with β for conditions $Q_0^+ = -Q_1^+$ and $Q_0^+ = -Q_1^-$ with pole-zero cancellation at $z^2 = 0$

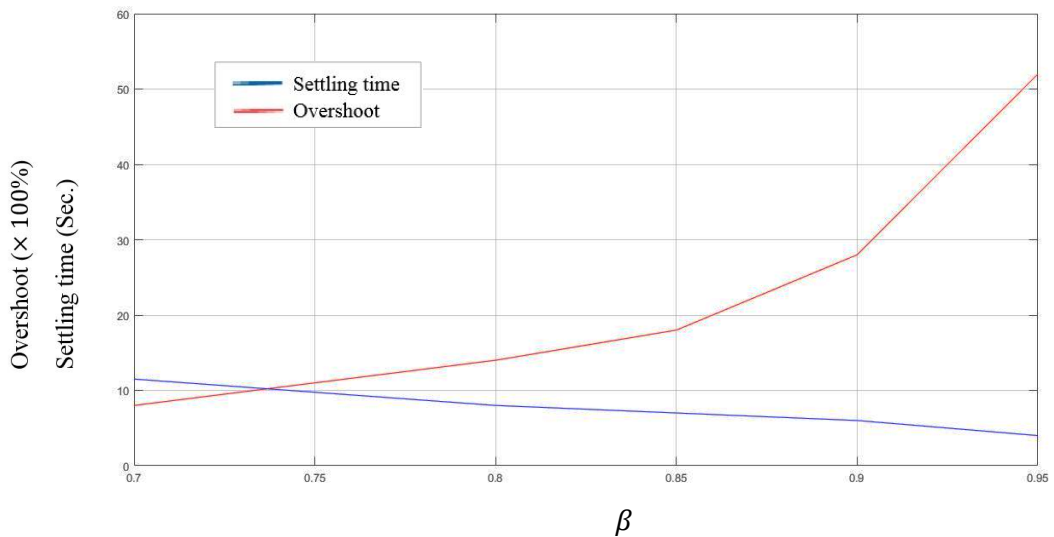


Fig. 2.9: Variation of settling time and maximum peak overshoot with β for condition $Q_0^+ = Q_1^-$ and $Q_0^+ = Q_1^+$ (with pole-zero cancellation at $z^2 = 0$)

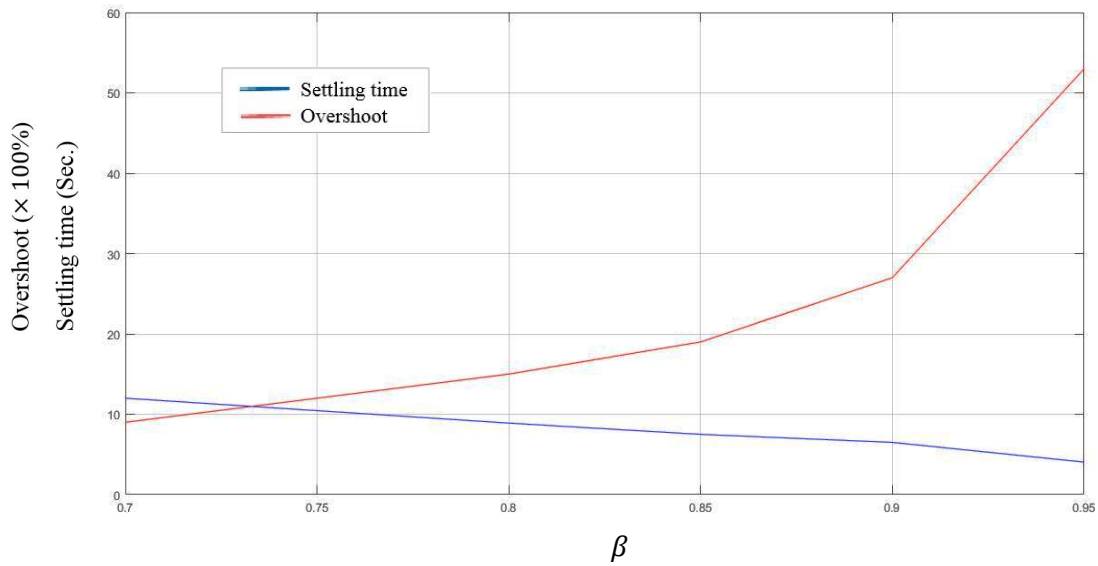


Fig. 2.10: Variation of settling time and maximum peak overshoot with β for condition $Q_0^+ = -Q_1^-$ and $Q_0^+ = -Q_1^+$ (with pole-zero cancellation at $z^2 = 0$)

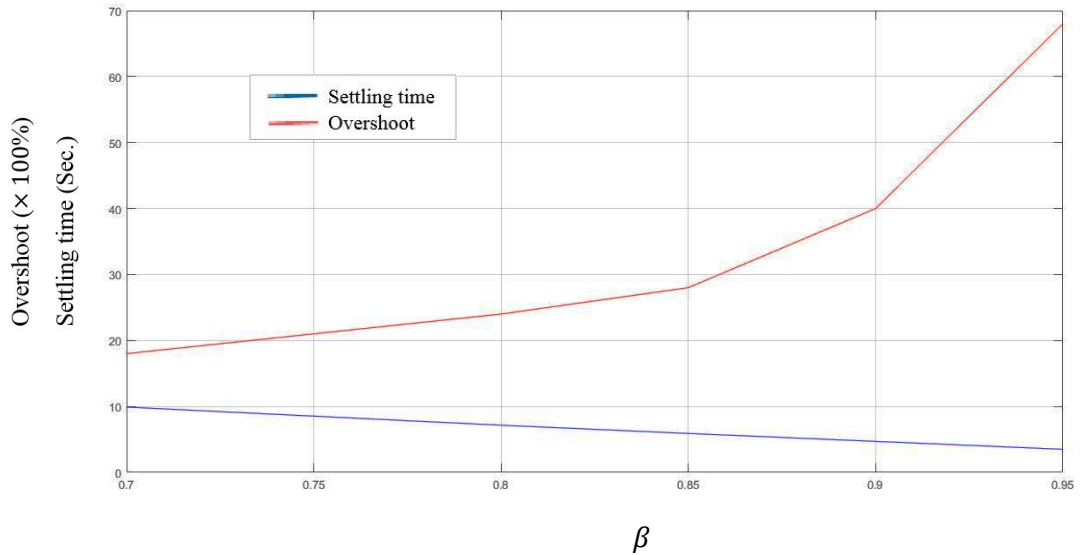


Fig. 2.11: Variation of settling time and maximum peak overshoot with β for condition $Q_0^+ = Q_1^-$ and $Q_0^+ = Q_1^+$ (with pole-zero cancellation at $z^2 = 0.1$)

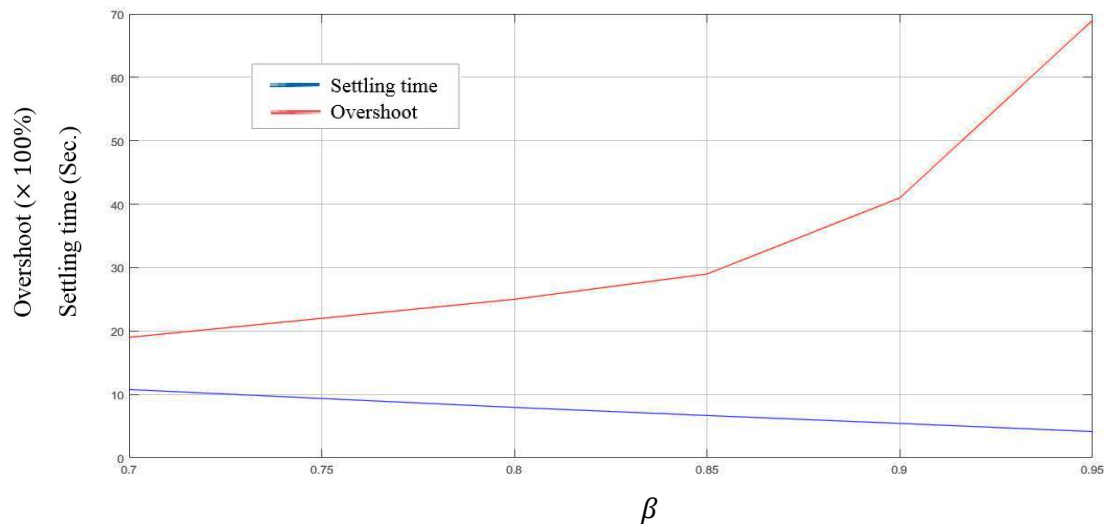


Fig. 2.12: Variation of settling time and maximum peak overshoot with β for condition $Q_0^+ = -Q_1^-$ and $Q_0^+ = -Q_1^+$ (with pole-zero cancellation at $z^2 = 0.1$)

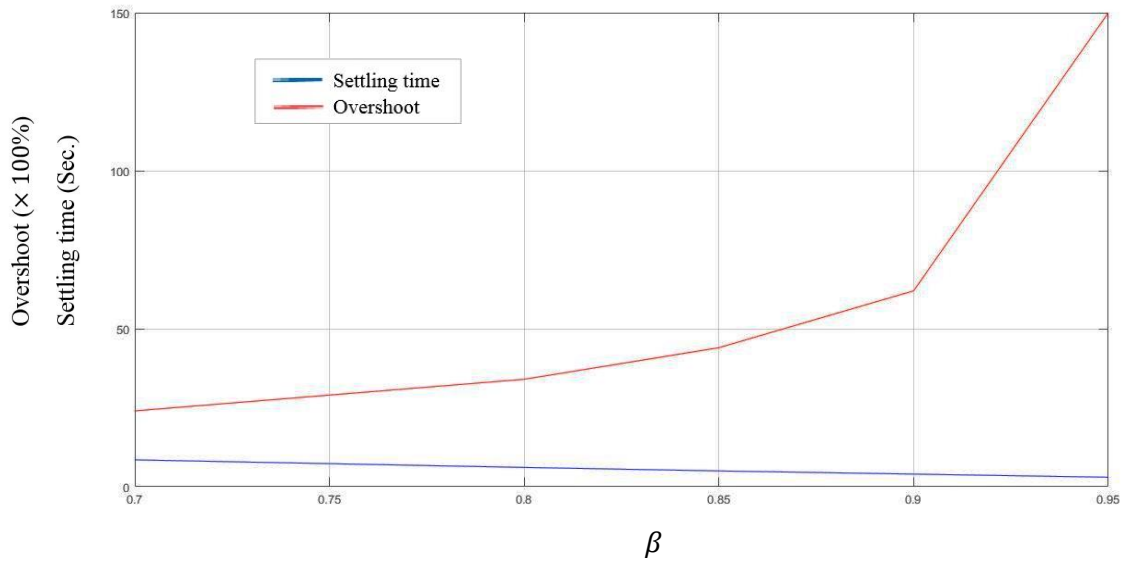


Fig. 2.13: Variation of settling time and maximum peak overshoot with β for condition $Q_0^+ = Q_1^-$ and $Q_0^+ = Q_1^+$ (with pole-zero cancellation at $z^2 = 0.2$)

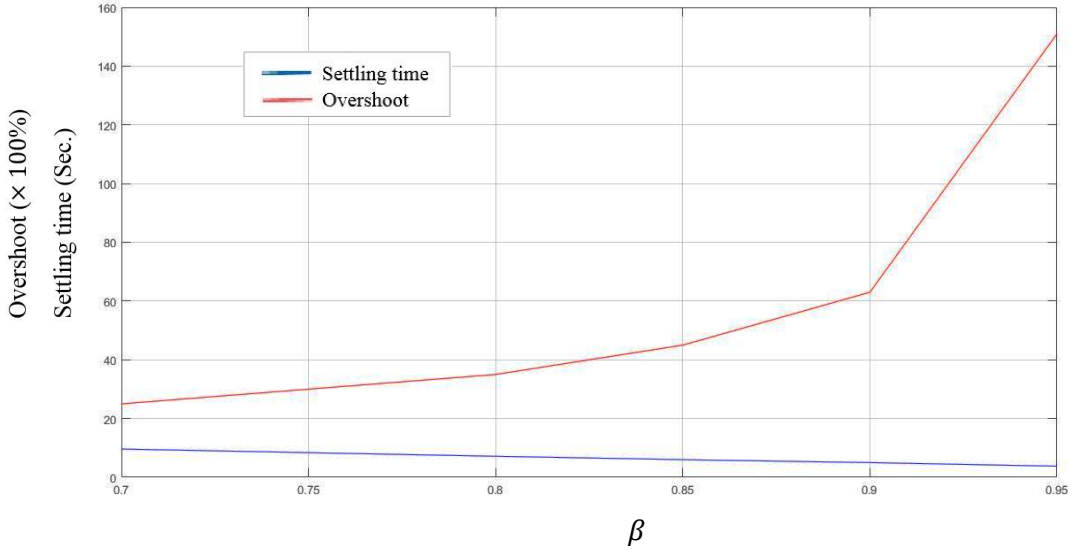


Fig. 2.14: Variation of settling time and maximum peak overshoot with β for condition $Q_0^+ = -Q_1^-$ and $Q_0^+ = -Q_1^+$ (with pole-zero cancellation at $z^2 = 0.2$)

II. With Augmentation $\frac{(z+1)}{z}$

The augmented transfer function is $G(z) = \frac{(z+1)(z-1.2)}{z(z-0.5)(z-1.5)}$

From (2.35) and (2.36) the order of the 2-periodic controller is $m = 2$ and number of controller zeros is 4

$$\hat{A}(z^2) = -z^2(z^2 - 2.25)(z^2 - 0.25)$$

$$\hat{P}(z^2) = z^2(z^2 - \alpha)$$

$$\hat{Z}(z^2) = k_z z^6(z^2 - 0.25)$$

$$\check{D}(z^2) = -z^4(z^2 - 0.25)$$

Further, note that α is the location of the controller pole which along with loop-gain k_z are the parameters that can be varied to obtain any desired closed loop pole as shown in the root locus of Fig. 2.15.

The effect of variation in the location of pole-zero cancellation on the system overall performance is discussed next.

The transfer function of overall system is

$$G_{loop2}(z) = \frac{z^2}{(z^2 - \alpha)(z^2 - 2.25)} \quad (2.64)$$

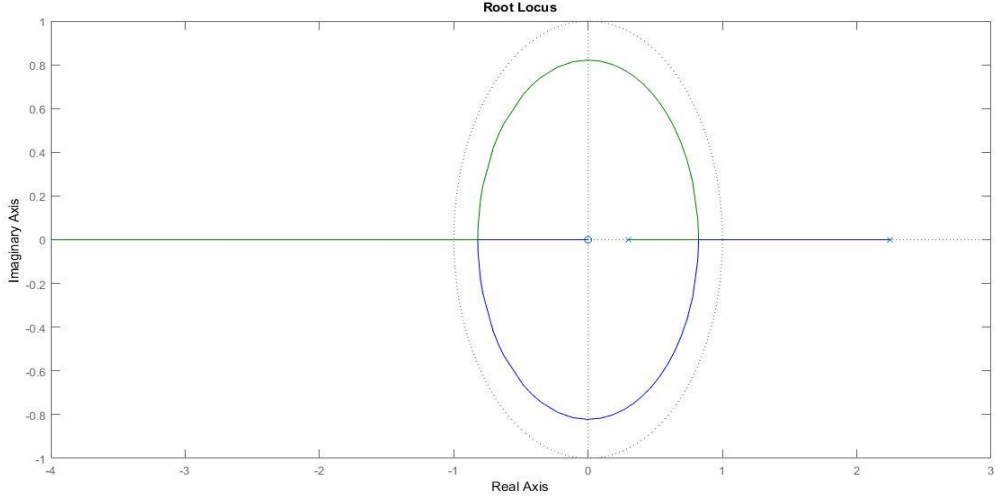


Fig. 2.15: Root locus of the system of (2.64) with $\alpha = 0.3$

Gain margin of overall system is calculated for different values of α . It is seen that as α comes closer to $z^2 = 0$, the gain margin decreases. The maximum gain margin is attained at $z^2 = 0.44$ (shown in Fig 2.13).

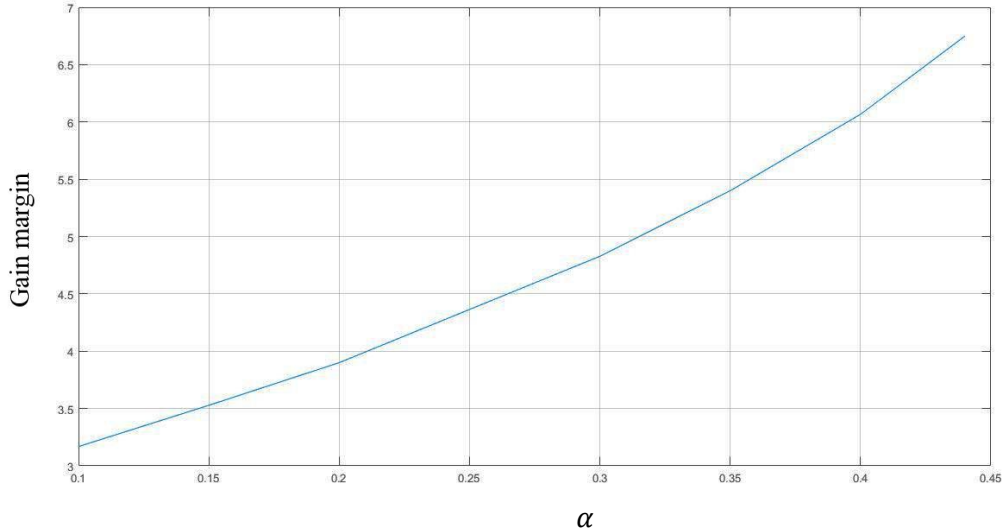


Fig. 2.16: Plot of gain margin with location of α

Now, response of the overall system i.e. $G_{loop2}(z)$ is recorded for different values of α with conditions $Q_0^+ = \pm Q_1^\pm$. It is observed that response curves are overdamped. So, there is no peak overshoot present. Settling times are noted for all the conditions and a comparative study is performed on the performance of controller for different values of α . Results showing these comparisons for aforesaid pole-zero cancellations at $z^2 = 0, 0.5, 0.75$ are given below. It is

obvious that as one moves α away from origin the closed loop poles also moves away from origin resulting in slower response with smaller overshoot.

Table 2.2: Variation of settling time and maximum peak undershoot with α for condition $Q_0^+ = Q_1^-$ and $Q_0^+ = -Q_1^-$ with pole-zero cancellation at $z^2 = 0.5$

| α | Condition | Settling time (t_s) | Maximum peak undershoot ($\times 100\%$) |
|----------|------------------|-------------------------|--|
| 0.1 | $Q_0^+ = Q_1^-$ | 28 | 2.808 |
| | $Q_0^+ = -Q_1^-$ | 29 | 2.8104 |
| 0.15 | $Q_0^+ = Q_1^-$ | 38 | 1.6425 |
| | $Q_0^+ = -Q_1^-$ | 39 | 1.642 |
| 0.2 | $Q_0^+ = Q_1^-$ | 44 | 1.36 |
| | $Q_0^+ = -Q_1^-$ | 45 | 1.361 |
| 0.3 | $Q_0^+ = Q_1^-$ | 72 | 0.589 |
| | $Q_0^+ = -Q_1^-$ | 73 | 0.58903 |
| 0.4 | $Q_0^+ = Q_1^-$ | 180 | 0.1072 |
| | $Q_0^+ = -Q_1^-$ | 185 | 0.1065 |

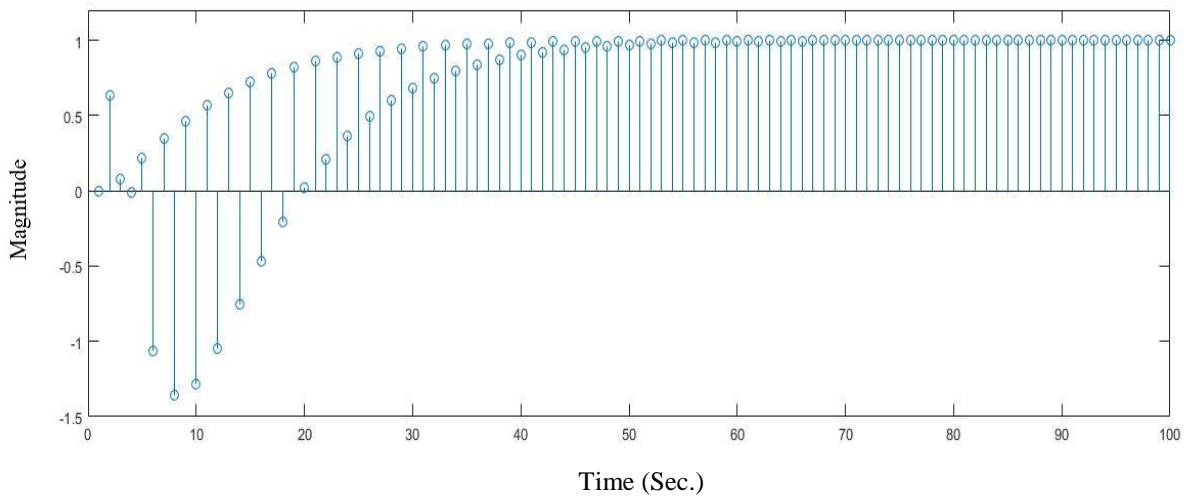


Fig. 2.17: Response using augmentation $\frac{(z-1)}{z}$ with $\alpha = 0.2$ for conditions $Q_0^+ = Q_1^-$ and $Q_0^+ = Q_1^+$ with pole-zero cancellation at $z^2 = 0$

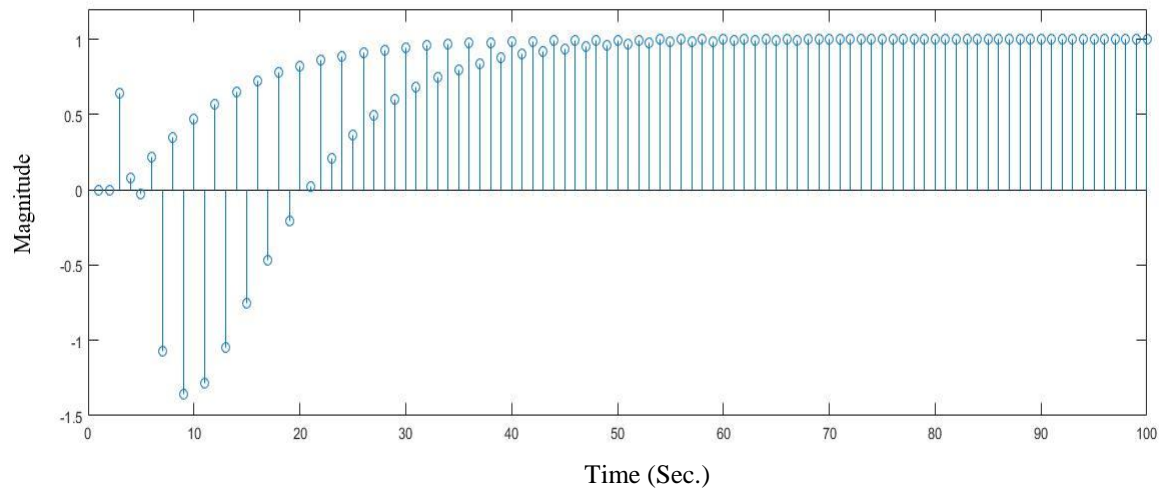


Fig. 2.18: Response using augmentation $\frac{(z-1)}{z}$ with $\alpha = 0.2$ for conditions $Q_0^+ = -Q_1^+$ and $Q_0^+ = -Q_1^-$ with pole-zero cancellation at $z^2 = 0$

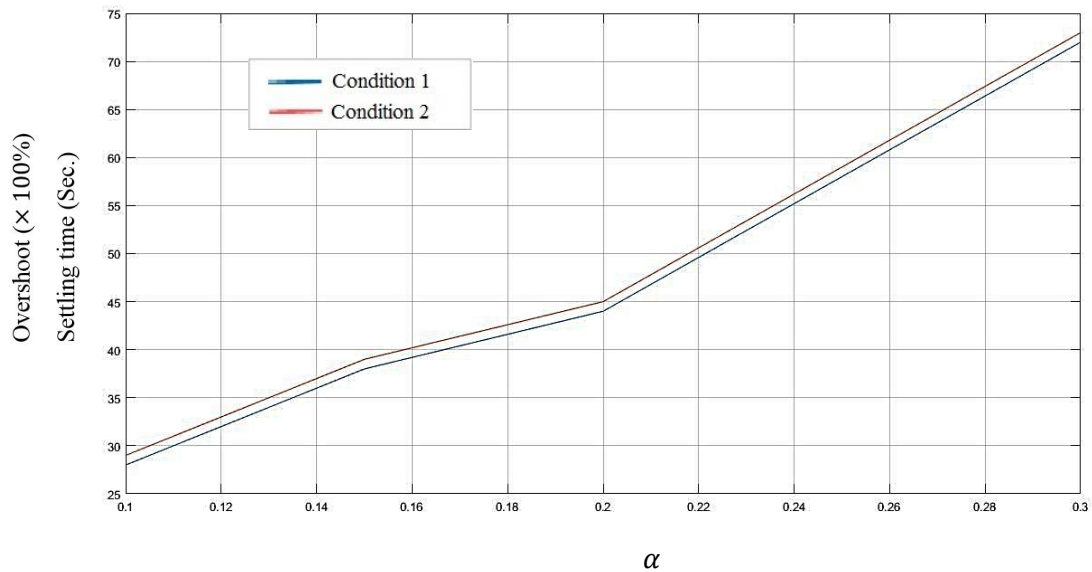


Fig. 2.19: Change in settling time with variation of α for conditions $Q_0^+ = Q_1^-$ and $Q_0^+ = -Q_1^-$ with pole-zero cancellation at $z^2 = 0$

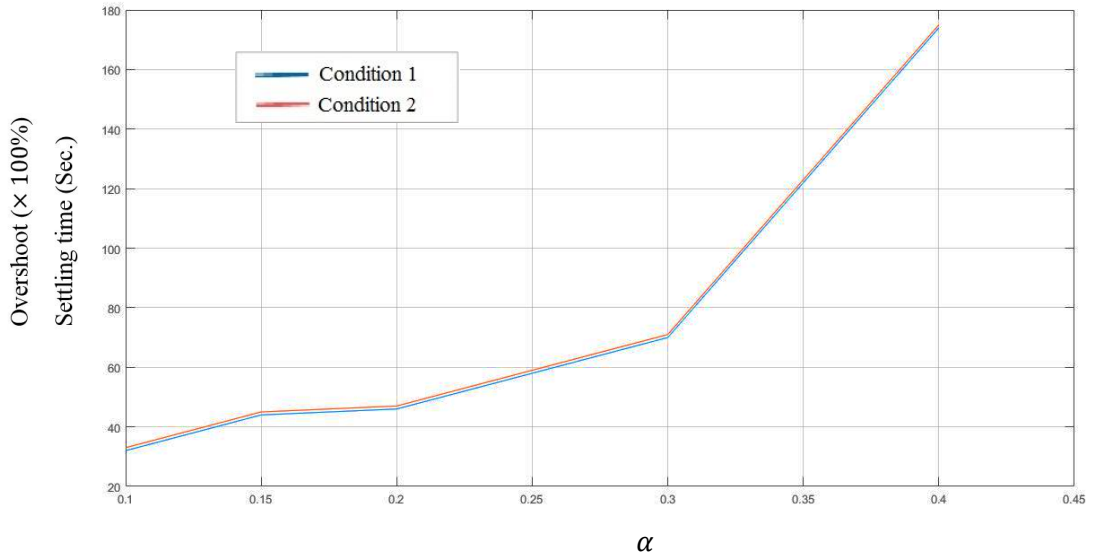


Fig. 2.20: Change in settling time with variation of α for conditions $Q_0^+ = Q_1^-$ and $Q_0^+ = -Q_1^-$ with pole-zero cancellation at $z^2 = 0.5$

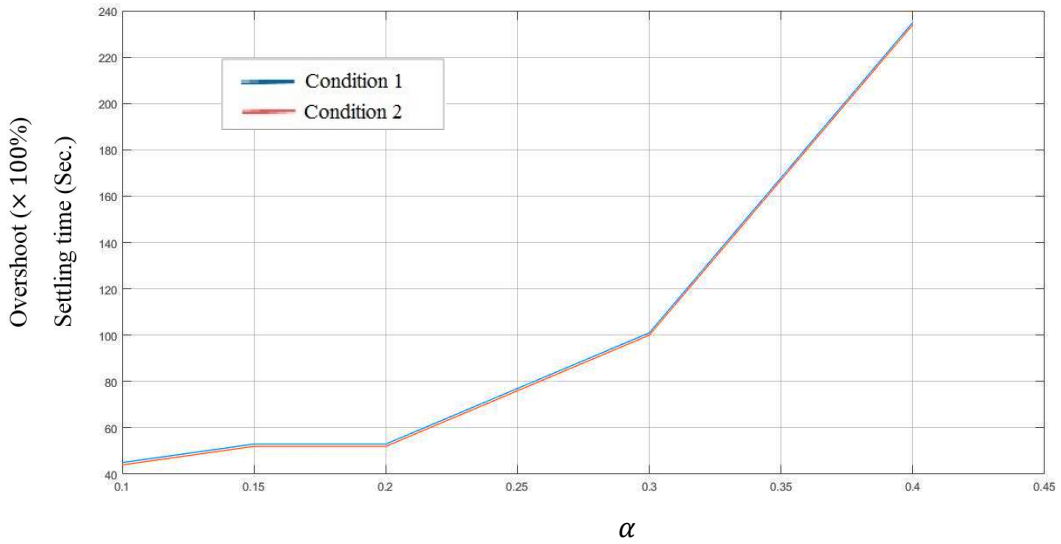


Fig. 2.21: Change in settling time with variation of α for conditions $Q_0^+ = Q_1^-$ and $Q_0^+ = -Q_1^-$ with pole-zero cancellation at $z^2 = 0.75$

III. With Augmentation $\frac{(z+1)}{(z-1)}$

The augmented transfer function is

$$G(z) = \frac{(z+1)(z-1.2)}{(z-0.5)(z-1)(z-1.5)}$$

From (2.35) and (2.36) the order of the 2-periodic controller is $m = 2$ and number of controller zeros is 4

$$\hat{A}(z^2) = -(z^2 - 1)(z^2 - 2.25)(z^2 - 0.25)$$

$$\hat{P}(z^2) = z^4$$

$$\hat{Z}(z^2) = k_z z^4(z^2 - 0.25)(z^2 - \beta)$$

$$\check{D}(z^2) = -z^4(z^2 - 0.25)$$

It can be noted from above equations that 1 pole-zero cancellation is performed at origin. These cancellations can be done at any other points too. Further, note that β is the location of the loop-zero which along with loop-gain k_z are the parameters that can be varied to obtain any desired closed loop pole.

If the pole-zero cancellations are performed on $z^2 = 0.5$ then equations of pole, zero and desired pole polynomial of the controller will become

$$\hat{P}(z^2) = (z^2 - 0.1)^2$$

$$\hat{Z}(z^2) = k_z (z^2 - 0.1)^2(z^2 - 0.25)(z^2 - \beta)$$

$$\check{D}(z^2) = -(z^2 - 0.1)^2(z^2 - 0.25)$$

Variations on the performance of the controller with the location of pole-zero cancellation is discussed later.

The loop transfer function of overall system is

$$G_{loop3}(z) = \frac{(z^2 - \beta)}{(z^2 - 1)(z^2 - 2.25)} \quad (2.65)$$

Root locus of the overall system and the curve depicting the change in gain margin with variation of β are same as shown in Fig 2.5 and Fig 2.6 respectively.

Now, response of the overall system i.e. $G_{loop1}(z)$ is recorded for different values of β with conditions $Q_0^+ = \pm Q_1^\pm$ (as shown for the augmentation I). Settling time and maximum peak overshoot are noted for all the conditions and a comparative study is performed on the performance of controller for different values of β . Plots showing these comparisons for aforesaid pole-zero cancellations at $z^2 = 0, 0.5, 0.75$ are shown next.

Table 2.3: Variation of settling time and maximum peak undershoot with β for condition $Q_0^+ = Q_1^-$ and $Q_0^+ = -Q_1^-$ with pole-zero cancellation at $z^2 = 0.5$

| β | Condition | Settling time (t_s) | Maximum peak overshoot ($\times 100\%$) |
|---------|------------------|-------------------------|---|
| 0.7 | $Q_0^+ = Q_1^-$ | 24 | 22.6 |
| | $Q_0^+ = -Q_1^-$ | 29 | 11 |
| 0.8 | $Q_0^+ = Q_1^-$ | 28 | 16.5 |
| | $Q_0^+ = -Q_1^-$ | 33 | 8 |
| 0.85 | $Q_0^+ = Q_1^-$ | 32 | 13.75 |
| | $Q_0^+ = -Q_1^-$ | 37 | 6.6296 |
| 0.9 | $Q_0^+ = Q_1^-$ | 40 | 11.1 |
| | $Q_0^+ = -Q_1^-$ | 45 | 5.3 |
| 0.95 | $Q_0^+ = Q_1^-$ | 60 | 8.5 |
| | $Q_0^+ = -Q_1^-$ | 63 | 4 |

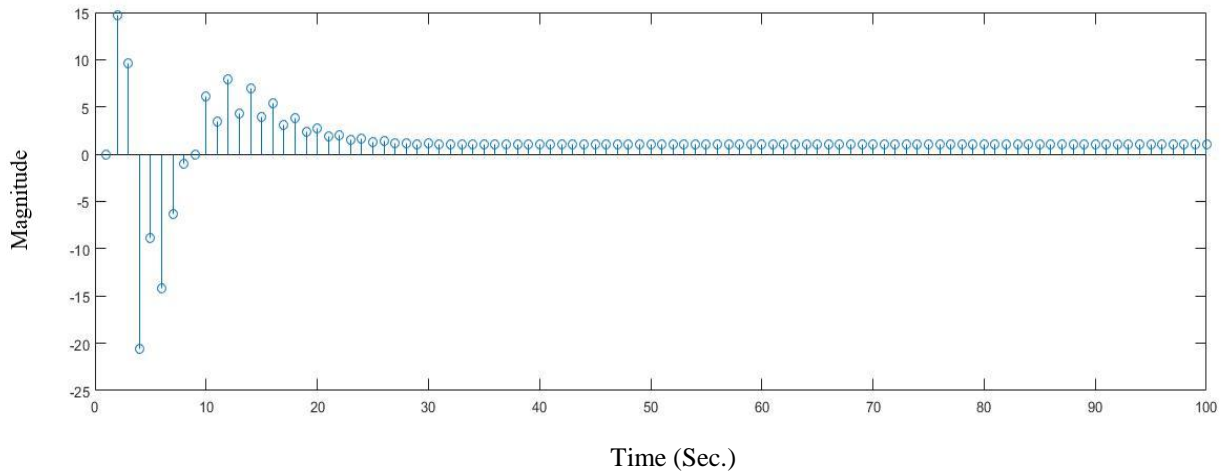


Fig. 2.22: Response using augmentation $\frac{(z+1)}{(z-1)}$ with $\beta = 0.85$ for conditions $Q_0^+ = Q_1^-$ and $Q_0^+ = Q_1^+$ with pole-zero cancellation at $z^2 = 0.5$

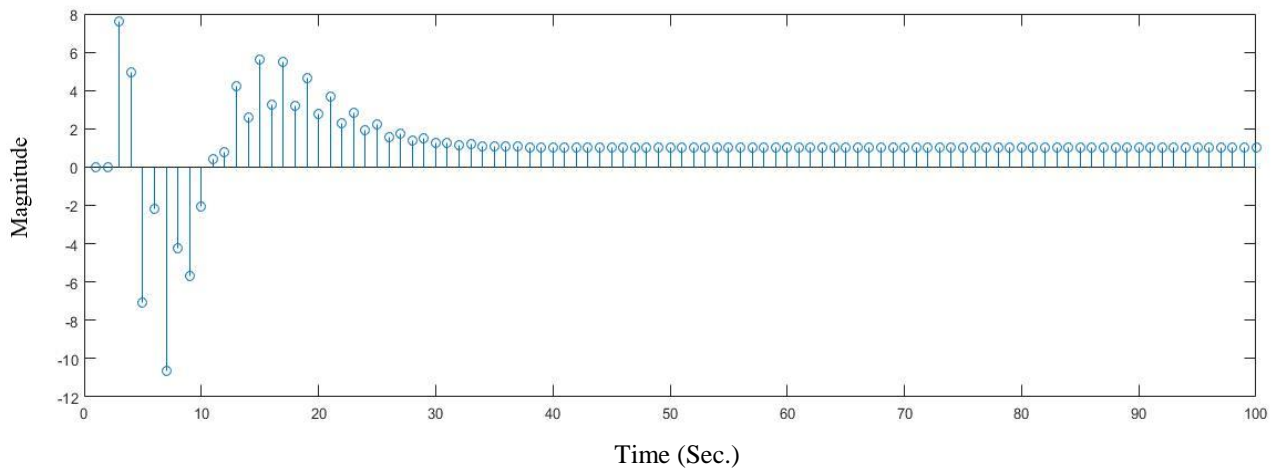


Fig. 2.23: Response using augmentation $\frac{(z+1)}{(z-1)}$ with $\beta = 0.85$ for conditions $Q_0^+ = -Q_1^+$ and $Q_0^+ = -Q_1^-$ with pole-zero cancellation at $z^2 = 0.5$

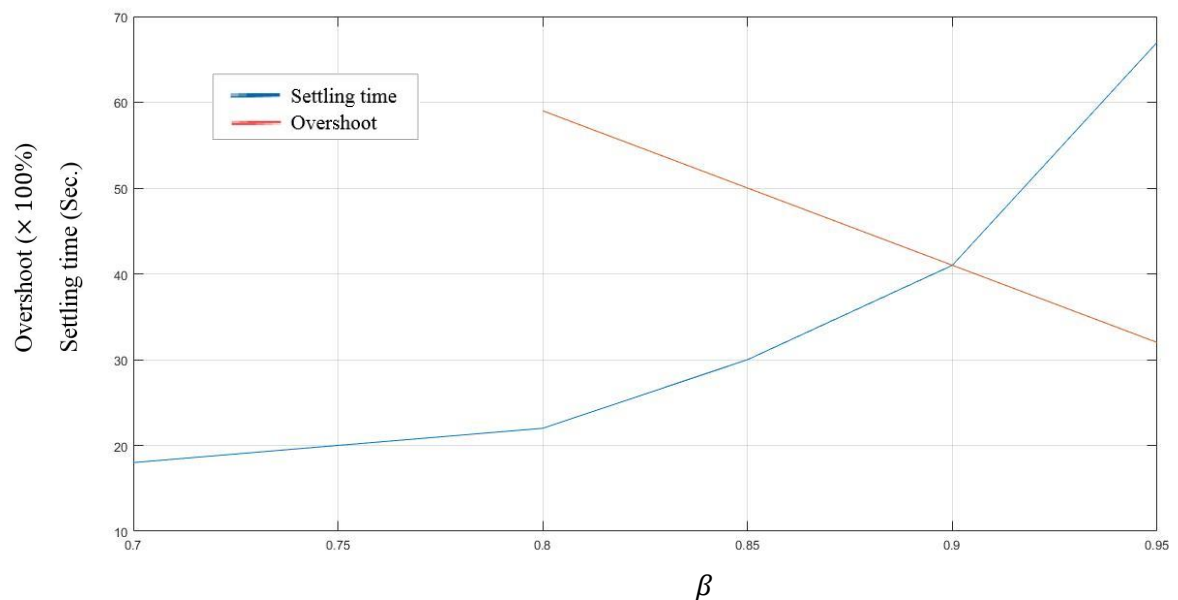


Fig. 2.24: Variation of settling time and maximum peak overshoot with β for condition $Q_0^+ = Q_1^-$ and $Q_0^+ = Q_1^+$ with pole-zero cancellation at $z^2 = 0$

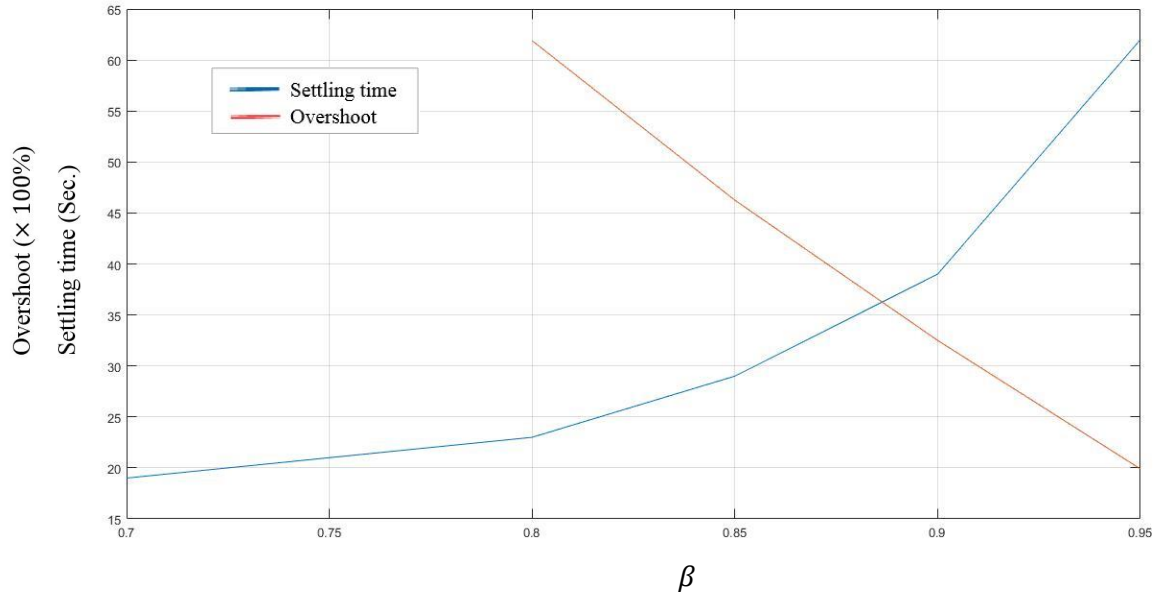


Fig. 2.25: Variation of settling time and maximum peak overshoot with β for condition $Q_0^+ = -Q_1^-$ and $Q_0^- = -Q_1^+$ with pole-zero cancellation at $z^2 = 0$

It is observed that the system becomes overdamped for $\beta = 0.7$ with pole-zero cancellation at $z^2 = 0$. So, overshoots are not present and the specified position is left blank in the fig 2.24 and 2.25.

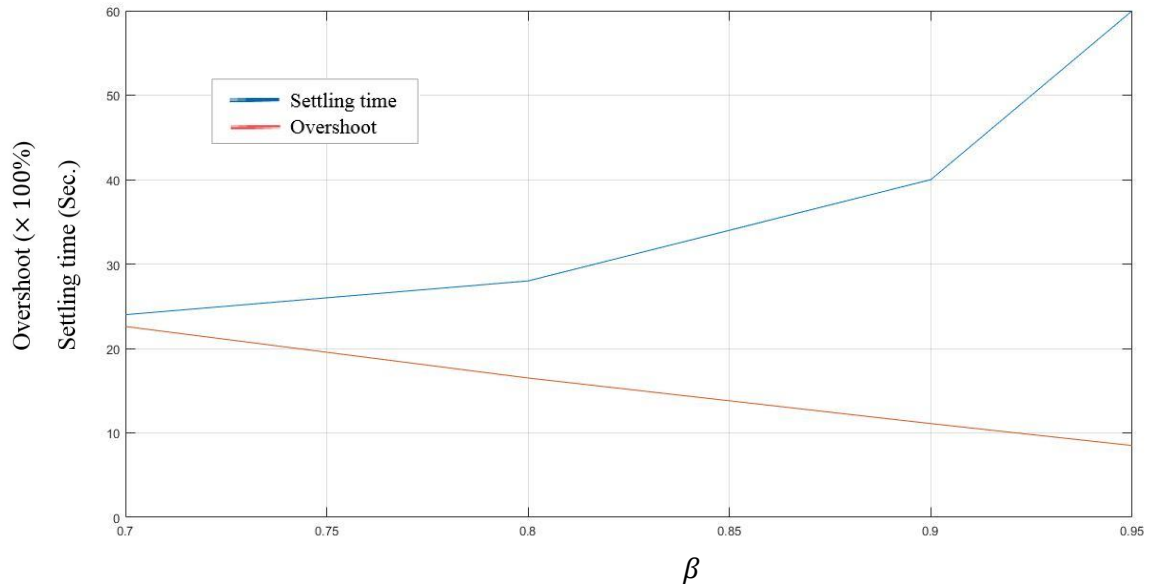


Fig. 2.26: Variation of settling time and maximum peak overshoot with β for condition $Q_0^+ = Q_1^-$ and $Q_0^- = Q_1^+$ with pole-zero cancellation at $z^2 = 0.5$

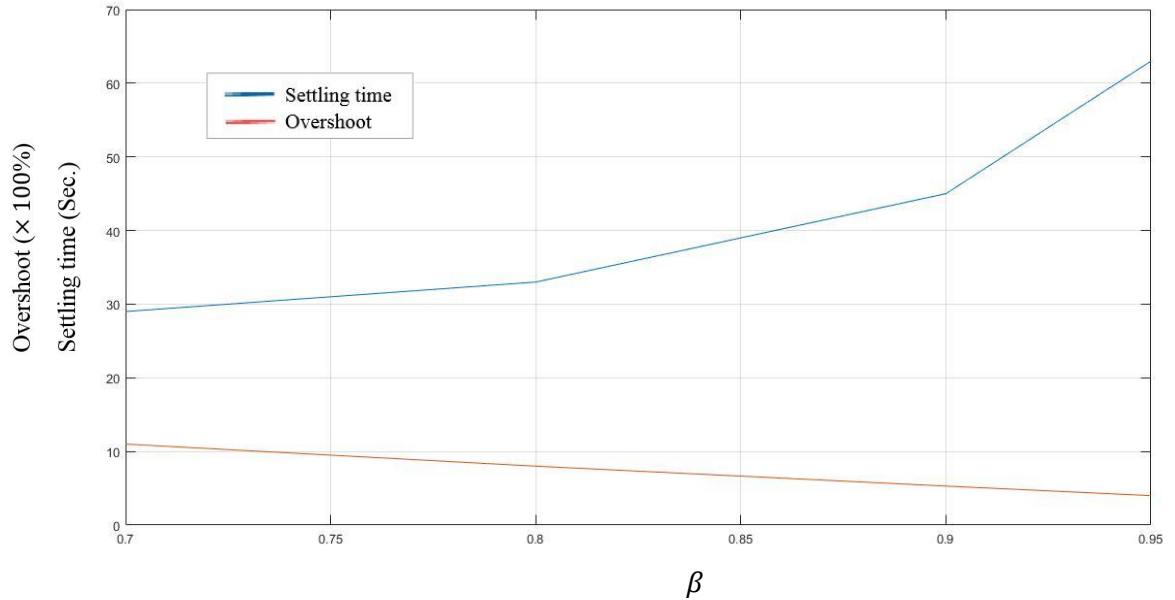


Fig. 2.27: Variation of settling time and maximum peak overshoot with β for condition $Q_0^+ = -Q_1^-$ and $Q_0^+ = -Q_1^+$ with pole-zero cancellation at $z^2 = 0.5$

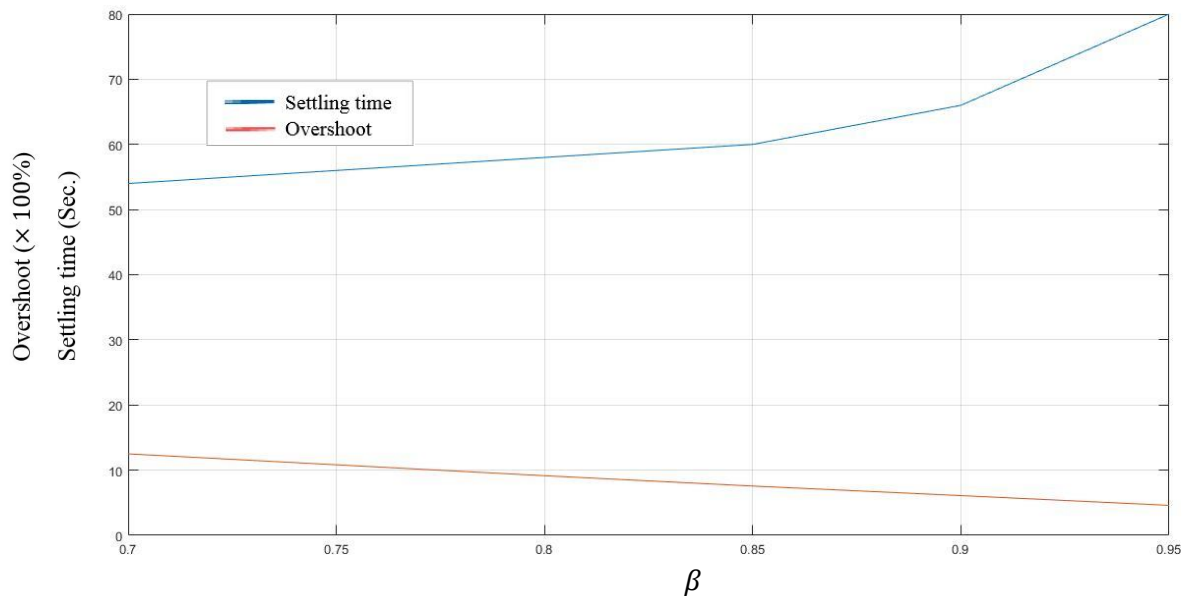


Fig. 2.28: Variation of settling time and maximum peak overshoot with β for condition $Q_0^+ = Q_1^-$ and $Q_0^+ = Q_1^+$ with pole-zero cancellation at $z^2 = 0.75$

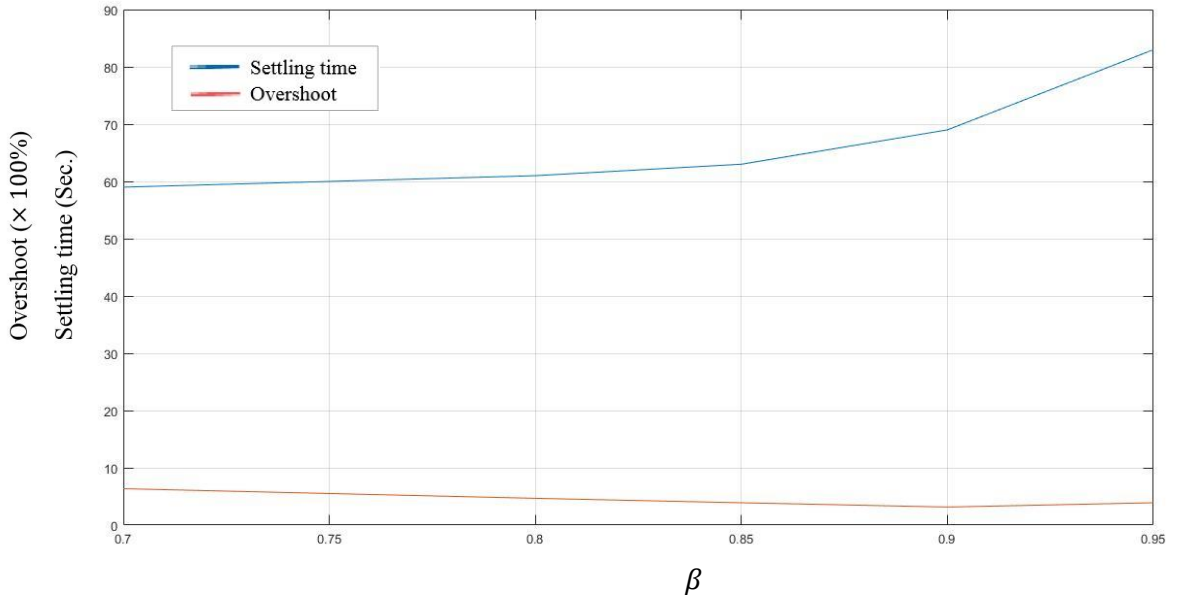


Fig. 2.29: Variation of settling time and maximum peak overshoot with β for condition $Q_0^+ = -Q_1^-$ and $Q_0^+ = -Q_1^+$ with pole-zero cancellation at $z^2 = 0.75$

2.5 Chapter Summary

In this chapter the compensation of SISO, NMP, Discrete-time LTI plants using 2-periodic controller is revisited and the results are discussed in details with respect to a nominal plant. It re-establishes the fact that a 2-periodic controller, by virtue of its loop-zero placement capability, yields better loop robustness as compared to its LTI counterpart. This chapter further presents the techniques used to eliminate the steady-state ripple in the output response. Finally, the chapter presents a detailed comparative study of a set of results that shows how the loop robustness and time response varies relative to the choice of controller parameters.

CHAPTER 3

2-DOF 2-Periodic Controller

3.1. Introduction

It is seen in Chapter 2, that for linear, SISO, discrete time-invariant plants with non-minimum phase zeros, 2-periodic controllers are capable of placing loop zeros and thus, satisfactory loop robustness is achieved. Also the ripple-problem from the steady-state step-response is eliminated by introducing LTI augmentations to the plant. However, these control schemes, increase the order of the controller required. This, in turn, increases the number of additional poles introduced in the closed-loop which slows down the transient response considerably. Such effects can be minimized by eliminating as many of additional closed-loop poles as possible. So, a 2 degrees-of-freedom controller configuration is used where the additional controller gains are used to cancel out the effect of some of the additional closed-loop poles.

In this chapter, 2-degrees-of-freedom 2-periodic controller in observer canonical configuration is considered (based on [27]). The performance of the controller has been analysed and compared with 1 degree-of-freedom 2-periodic controller. Numerical examples are also shown to illustrate the results.

3.2 Design of 2-DOF 2-Periodic Controller

Let us consider a SISO, LDTI, n^{th} order plant $G(z) = k \frac{b(z)}{a(z)}$

$$\begin{aligned} \text{Where, } \quad a(z) &= z^n + a_{n-1}z^{n-1} + \cdots + a_1z + a_0 \\ b(z) &= z^r + b_{r-1}z^{r-1} + \cdots + b_1z + b_0 \quad \text{with } r < n \end{aligned} \tag{3.1}$$

Considering a m^{th} order 2-DOF 2-periodic controller (Fig. 3.1), where the controller gains Following [27], K_i, D_i, C_i can be expressed as,

$$\begin{aligned} K_i &= k_{i,0} + (-1)^N k_{i,1} \\ D_i &= d_{i,0} + (-1)^N d_{i,1}, \quad \text{for } i = 0, 1, \dots, m \\ C_i &= c_{i,0} + (-1)^N c_{i,1}, \quad \text{for } i = 0, 1, \dots, (m-1) \end{aligned} \tag{3.2}$$

Recasting the system as,

$$\begin{aligned} P_0 &= z^m + c_{m-1,0}z^{m-1} + \cdots + c_{1,0}z + c_{0,0} \\ P_i &= c_{m-1,i}z^{m-1} + \cdots + c_{1,i}z + c_{0,i}, \quad \text{for } i = 0, 1, \dots, (m-1) \end{aligned}$$

$$\begin{aligned} Q_i &= d_{m,i}z^m + d_{m-1,i}z^{m-1} + \cdots + d_{0,i}, & \text{for } i = 0, 1, \dots, m \\ H_i &= k_{m,i}z^m + k_{m-1,i}z^{m-1} + \cdots + k_{0,i}, & \text{for } i = 0, 1, \dots, m \end{aligned} \quad (3.3)$$

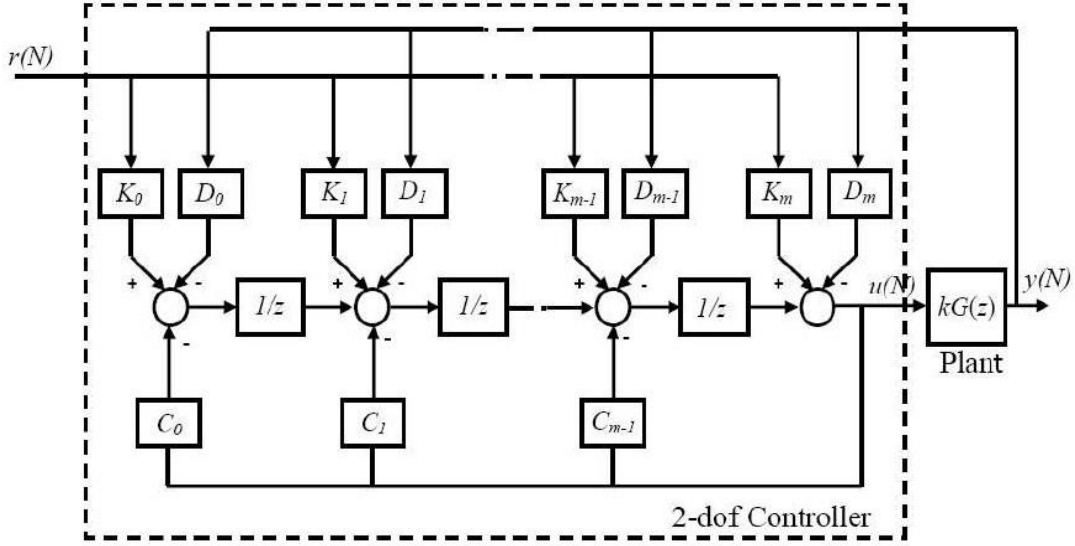


Fig. 3.1: 2-DOF periodic controller

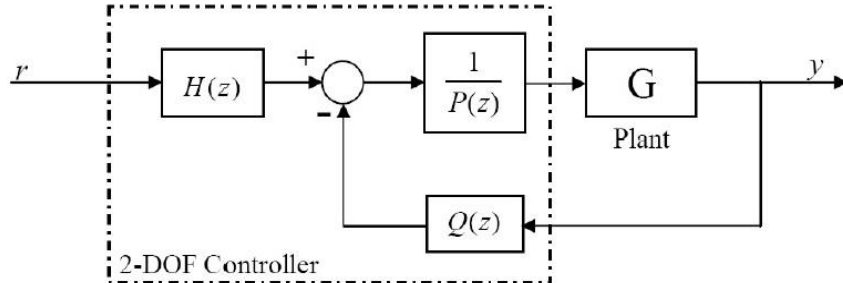


Fig. 3.2: 2-DOF LTI controller configuration

So, we can write as,

$$\begin{aligned} Q(z) &= (d_{m,0}z^m + d_{m-1,0}z^{m-1} + \cdots + d_{1,0}z + d_{0,0}) + \\ &\quad (-1)^N(d_{m,1}z^m + d_{m-1,1}z^{m-1} + \cdots + d_{1,1}z + d_{0,1}) \end{aligned} \quad (3.4)$$

$$\begin{aligned} P(z) &= (z^m + c_{m-1,0}z^{m-1} + \cdots + c_{1,0}z + c_{0,0}) + \\ &\quad (-1)^N(c_{m-1,1}z^{m-1} + \cdots + c_{1,1}z + c_{0,1}) \end{aligned} \quad (3.5)$$

$$\begin{aligned} H(z) &= (k_{m,0}z^m + k_{m-1,0}z^{m-1} + \cdots + k_{1,0}z + k_{0,0}) + \\ &\quad (-1)^N(k_{m,1}z^m + k_{m-1,1}z^{m-1} + \cdots + k_{1,1}z + k_{0,1}) \end{aligned} \quad (3.6)$$

3.2.1 Closed Loop Characteristic Equation

Let, for any polynomial $f(z)$, $f^+ = f(z)$ and $f^- = f(-z)$

Time domain lifting theory is applied to the controller and the plant. The transfer matrix of the polynomial $Q(z)$ becomes,

$$\bar{Q}(z^2) = \begin{bmatrix} Q_{11}(z^2) & z^{-1}Q_{12}(z^2) \\ zQ_{21}(z^2) & Q_{22}(z^2) \end{bmatrix} \quad (3.7)$$

where, $Q_{11} = Q_0^+ + Q_0^- + Q_1^+ + Q_1^-$

$$Q_{12} = Q_0^+ - Q_0^- + Q_1^+ - Q_1^-$$

$$Q_{21} = Q_0^+ - Q_0^- - Q_1^+ + Q_1^-$$

$$Q_{22} = Q_0^+ + Q_0^- - Q_1^+ - Q_1^- \quad (3.8)$$

The lifted transfer matrix of the polynomial $P(z)$,

$$\bar{P}(z^2) = \frac{1}{2} \begin{bmatrix} P_{11}(z^2) & z^{-1}P_{12}(z^2) \\ zP_{21}(z^2) & P_{22}(z^2) \end{bmatrix} \quad (3.9)$$

where , $P_{11} = P_0^+ + P_0^- + P_1^+ + P_1^-$

$$P_{12} = P_0^+ - P_0^- + P_1^+ - P_1^-$$

$$P_{21} = P_0^+ - P_0^- - P_1^+ + P_1^-$$

$$P_{22} = P_0^+ + P_0^- - P_1^+ - P_1^- \quad (3.10)$$

The closed loop controller transfer function,

$$C(z, N) = [Q(z)][P(z)]^{-1}$$

So, from (3.7) and (3.9),

$$\bar{C}(z^2) = \frac{1}{\Delta_c} \begin{bmatrix} C_{11}(z^2) & z^{-1}C_{12}(z^2) \\ zC_{21}(z^2) & C_{22}(z^2) \end{bmatrix} \quad (3.11)$$

where,

$$\Delta_c = 2(P_0^+P_0^- - P_1^+P_1^-)$$

$$C_{11} = Q_0^+P_0^- + Q_0^-P_0^+ - Q_0^+P_1^- - Q_0^-P_1^+ + Q_1^+P_0^- + Q_1^-P_0^+ - Q_1^+P_1^- - Q_1^-P_1^+$$

$$C_{12} = Q_0^+P_0^- - Q_0^-P_0^+ + Q_0^+P_1^- - Q_0^-P_1^+ + Q_1^+P_0^- - Q_1^-P_0^+ + Q_1^+P_1^- - Q_1^-P_1^+$$

$$C_{21} = Q_0^+P_0^- - Q_0^-P_0^+ - Q_0^+P_1^- + Q_0^-P_1^+ - Q_1^+P_0^- + Q_1^-P_0^+ + Q_1^+P_1^- - Q_1^-P_1^+$$

$$C_{22} = Q_0^+P_0^- + Q_0^-P_0^+ + Q_0^+P_1^- + Q_0^-P_1^+ - Q_1^+P_0^- - Q_1^-P_0^+ - Q_1^+P_1^- - Q_1^-P_1^+ \quad (3.12)$$

Now, the lifted transfer matrix of the plant,

$$\bar{G}(z^2) = \frac{1}{\Delta_c} \begin{bmatrix} G_{11}(z^2) & z^{-1}G_{12}(z^2) \\ zG_{21}(z^2) & G_{22}(z^2) \end{bmatrix} \quad (3.13)$$

where, $\Delta_c = \frac{1}{2a^+a^-}$

$$\begin{aligned} G_{11} &= G_{22} = b^+a^- + b^-a^+ \\ G_{12} &= G_{21} = b^+a^- - b^-a^+ \end{aligned} \quad (3.14)$$

The characteristic equation of closed loop system is given by

$$\Delta = \det[I + K\bar{G}\bar{C}] \quad (3.15)$$

Substituting the values of 2×2 transfer matrices of \bar{G} and \bar{C} from equation (3.11) and (3.13) to the characteristic equation of (3.15), we get,

$$\begin{aligned} \Delta = a^+a^-(P_0^+P_0^- - P_1^+P_1^-) + K [b^+a^-(Q_0^+P_0^- - Q_1^-P_1^+) + b^-a^+(Q_0^-P_0^+ - Q_1^+P_1^-)] \\ + K^2b^+b^-(Q_0^+Q_0^- - Q_1^+Q_1^-) \end{aligned} \quad (3.16)$$

Special cases of 2-periodic controller (i.e. conditions $Q_0^+ = \pm Q_1^\pm$) which omits the coefficients of K^2 term of the closed loop characteristic equation will be discussed in the next section.

3.2.2 Loop Zero Placement

From the characteristic equation of (3.16), the plant zeros are the co-efficient of K^2 term. Due to the presence of term, loop-zeros cannot be placed arbitrarily. But coefficient of K term does not contain such term and roots of this coefficient can be assigned to the required places. Therefore, if coefficient of K^2 term is made equal to zero then coefficient of K term would determine the locations of loop-zeros. Thus the zero placement is achieved. To make the K^2 term equal to zero, the following four conditions are used,

- i. $Q_0^+ = Q_1^-$
- ii. $Q_0^+ = -Q_1^-$
- iii. $Q_0^+ = Q_1^+$
- iv. $Q_0^+ = -Q_1^+$

The equation (3.16) now becomes,

$$\Delta = a^+a^-(P_0^+P_0^- - P_1^+P_1^-) + K [b^+a^-(Q_0^+P_0^- - Q_1^-P_1^+) + b^-a^+(Q_0^-P_0^+ - Q_1^+P_1^-)] \quad (3.17)$$

The equation (3.17) can be written as,

$$\hat{A}(z^2)\hat{P}(z^2) + \hat{Z}(z^2) = \hat{\Delta}(z^2) = \check{\Delta}(z^2)\check{D}(z^2) = 0 \quad (3.18)$$

where,

$$\begin{aligned} \hat{A}(z^2) &= \text{Plant poles} = a^+ a^- \\ &= a_0 + a_2 z^2 + \dots + (-1)^n z^{2n} \end{aligned} \quad (3.19)$$

$$\begin{aligned} \hat{P}(z^2) &= \text{Controller poles} = (P_0^+ P_0^- - P_1^+ P_1^-) \\ &= \hat{p}_0 + \hat{p}_2 z^2 + \dots + (-1)^m z^{2m} \end{aligned} \quad (3.20)$$

$$\begin{aligned} \hat{Z}(z^2) &= \text{Zero polynomial of the overall system} \\ &= K [b^+ a^- (Q_0^+ P_0^- - Q_1^- P_1^+) + b^- a^+ (Q_0^- P_0^+ - Q_1^+ P_1^-)] \\ &= r_0 + r_2 z^2 + \dots + r_{2\theta} z^{2\theta} \end{aligned} \quad (3.21)$$

$\check{\Delta}(z^2)$ = Desired closed loop poles

$\check{D}(z^2)$ = Additional closed loop poles

From the above equations it can be noted that the controller pole polynomial and the loop-zero polynomial both are assignable. So, by adjusting the parameters of zero polynomial, zero placement can be achieved.

3.3 Controller Synthesis Part I: Loop-Zero and Pole Placement

In this section, the closed loop poles and the loop-zeros associated with the K-term of closed loop characteristic equation (equation 3.17), are placed in desired location.

3.3.1 Order of the Controller

It can be observed from (3.19) and (3.20), the degree of polynomials $\hat{A}(z^2)$ and $\hat{P}(z^2)$ are $2n$ and $2m$ respectively. The degree of the polynomial $\hat{Z}(z^2)$ can be defined as,

$$\theta = m + \vartheta$$

$$\text{With } \vartheta = n - I^+\left\{\frac{(n-r)}{2}\right\} \quad (3.22)$$

where,

I^+ is the ceiling operator,

θ is the total number of assignable loop-zeros,

ϑ is the assignable plant zeros which depends upon the relative order of the plant.

From (3.5) and (3.18), the total number of assignable coefficients is $(2m + m)$ to place m controller poles and $(m + \vartheta)$ loop zeros. The order of the controller is defined by,

$$m \geq \vartheta = n - I^+ \left\{ \frac{(n-r)}{2} \right\} \quad (3.23)$$

3.3.2 Evaluation of Controller Parameters

Controller parameters are evaluated by solving the characteristic equation. The controller is synthesized using approach of [3]. It is a two-stage method. In Stage-I, an intermediate polynomial is obtained and in Stage-II, controller parameters are calculated from the intermediate polynomial.

Stage I:

Let,

$$\begin{aligned} \hat{B}(z) &= b^+ a^- = [\hat{b}_0 + \hat{b}_2 z^2 + \dots + \hat{b}_{2\varphi_1} z^{2\varphi_1}] + z[\hat{b}_1 + \hat{b}_3 z^2 + \dots + \hat{b}_{2\varphi_2+1} z^{2\varphi_2}] \\ &= \hat{B}_e(z^2) + z\hat{B}_d(z^2) \end{aligned} \quad (3.24)$$

With $\varphi_1 = I^- \left\{ \frac{n+r}{2} \right\}$ and $\varphi_2 = I^- \left\{ \frac{n+r-1}{2} \right\}$

$$\begin{aligned} \hat{L}(z) &= (Q_0^+ P_0^- - Q_1^- P_1^+) \\ &= [\hat{l}_0 + \hat{l}_2 z^2 + \dots + \hat{l}_{2m} z^{2m}] + z[\hat{l}_1 + \hat{l}_3 z^2 + \dots + \hat{l}_{2m-1} z^{2(m-1)}] \\ &= \hat{L}_e(z^2) + z\hat{L}_d(z^2) \end{aligned} \quad (3.25)$$

From (3.24), (3.25) we obtain,

$$\begin{aligned} \hat{Z}(z^2) &= \hat{B}^+ \hat{L}^+ + \hat{B}^- \hat{L}^- = 2\hat{B}_e(z^2)\hat{L}_e(z^2) + 2z^2\hat{B}_d(z^2)\hat{L}_d(z^2) \\ &= r_0 + r_2 z^2 + \dots + r_{2\theta} z^{2\theta} \end{aligned} \quad (3.26)$$

Now, using (3.24), (3.25) and (3.26) the Sylvester matrix like equation is obtained below,

$$\begin{bmatrix} r_0 \\ r_2 \\ r_4 \\ \vdots \\ r_{2\theta} \end{bmatrix} = \begin{bmatrix} \hat{b}_0 & \dots & 0 & 0 & \dots & 0 \\ \hat{b}_2 & \dots & 0 & \hat{b}_1 & \dots & 0 \\ \hat{b}_4 & \dots & 0 & \hat{b}_3 & \dots & 0 \\ \vdots & \ddots & \vdots & \vdots & \ddots & \vdots \\ 0 & \dots & \hat{b}_{2\varphi_1} & 0 & \dots & \hat{b}_{2\varphi_2+1} \end{bmatrix} \begin{bmatrix} \hat{l}_0 \\ \vdots \\ \hat{l}_{2m} \\ \hat{l}_1 \\ \vdots \\ \hat{l}_{2m-1} \end{bmatrix} \quad (3.27)$$

Equation (3.27) will be a consistent set of equations if the conditions of section 2.2.4 are satisfied.

Stage II:

Polynomial $\hat{L}(z)$ which is obtained in stage-I, now, will be divided into two parts for all four conditions $Q_0^+ = \pm Q_1^\pm$ and will be suitably assigned to pole polynomials to calculate the controller parameters.

Condition I: $Q_0^+ = Q_1^-$

From (3.25) we get, $\hat{L}(z) = Q_0^-(P_0^+ - P_1^-)$

Then, to find Q_0^- and $(P_0^+ - P_1^-)$, polynomial $\hat{L}(z)$ is divided into two parts such that

- i. Both the halves are real polynomials (i.e., a complex root and its conjugate should be present in the same half).
- ii. At least one of the halves has no even factor.

If the factor that satisfies the 2nd condition is, in addition, monic, then the same can be chosen as $(P_0^+ - P_1^-)$ and the rest would be Q_0^- . Values of $d_{i,0}$ and $d_{i,1}$ (for $i = 0, 1, \dots, m$) can be directly obtained from Q_0^- and Q_1^+ . Calculations for finding $c_{i,0}$ and $c_{i,1}$ (for $i = 0, 1, \dots, m-1$) are shown below.

Let,

$$(P_0^+ - P_1^-) = \Gamma(z) = \gamma_0 + \gamma_1 z + \dots + \gamma_m z^m \quad (3.28)$$

From (3.5), (3.28) it is obtained,

$$(P_0^+ \Gamma^- - P_1^- \Gamma^+) = \hat{P}(z^2) + \Gamma^+ \Gamma^- \quad (3.29)$$

Now, comparing both sided of the equation (3.29), we get,

$$\begin{bmatrix} \gamma_0 & 0 & 0 & 0 & \dots & 0 & 0 \\ \gamma_2 & -\gamma_1 & \gamma_0 & 0 & \dots & 0 & 0 \\ \gamma_4 & -\gamma_3 & \gamma_2 & -\gamma_1 & \dots & 0 & 0 \\ \vdots & \vdots & \vdots & \ddots & \vdots & \vdots & \vdots \\ 0 & 0 & 0 & 0 & \dots & (-1)^{m-1} \gamma_{m-1} & (-1)^m \gamma_{m-2} \\ 0 & 0 & 0 & 0 & \dots & 0 & (-1)^m \gamma_m \end{bmatrix} \begin{bmatrix} C_{0,0} \\ C_{1,0} \\ C_{2,0} \\ \vdots \\ C_{(m-1),0} \\ 1 \end{bmatrix} = \begin{bmatrix} \hat{p}_0 + \gamma_0^2 \\ \hat{p}_2 + 2\gamma_0\gamma_2 - \gamma_1^2 \\ \hat{p}_4 + \gamma_0\gamma_4 - 2\gamma_1\gamma_3 + \gamma_2^2 \\ \vdots \\ \hat{p}_{2(m-1)} + 2(-1)^m \gamma_m \gamma_{m-2} - (-1)^{(m-1)} \gamma_{m-1}^2 \\ (-1)^m + (-1)^m \gamma_m^2 \end{bmatrix} \quad (3.30)$$

The coefficients of P_0 i.e. $C_{0,0}, C_{1,0}, C_{2,0}, \dots, C_{(m-1),0}$ can be obtained by solving equation (3.30). Using these values, coefficients of P_1 i.e. $C_{0,1}, C_{1,1}, C_{2,1}, \dots, C_{(m-1),1}$ can be calculated from the following equation,

$$C_{i,1} = (-1)^i(C_{i,0} - \gamma_0) \quad \text{with } i = 0, 1, \dots, (m-1) \quad (3.31)$$

Condition II: $Q_0^+ = -Q_1^-$

From (3.25) we get, $\hat{L}(z) = Q_0^-(P_0^+ + P_1^-)$

Now, procedures shown for condition can be followed. But equation for obtaining coefficients of P_1 from coefficients of P_0 will change and become as follows.

$$C_{i,1} = (-1)^i(\gamma_0 - C_{i,0}) \quad \text{with } i = 0, 1, \dots, (m-1) \quad (3.32)$$

Condition III: $Q_0^+ = Q_1^+$

In order to extract the factor Q_0 from $\hat{L}(z)$, the following condition must be considered.

$$Q_i^+ = (-1)^m Q_i^- \quad \text{with } i = 0, 1$$

m is the controller order.

From (3.25) we get,

$$\hat{L}(z) = Q_0^-(P_0^+ - (-1)^m P_1^-)$$

Now, procedures shown for condition can be followed. But equation for obtaining coefficients of P_1 from coefficients of P_0 will change and become as follows.

Condition IV: $Q_0^+ = -Q_1^+$

In order to extract the factor Q_0 from $\hat{L}(z)$, the following condition must be considered.

$$Q_i^+ = (-1)^m Q_i^- \quad \text{with } i = 0, 1$$

m is the controller order.

From (3.25) we get, $\hat{L}(z) = Q_0^-(P_0^+ + (-1)^m P_1^-)$

Now, procedures shown for condition can be followed. But equation for obtaining coefficients of P_1 from coefficients of P_0 will change and become as follows.

3.4 Controller Synthesis Part II: Model Matching

The standard model-matching problem consists of making a given plant behave like another model plant of same or reduced order. If a 1 degree of freedom LTI controller is used to compensate a plant containing unstable poles and/or NMP zeros, then it cannot perform the reduced order or the same order model matching. However, 2 degree of freedom LTI controllers can achieve same order model-matching (for plants not containing NMP zeros). In order to do so the input gains associated with a 2-DOF controller need to be chosen such that they cancel out the effect of additional poles introduced in the closed-loop transfer function by the controller. However, these controllers cannot alter the NMP zeros. On the other hand, 2-periodic 2-DOF controllers can alter the loop zeros and the effect of the additional poles introduced by the controller can be eliminated by introducing the input gains K_i . This technique of achieving model matching is discussed in this section.

The closed loop transfer function can be expressed as

$$G_{CL}(z^2) = [I + K\bar{G}P^{-1}Q]^{-1}\bar{G}P^{-1}\bar{H} \quad (3.33)$$

At first considering case $Q_0^+ = Q_1^+$,

This case corresponds to condition-III of section 3.3.2, stage-II. The additional condition is

$$Q_i^+ = (-1)^m Q_i^- \quad \text{with } i = 0, 1 \quad (3.34)$$

For $m = \text{even}$, we get (from equation 3.34),

$$Q_0^+ = Q_0^-$$

$$\text{and} \quad Q_1^+ = Q_1^-$$

The lifted representation of $Q(z, N)$ becomes

$$\bar{Q}(z^2) = \begin{bmatrix} (Q_0^+ + Q_1^+) & 0 \\ 0 & 0 \end{bmatrix} = \begin{bmatrix} 2Q_0^+ & 0 \\ 0 & 0 \end{bmatrix} \quad (3.35)$$

Now, considering an additional condition

$$P_i^+ = P_i^- = P_i \quad \text{with } i = 0, 1$$

Then the open-loop controller pole polynomial $\hat{P}(z^2)$ from (3.20) becomes

$$\begin{aligned} \hat{P}(z^2) &= (P_0^+ P_0^- - P_1^+ P_1^-) = (P_0^2 - P_1^2) \\ &= (P_0 + P_1)(P_0 - P_1) \triangleq \check{k}_1 \check{k}_2 \end{aligned} \quad (3.36)$$

$$\text{where,} \quad \check{k}_1 = (P_0^+ + P_1^+) = (P_0 + P_1)$$

$$\check{k}_2 = (P_0^+ - P_1^+) = (P_0 - P_1)$$

The corresponding lifted representation of $P(z,N)$ becomes

$$\bar{P}(z^2) = \begin{bmatrix} (P_0 + P_1) & 0 \\ 0 & (P_0 - P_1) \end{bmatrix} = \begin{bmatrix} \check{k}_1 & 0 \\ 0 & \check{k}_2 \end{bmatrix} \quad (3.37)$$

The loop-zero polynomial $\hat{Z}(z)$ and polynomial $\hat{L}(z)$ can be recasted as

$$\begin{aligned} \hat{Z}(z^2) &= K [\hat{B}^+ Q_0^+(P_0^+ - P_1^+) + \hat{B}^- Q_0^+(P_0^+ - P_1^+)] \\ &= 2\hat{B}_e Q_0^+(P_0^+ - P_1^+) = 2\hat{B}_e Q_0^+ \check{k}_2 \end{aligned} \quad (3.38)$$

$$\hat{L}(z) = Q_0^+(P_0^+ - P_1^-) = Q_0^+(P_0^+ - P_1^+) \quad (3.39)$$

If we choose $Q_0^+ = l_{2m}(P_0^+ + P_1^+) = l_{2m}\check{k}_1$

Then from (3.39) and (3.28), $\hat{L}(z)$ and $\Gamma(z)$ becomes

$$\hat{L}(z) = l_{2m}(P_0^+ + P_1^+)(P_0^+ - P_1^-) = l_{2m}\check{k}_1\check{k}_2 \quad (3.40)$$

$$\Gamma(z) = (P_0^+ - P_1^-) = (P_0^+ - P_1^+) = \check{k}_2 \quad (3.41)$$

Now, choosing $H_0^+ = H_0^- = P_0^+ = P_0^- = H_0$ and $H_1^+ = H_1^- = P_1^+ = P_1^- = H_1$

The corresponding lifted representation of $H(z,N)$ becomes

$$\bar{H}(z^2) = \begin{bmatrix} (H_0 + H_1) & 0 \\ 0 & (H_0 - H_1) \end{bmatrix} = \begin{bmatrix} \check{k}_1 & 0 \\ 0 & \check{k}_2 \end{bmatrix} \quad (3.42)$$

Lifted plant transfer matrix is found to be

$$\bar{G}(z^2) = \frac{1}{d} \begin{bmatrix} n_1(z^2) & z^{-2}n_2(z^2) \\ n_2(z^2) & n_1(z^2) \end{bmatrix} \quad (3.43)$$

$$\begin{aligned} \text{where, } d &= \frac{1}{2a^+a^-} \\ n_1 &= b^+a^- + b^-a^+ \\ n_2 &= z(b^+a^- - b^-a^+) \end{aligned} \quad (3.44)$$

After simplification closed loop transfer matrix becomes

$$\begin{aligned} G_{CL}(z^2) &= [I + K\bar{G}P^{-1}Q]^{-1}\bar{G}P^{-1}\bar{H} \\ &= \frac{1}{\Delta_c} \begin{bmatrix} n_1\check{k}_1 & z^{-2}n_2\check{k}_1 \\ n_2\check{k}_1 & n_1\check{k}_1 + \frac{2Q_0^+}{d}(n_1^2 - z^{-2}n_2^2) \end{bmatrix} \bar{H} \end{aligned} \quad (3.45)$$

$$\text{where, } \Delta_c = 2Q_0^+n_1 + d\check{k}_1 \quad (3.46)$$

From (3.44), we get,

$$n_1^2 - z^{-2}n_2^2 = b^+b^-a^+a^-$$

$$\text{So } (n_1^2 - z^{-2}n_2^2)/d = b^+b^-$$

and with the choice $Q_0^+ = l_{2m}\check{k}_1$, transfer matrix of (3.45) is simplified as

$$G_{CL}(z^2) = \frac{1}{d+2l_{2m}n_1} \begin{bmatrix} n_1 & z^{-2}n_2 \\ n_2 & n_1 + 2l_{2m}b^+b^- \end{bmatrix} \quad (3.47)$$

Now, the even and odd instant outputs (Y) to step input (U) will be

$$\begin{aligned} \begin{bmatrix} Y_e(z^2) \\ Y_d(z^2) \end{bmatrix} &= G_{CL}(z^2) \begin{bmatrix} U_e(z^2) \\ U_d(z^2) \end{bmatrix} \\ &= \frac{1}{d+2l_{2m}n_1} \begin{bmatrix} n_1 + z^{-2}n_2 \\ (n_2 + n_1) + 2l_{2m}b^+b^- \end{bmatrix} \frac{z^2}{(z^2-1)} \end{aligned} \quad (3.48)$$

For $m = \text{odd}$, we get (from equation 3.34),

$$Q_0^+ = -Q_0^-$$

$$\text{and } Q_1^+ = -Q_1^-$$

Now, in this case we consider $Q_0^+ = Q_1^+ = -l_{2m}\check{k}_1$

The controller transfer matrix is calculated as

$$\bar{C}(z^2) = \begin{bmatrix} -2l_{2m} & 0 \\ 0 & 0 \end{bmatrix} \quad (3.49)$$

The closed-loop transfer matrix would become

$$G_{CL}(z^2) = \frac{1}{d-2l_{2m}n_1} \begin{bmatrix} z^{-3}n_2 & zn_1 \\ z^{-1}(n_1 - 2l_{2m}b^+b^-) & z^{-1}n_2 \end{bmatrix} \quad (3.50)$$

Now, the even and odd instant outputs (Y) to step input (U) will be

$$\begin{aligned} \begin{bmatrix} Y_e(z^2) \\ Y_d(z^2) \end{bmatrix} &= G_{CL}(z^2) \begin{bmatrix} U_e(z^2) \\ U_d(z^2) \end{bmatrix} \\ &= \frac{1}{d-2l_{2m}n_1} \begin{bmatrix} z(n_1 + z^{-4}n_2) \\ z^{-1}\{(n_1 + n_2) - 2l_{2m}b^+b^-\} \end{bmatrix} \frac{z^2}{(z^2-1)} \end{aligned} \quad (3.51)$$

Similarly, the closed-loop transfer matrix corresponding to the remaining three cases (i.e. $Q_0^+ = -Q_1^+$, $Q_0^+ = Q_1^-$, $Q_0^+ = -Q_1^-$) can be obtained.

3.4.1 Numerical example

Example 3.4.1: Considering the plant of Example 2.3.1, it will now be compensated using a 2 DOF 2-periodic controller.

Consider a 2-periodic controller of the form of Fig. 3.1, of order $m = 1$ and number of controller zeros is 2.

$$\hat{A}(z^2) = (z^2 - 2.25)(z^2 - 0.25)$$

$$\hat{P}(z^2) = -(z^2 - 0.2)$$

$$\hat{Z}(z^2) = k_z z^2(z^2 - 0.25)$$

$$\check{D}(z^2) = -(z^2 - 0.25)$$

The loop-transfer function of overall system is

$$G_{loop}(z) = \frac{z^2}{(z^2 - 0.2)(z^2 - 2.25)} \quad (3.52)$$

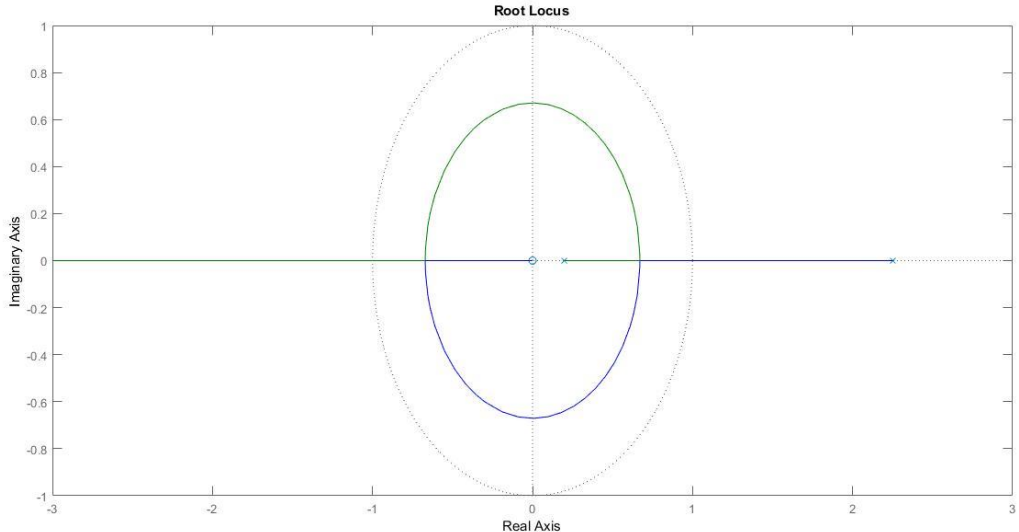


Fig. 3.3: Root locus of the system of (2.52)

The controller parameters are evaluated using technique of section 3.3 and 3.4. and response for the conditions $Q_0^+ = Q_1^-$ and $Q_0^+ = -Q_1^+$ are presented below.

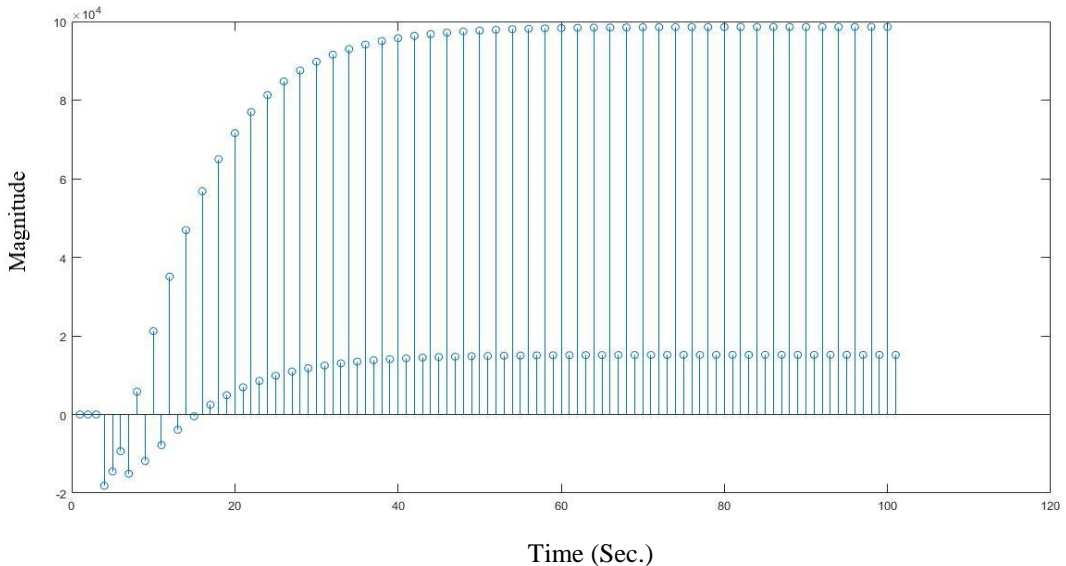


Fig. 3.4: Response of the plant with 2 DOF 2-periodic controller for conditions $Q_0^+ = Q_1^-$ and $Q_0^+ = -Q_1^+$

3.5 Ripple-Free Response

In example 3.4.1, 2-DOF 2-periodic controller design for a second order plant is demonstrated. It is observed that a 2-periodic oscillation is present in the steady-state response, which make the controller inconvenient. In this section, techniques of removing those ripples are discussed.

The steady-state step-response of a 2-periodically compensated system would be ripple-free if the loop contains any of the following time-invariant components,

- i. $\frac{z}{(z-1)}$
- ii. $\frac{(z+1)}{z}$
- iii. $\frac{(z+1)}{(z-1)}$

Proof: The lifted transform domain relation between the reference input and error is

$$\begin{bmatrix} E_e(z^2) \\ E_o(z^2) \end{bmatrix} = [I + K\bar{G}\bar{C}]^{-1} \begin{bmatrix} R_e(z^2) \\ R_o(z^2) \end{bmatrix}$$

Considering a step input for which $\begin{bmatrix} R_e(z^2) \\ R_o(z^2) \end{bmatrix} = \begin{bmatrix} 1 \\ 1 \end{bmatrix} \frac{z^2}{(z^2-1)}$

$$\begin{bmatrix} E_e(z^2) \\ E_o(z^2) \end{bmatrix} = \frac{1}{\Delta} \begin{bmatrix} \Delta_c d - z^{-1}(n_1 - n_2)C_{12} + (n_1 - z^{-2}n_2)C_{22} \\ \Delta_c d - (n_1 - n_2)C_{12} + z(n_1 - z^{-2}n_2)C_{22} \end{bmatrix} \frac{z^2}{(z^2 - 1)} \quad (3.53)$$

Where $d = a^+a^-$

$$\Delta = \Delta_c d + (C_{11} + C_{22})n_1 + z^{-1}(C_{21} + C_{12})n_2 + b^+b^-$$

$$n_1 = (b^+a^- + b^-a^+)$$

$$n_2 = z(b^+a^- - b^-a^+)$$

$$\text{So, } n_1 - n_2 = (1 - z)b^+a^- + (1 + z)b^-a^+$$

$$n_1 - z^{-2}n_2 = z^{-1}[(z - 1)b^+a^- + (1 + z)b^-a^+]$$

The steady state errors are calculated using the final value theorem and given by,

$$\begin{bmatrix} E_{e,ss} \\ E_{o,ss} \end{bmatrix} = \lim_{z^2 \rightarrow 1} \frac{z^2}{\Delta} \begin{bmatrix} \Delta_c d - z^{-1}(n_1 - n_2)C_{12} + (n_1 - z^{-2}n_2)C_{22} \\ \Delta_c d - (n_1 - n_2)C_{12} + z(n_1 - z^{-2}n_2)C_{22} \end{bmatrix} \quad (3.54)$$

It is clear from the above equation (3.54) that steady state ripples are introduced in even instants by the term $\{-z^{-1}(n_1 - n_2)C_{12} + (n_1 - z^{-2}n_2)C_{22}\}$ and $\{-(n_1 - n_2)C_{12} + z(n_1 - z^{-2}n_2)C_{22}\}$ in odd instants. So, to make the response ripple free, we need to make $(n_1 - n_2)$ and $(n_1 - z^{-2}n_2)$ equal to zero. This can be achieved if a $(z^2 - 1)$ term is present in $(n_1 - n_2)$ and $(n_1 - z^{-2}n_2)$, which will become zero due to the limit $(z^2 \rightarrow 1)$.

So, if the plant contains either a pole at 1 or a zero at -1 or both i.e. a denominator factor $(z - 1)$ or a numerator factor $(z + 1)$ or both, then the steady state response will not contain any ripple. If the plant does not contain any of those terms, then it should be multiplied by any of such factors before designing the periodic controller. The effects of the presence of the factors $\frac{z}{(z-1)}$, $\frac{(z+1)}{z}$ and $\frac{(z+1)}{(z-1)}$ in plant model is discussed next.

i. Pole at 1: If the plant denominator contains a factor $(z - 1)$ then the plant transfer function can be expressed as

$$G(z) = K \frac{b(z)}{a(z)} = K \frac{b(z)}{\check{a}(z)(z-1)} = K \frac{b(z)(-1)^n \check{a}(-z)(z+1)}{\check{a}(z)(-1)^n \check{a}(-z)(z^2-1)} = \frac{\check{n}(z)(z+1)}{\check{d}(z)(z^2-1)} \quad (3.55)$$

$$\text{as } b(z)(-1)^n \check{a}(-z) = \check{n}(z)$$

$$\check{a}(z)(-1)^n \check{a}(-z) = \check{d}(z)$$

Now, the lifted transfer function becomes

$$\begin{aligned}
G(z^2) &= \frac{[\check{n}_1(z^2) + z^{-1}\check{n}_2(z^2)](z+1)}{\check{d}(z)(z^2-1)} \\
&= \frac{[\check{n}_1(z^2) + \check{n}_2(z^2)] + z^{-1}[z^2\check{n}_1(z^2) + \check{n}_2(z^2)]}{\check{d}(z)(z^2-1)} \\
&= \frac{[n_1(z^2) + z^{-1}n_2(z^2)]}{\check{d}(z)(z^2-1)}
\end{aligned} \tag{3.56}$$

$$\begin{aligned}
\text{As } [\check{n}_1(z^2) + \check{n}_2(z^2)] &= n_1(z^2) \\
[z^2\check{n}_1(z^2) + \check{n}_2(z^2)] &= n_2(z^2)
\end{aligned} \tag{3.57}$$

Now, from (2.57) we get,

$$\begin{aligned}
n_1 - n_2 &= -(z^2 - 1)\check{n}_1(z^2) \\
n_1 - z^{-2}n_2 &= z^{-2}(z^2 - 1)\check{n}_1(z^2)
\end{aligned} \tag{3.58}$$

From (3.54) and (3.58) we get,

$$\begin{aligned}
[E_{e,ss}] &= \lim_{z^2 \rightarrow 1} \frac{z^2}{\Delta} \left[\Delta_c d + z^{-1}(z^2 - 1)\check{n}_1(z^2)C_{12} + z^{-2}(z^2 - 1)\check{n}_1(z^2)C_{22} \right] \\
&= \lim_{z^2 \rightarrow 1} \frac{z^2}{\Delta} \left[\Delta_c d \right]
\end{aligned} \tag{3.59}$$

It can be concluded from (3.59) that the presence of a pole at 1 in plant transfer function make the response ripple free.

ii. Zero at -1: If the plant numerator contains a factor $(z + 1)$ then the plant transfer function can be expressed as

$$G(z) = K \frac{b(z)}{a(z)} = K \frac{\check{b}(z)(z+1)}{a(z)} = K \frac{\check{b}(z)(-1)^n a(-z)(z+1)}{a(z)(-1)^n a(-z)} = \frac{\check{n}(z)(z+1)}{\check{d}(z)} \tag{3.60}$$

$$\begin{aligned}
\text{As } \check{b}(z)(-1)^n a(-z) &= \check{n}(z) \\
a(z)(-1)^n a(-z) &= \check{d}(z)
\end{aligned}$$

Now, the lifted transfer function becomes

$$\begin{aligned}
G(z^2) &= \frac{[\check{n}_1(z^2) + z^{-1}\check{n}_2(z^2)](z+1)}{\check{d}(z)(z^2-1)} = \frac{[\check{n}_1(z^2) + \check{n}_2(z^2)] + z^{-1}[z^2\check{n}_1(z^2) + \check{n}_2(z^2)]}{\check{d}(z)} \\
&= \frac{[n_1(z^2) + z^{-1}n_2(z^2)]}{\check{d}(z)}
\end{aligned} \tag{3.61}$$

$$\text{As } [\check{n}_1(z^2) + \check{n}_2(z^2)] = n_1(z^2)$$

$$[z^2 \tilde{n}_1(z^2) + \tilde{n}_2(z^2)] = n_2(z^2) \quad (3.62)$$

Now, from (3.62) we get,

$$\begin{aligned} n_1 - n_2 &= -(z^2 - 1) \tilde{n}_1(z^2) \\ n_1 - z^{-2}n_2 &= z^{-2}(z^2 - 1) \tilde{n}_1(z^2) \end{aligned} \quad (3.63)$$

From (3.54) and (3.63) we get,

$$\begin{aligned} \left[\frac{E_{e,ss}}{E_{o,ss}} \right] &= \lim_{z^2 \rightarrow 1} \frac{z^2}{\Delta} \left[\frac{\Delta_c d + z^{-1}(z^2 - 1) \tilde{n}_1(z^2) C_{12} + z^{-2}(z^2 - 1) \tilde{n}_1(z^2) C_{22}}{\Delta_c d + (z^2 - 1) \tilde{n}_1(z^2) C_{12} + z^{-1}(z^2 - 1) \tilde{n}_1(z^2) C_{22}} \right] \\ &= \lim_{z^2 \rightarrow 1} \frac{z^2}{\Delta} \left[\frac{\Delta_c d}{\Delta_c d} \right] \end{aligned} \quad (3.64)$$

It can be concluded from (3.64) that the presence of a zero at -1 in plant transfer function make the response ripple free.

- iii. **A Pole at 1 and a zero at -1:** As we know from (3.59) and (3.64) that the presence of a pole at 1 or a zero at -1 in plants transfer function makes the response ripple free. So, presence of both will also eliminate ripple in steady state response. It is proved in the following section.

The plant transfer function can be expressed as

$$G(z) = K \frac{b(z)}{a(z)} = K \frac{\check{b}(z)(z+1)}{\check{a}(z)(z-1)} = K \frac{\check{b}(z)(-1)^n \check{a}(-z)(z+1)}{\check{a}(z)(-1)^n \check{a}(-z)(z-1)} = \frac{\check{n}(z)(z+1)}{\check{d}(z)(z-1)} \quad (3.65)$$

$$\begin{aligned} \text{As } \check{b}(z)(-1)^n \check{a}(-z) &= \check{n}(z) \\ \check{a}(z)(-1)^n \check{a}(-z) &= \check{d}(z) \end{aligned}$$

Now, the lifted transfer function becomes

$$\begin{aligned} G(z^2) &= \frac{[\check{n}_1(z^2) + z^{-1}\check{n}_2(z^2)](z+1)}{\check{d}(z)(z-1)} = \frac{[\check{n}_1(z^2) + \check{n}_2(z^2)] + z^{-1}[z^2\check{n}_1(z^2) + \check{n}_2(z^2)]}{\check{d}(z)(z-1)} \\ &= \frac{[n_1(z^2) + z^{-1}n_2(z^2)]}{\check{d}(z)(z-1)} \end{aligned} \quad (3.66)$$

$$\begin{aligned} \text{as } [\check{n}_1(z^2) + \check{n}_2(z^2)] &= n_1(z^2) \\ [z^2\check{n}_1(z^2) + \check{n}_2(z^2)] &= n_2(z^2) \end{aligned} \quad (3.67)$$

Now, from (3.67) we get,

$$\begin{aligned} n_1 - n_2 &= -(z^2 - 1) \tilde{n}_1(z^2) \\ n_1 - z^{-2}n_2 &= z^{-2}(z^2 - 1) \tilde{n}_1(z^2) \end{aligned} \quad (3.68)$$

From (3.54) and (3.68) we get,

$$\begin{aligned} \begin{bmatrix} E_{e,ss} \\ E_{o,ss} \end{bmatrix} &= \lim_{z^2 \rightarrow 1} \frac{z^2}{\Delta} \begin{bmatrix} \Delta_c d + z^{-1}(z^2 - 1) \tilde{n}_1(z^2) C_{12} + z^{-2}(z^2 - 1) \tilde{n}_1(z^2) C_{22} \\ \Delta_c d + (z^2 - 1) \tilde{n}_1(z^2) C_{12} + z^{-1}(z^2 - 1) \tilde{n}_1(z^2) C_{22} \end{bmatrix} \\ &= \lim_{z^2 \rightarrow 1} \frac{z^2}{\Delta} \begin{bmatrix} \Delta_c d \\ \Delta_c d \end{bmatrix} \end{aligned} \quad (3.69)$$

From the above equation (3.69) we can see that the response has become ripple free.

3.5.1 Numerical example

Example 3.5.1: Considering the plant of Example 2.3.1, it will now be compensated to obtain a reduced order system with robust ripple-free steady-state step response.

It is observed that 2-DOF system provides better result in presence of a zero at -1 i.e. with augmentations $\frac{(z+1)}{z}$ and $\frac{(z+1)}{(z-1)}$ but results with augmentation $\frac{z}{(z-1)}$ are not satisfactory. controller parameter evaluation and step responses with augmentations $\frac{(z+1)}{z}$ and $\frac{(z+1)}{(z-1)}$ are presented below.

I. With Augmentation $\frac{(z+1)}{z}$

The augmented transfer function is

$$G(z) = \frac{(z+1)(z-1.2)}{z(z-0.5)(z-1.5)}$$

From (3.22) and (3.23), the order of the 2-periodic controller m is 2 and number of controller zeros is 4.

$$\begin{aligned} \hat{A}(z^2) &= -z^2(z^2 - 2.25)(z^2 - 0.25) \\ \hat{P}(z^2) &= z^2(z^2 - \alpha) \\ \hat{Z}(z^2) &= k_z z^6(z^2 - 0.25) \\ \check{D}(z^2) &= -z^4(z^2 - 0.25) \end{aligned}$$

It can be noted from above equations that 1 pole-zero cancellation is performed at origin. These cancellations can be done at any other location.

Variations on the performance of the controller with the location of pole-zero cancellation is discussed later.

The transfer function of overall system is

$$G_{loop1}(z) = \frac{z^2}{(z^2 - \alpha)(z^2 - 2.25)} \quad (3.70)$$

The root locus of system of (3.70) is shown below (fig. 3.5),

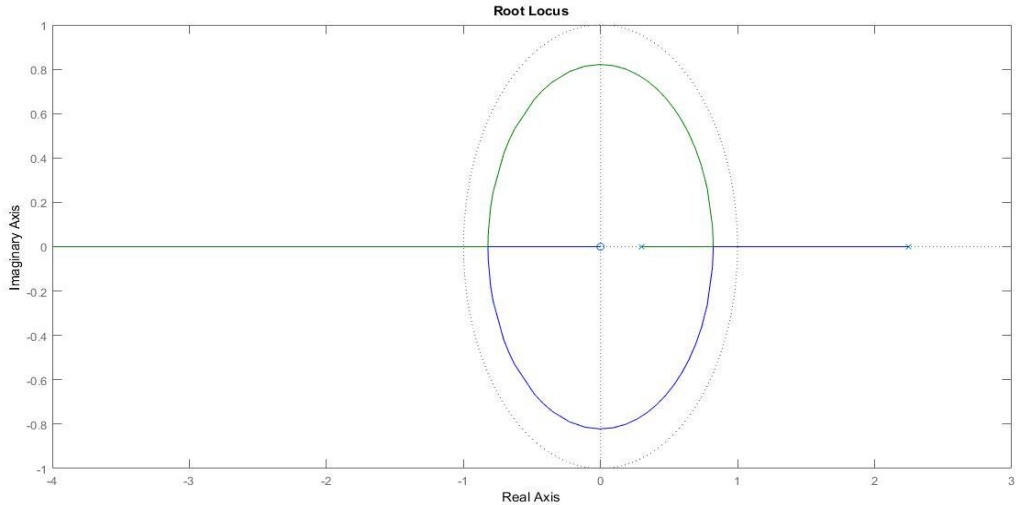


Fig. 3.5: Root locus of the system of (3.34) with $\alpha = 0.3$

Gain margin of overall system is calculated for different values of α . It is seen that as α comes closer to $z^2 = 0$, the gain margin decreases. The maximum gain margin is attained at $z^2 = 0.44$ (shown in fig. 3.2).

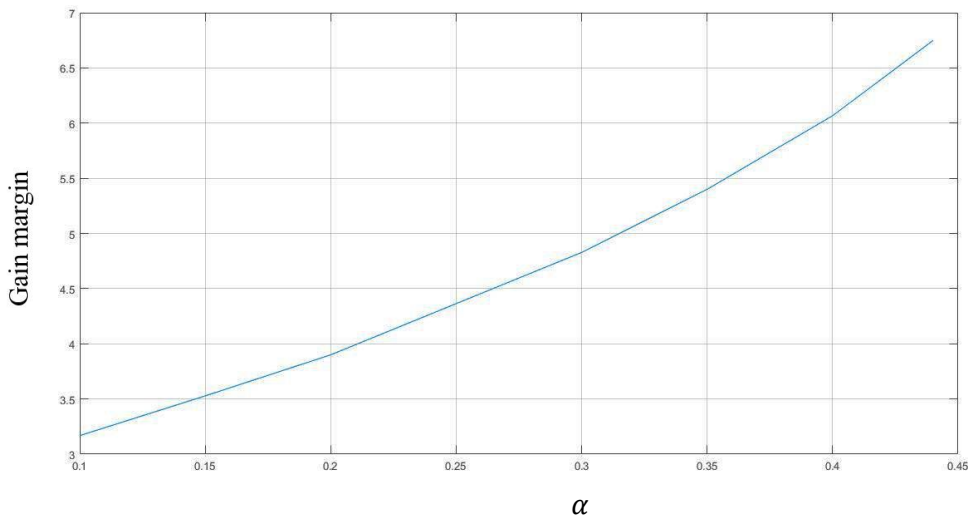


Fig. 3.6: Plot of gain margin with location of α

Now, response of the overall system i.e. $G_{loop1}(z)$ is recorded for different values of α with conditions $Q_0^+ = \pm Q_1^\pm$. It is observed that response curves follow the characteristics of non-minimum phase systems i.e. goes through undershoot initially and then rises upto the final value. Settling times and maximum peak undershoots are noted for all the conditions and a comparative study is presented on the performance of controller for different values of α . Plots showing these comparisons for aforesaid pole-zero cancellations at $z^2 = 0, 0.5, 0.75$ are given below.

Table 3.1: Variation of settling time and maximum peak undershoot with α for condition $Q_0^+ = Q_1^-$ and $Q_0^+ = -Q_1^-$ with pole-zero cancellation at $z^2 = 0$

| α | Condition | Settling time (t_s) | Maximum peak under shoot (%) |
|----------|------------------|-------------------------|------------------------------|
| 0.1 | $Q_0^+ = Q_1^-$ | 26 | 33.373 |
| | $Q_0^+ = -Q_1^-$ | 25 | 36.5 |
| 0.15 | $Q_0^+ = Q_1^-$ | 37 | 22.254 |
| | $Q_0^+ = -Q_1^-$ | 35 | 23.05 |
| 0.2 | $Q_0^+ = Q_1^-$ | 39 | 20.685 |
| | $Q_0^+ = -Q_1^-$ | 37 | 21.845 |
| 0.3 | $Q_0^+ = Q_1^-$ | 65 | 7.256 |
| | $Q_0^+ = -Q_1^-$ | 63 | 8.323 |
| 0.4 | $Q_0^+ = Q_1^-$ | 173 | 0.9445 |
| | $Q_0^+ = -Q_1^-$ | 171 | 1.068 |

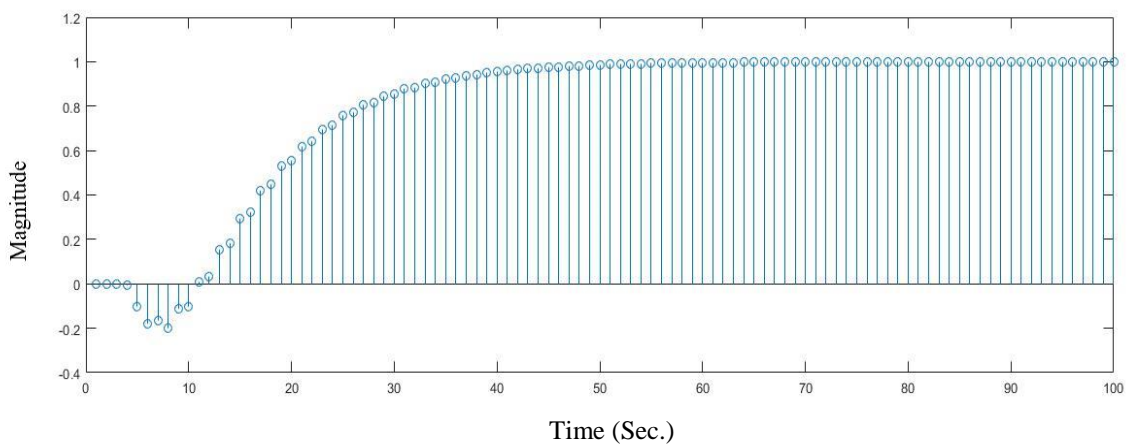


Fig. 3.7: Response using augmentation $\frac{z+1}{z}$ with $\alpha = 0.2$ for conditions $Q_0^+ = Q_1^-$ and $Q_0^+ = Q_1^+$ with pole-zero cancellation at $z^2 = 0$

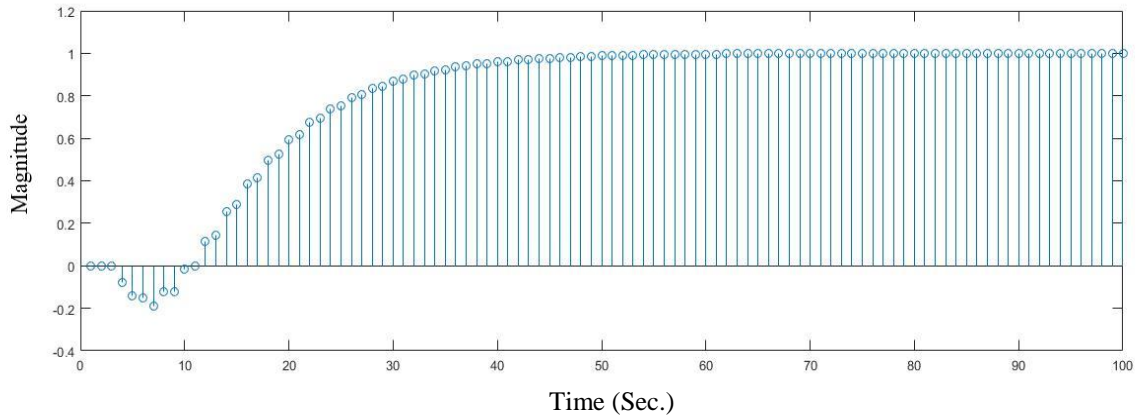


Fig. 3.8: Response using augmentation $\frac{z+1}{z}$ with $\alpha = 0.2$ for conditions $Q_0^+ = -Q_1^+$ and $Q_0^- = -Q_1^-$ with pole-zero cancellation at $z^2 = 0$

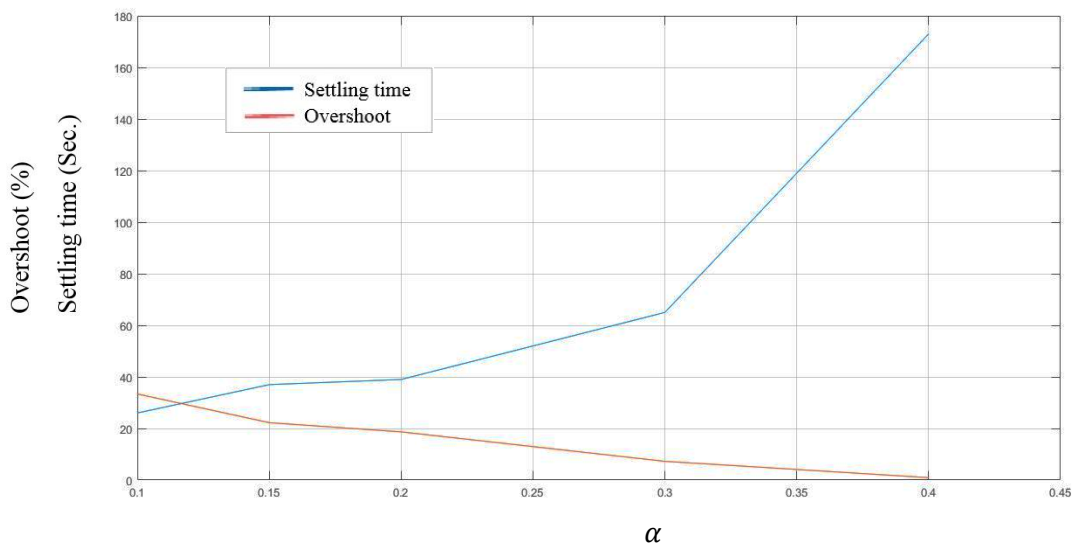


Fig. 3.9: Variation of settling time and maximum peak undershoot with α for condition $Q_0^+ = Q_1^-$ and $Q_0^+ = Q_1^+$ with pole-zero cancellation at $z^2 = 0$

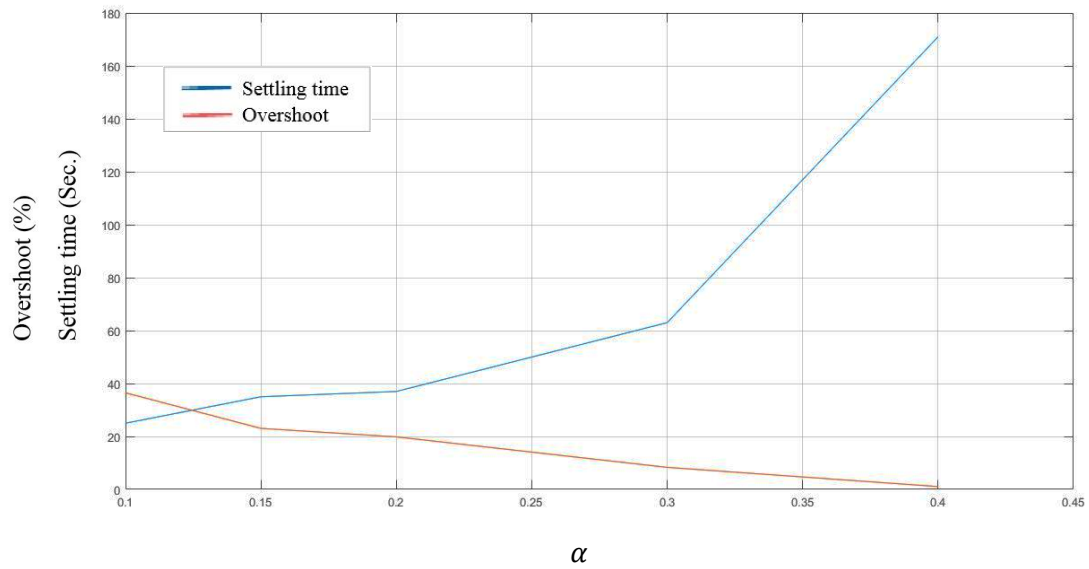


Fig. 3.10: Variation of settling time and maximum peak undershoot with α for condition $Q_0^+ = -Q_1^-$ and $Q_0^+ = -Q_1^+$ with pole-zero cancellation at $z^2 = 0$

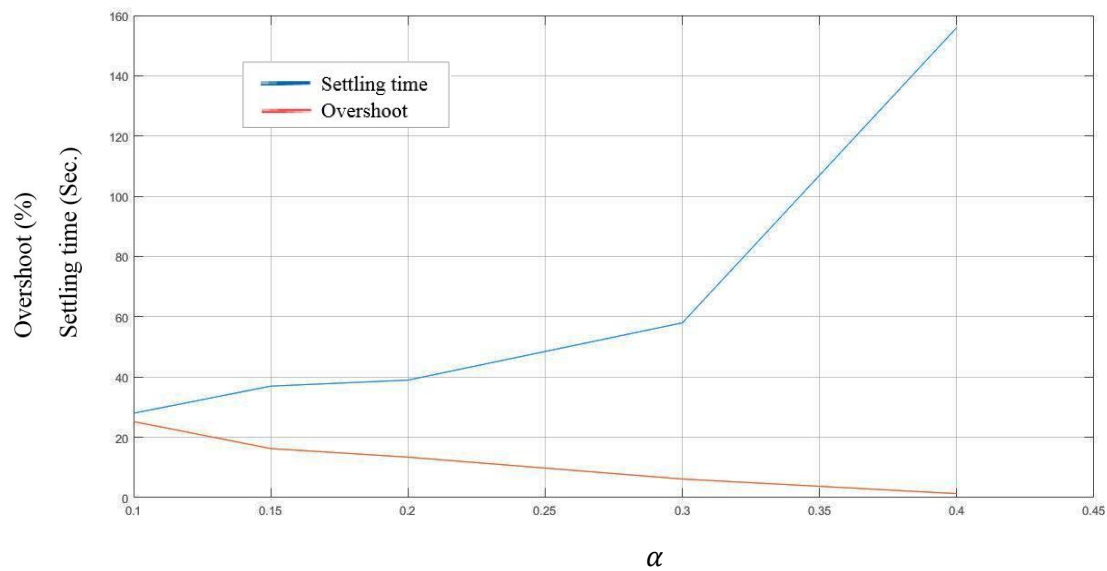


Fig. 3.11: Variation of settling time and maximum peak undershoot with α for condition $Q_0^+ = Q_1^-$ and $Q_0^+ = Q_1^+$ with pole-zero cancellation at $z^2 = 0.5$

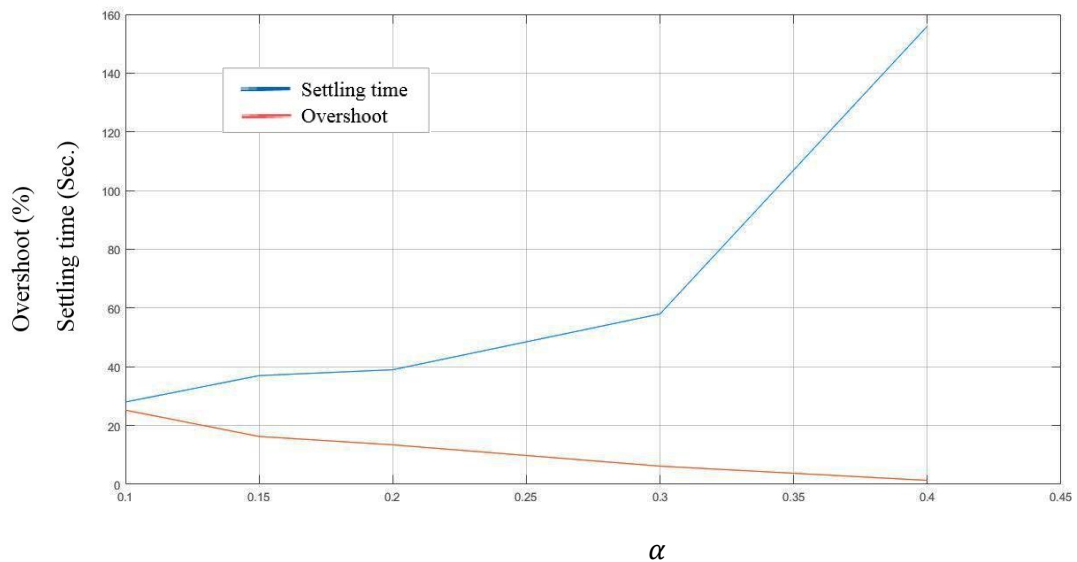


Fig. 3.12: Variation of settling time and maximum peak undershoot with α for condition $Q_0^+ = -Q_1^-$ and $Q_0^- = -Q_1^+$ with pole-zero cancellation at $z^2 = 0.5$

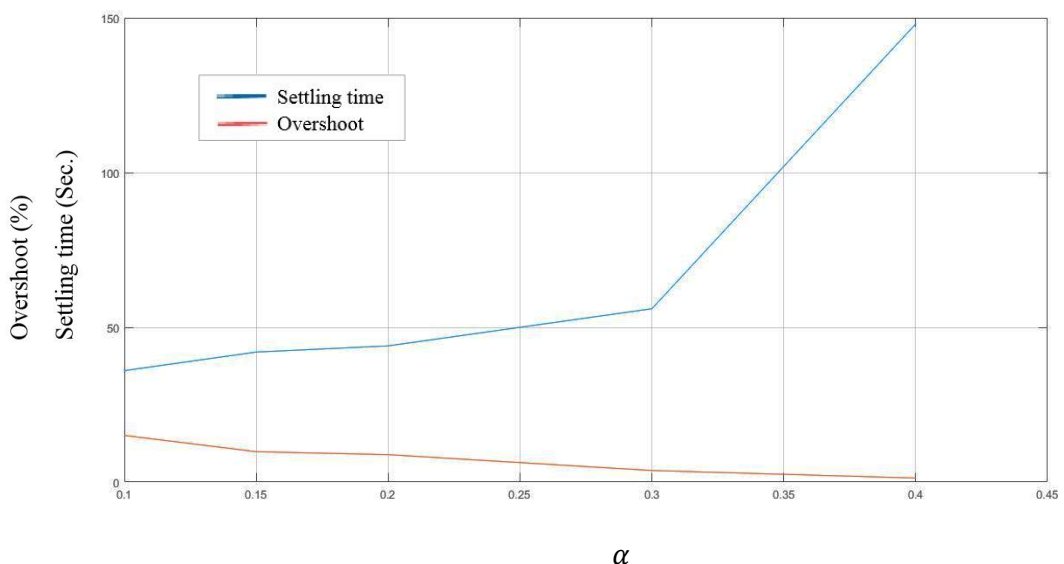


Fig. 3.13: Variation of settling time and maximum peak undershoot with α for condition $Q_0^+ = Q_1^-$ and $Q_0^- = Q_1^+$ with pole-zero cancellation at $z^2 = 0.75$

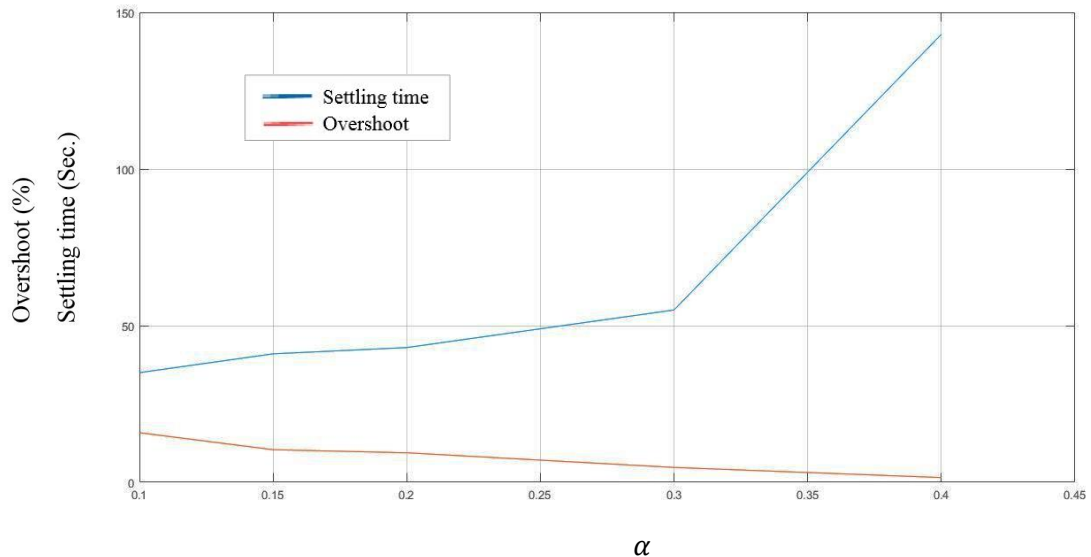


Fig. 3.14: Variation of settling time and maximum peak undershoot with α for condition $Q_0^+ = -Q_1^-$ and $Q_0^+ = -Q_1^+$ with pole-zero cancellation at $z^2 = 0.75$

II. With Augmentation $\frac{(z+1)}{(z-1)}$

The augmented transfer function is

$$G(z) = \frac{(z+1)(z-1.2)}{(z-0.5)(z-1)(z-1.5)}$$

From (3.22) and (3.23) the order of the 2-periodic controller m is 2 and number of controller zeros is 4

$$\begin{aligned}\hat{A}(z^2) &= -(z^2 - 1)(z^2 - 2.25)(z^2 - 0.25) \\ \hat{P}(z^2) &= z^4 \\ \hat{Z}(z^2) &= k_z z^4(z^2 - 0.25)(z^2 - \beta) \\ \check{D}(z^2) &= -z^4(z^2 - 0.25)\end{aligned}$$

It can be noted from above equations that 1 pole-zero cancellation is performed at origin. These cancellations can be done at any other location.

Variations on the performance of the controller with the location of pole-zero cancellation is discussed later.

The loop transfer function of overall system is

$$G_{loop2}(z) = \frac{(z^2 - \beta)}{(z^2 - 1)(z^2 - 2.25)} \quad (3.70)$$

Root locus corresponding to system (3.70) is shown in Fig. 3.13.

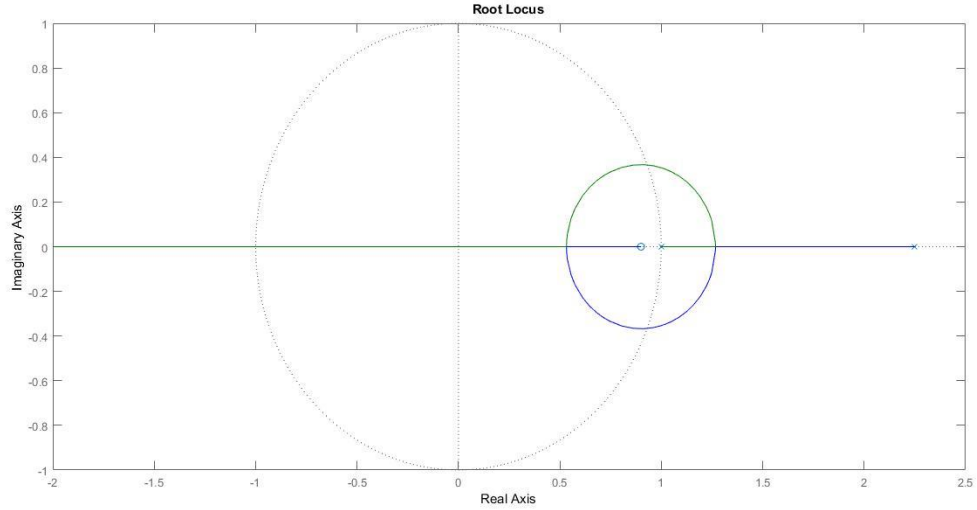


Fig. 3.15: Root locus of the system of (3.70) with $\beta = 0.9$

Gain margin of overall system is calculated for different values of β . It is seen that as β comes closer to $z^2 = 1$, the gain margin increases (as shown in Fig. 3.14).

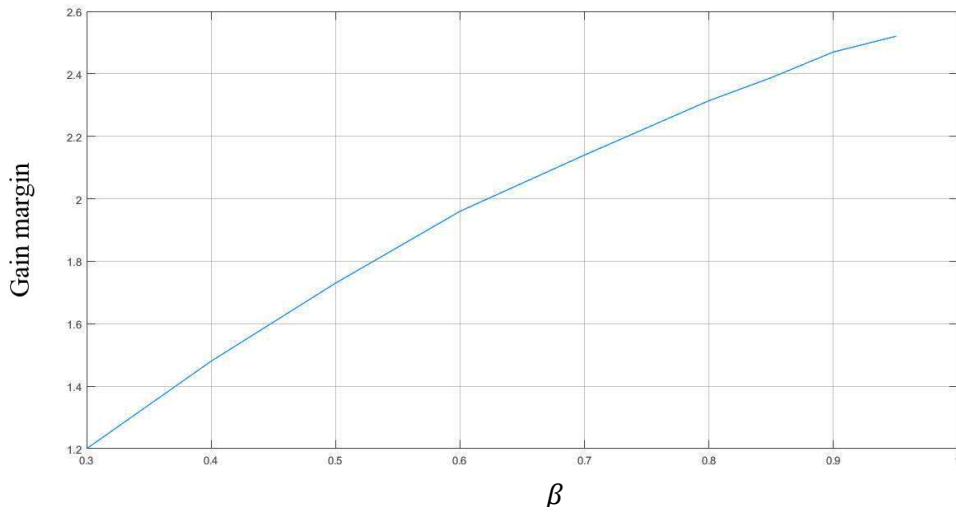


Fig. 3.16: Plot of gain margin with location of β

Now, response of the overall system i.e. $G_{loop2}(z)$ is recorded for different values of β with conditions $Q_0^+ = \pm Q_1^\pm$. Settling time and maximum peak undershoot are noted for all the conditions and a comparative study is presented on the performance of controller for different values of β . Plots showing these comparisons for aforesaid pole-zero cancellations at $z^2 = 0, 0.5, 0.75$ are given below.

Table 3.2: Variation of settling time and maximum peak undershoot with β for condition $Q_0^+ = Q_1^-$ and $Q_0^+ = -Q_1^-$ with pole-zero cancellation at $z^2 = 0$

| β | Condition | Settling time (t_s) | Maximum peak undershoot (%) |
|---------|------------------|-------------------------|-----------------------------|
| 0.7 | $Q_0^+ = Q_1^-$ | 18 | 81.89 |
| | $Q_0^+ = -Q_1^-$ | 16 | 83.25 |
| 0.8 | $Q_0^+ = Q_1^-$ | 20 | 47.1 |
| | $Q_0^+ = -Q_1^-$ | 19 | 47.5 |
| 0.85 | $Q_0^+ = Q_1^-$ | 22 | 34.25 |
| | $Q_0^+ = -Q_1^-$ | 21 | 35 |
| 0.9 | $Q_0^+ = Q_1^-$ | 27 | 25.8 |
| | $Q_0^+ = -Q_1^-$ | 26 | 26.18 |
| 0.95 | $Q_0^+ = Q_1^-$ | 39 | 13.5 |
| | $Q_0^+ = -Q_1^-$ | 38 | 13.638 |

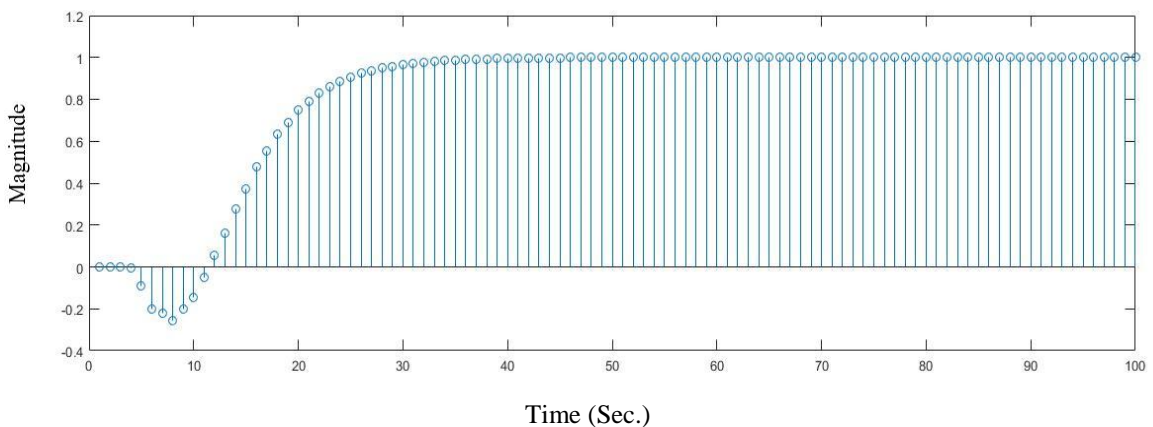


Fig. 3.17: Response using augmentation $\frac{(z+1)}{(z-1)}$ with $\beta = 0.9$ for conditions $Q_0^+ = Q_1^-$ and $Q_0^+ = Q_1^+$ with pole-zero cancellation at $z^2 = 0.5$

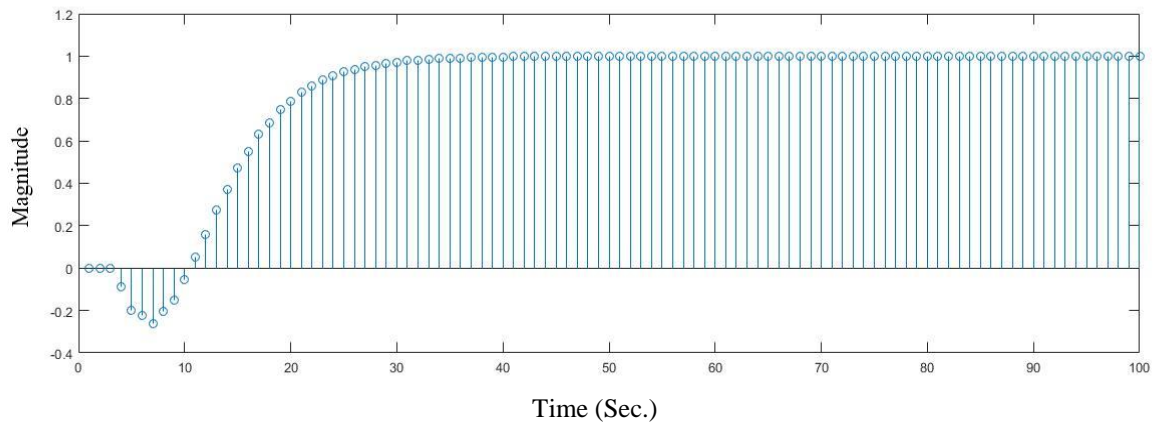


Fig. 3.18: Response using augmentation $\frac{(z+1)}{(z-1)}$ with $\beta = 0.9$ for conditions $Q_0^+ = -Q_1^+$ and $Q_0^- = -Q_1^-$ with pole-zero cancellation at $z^2 = 0.5$

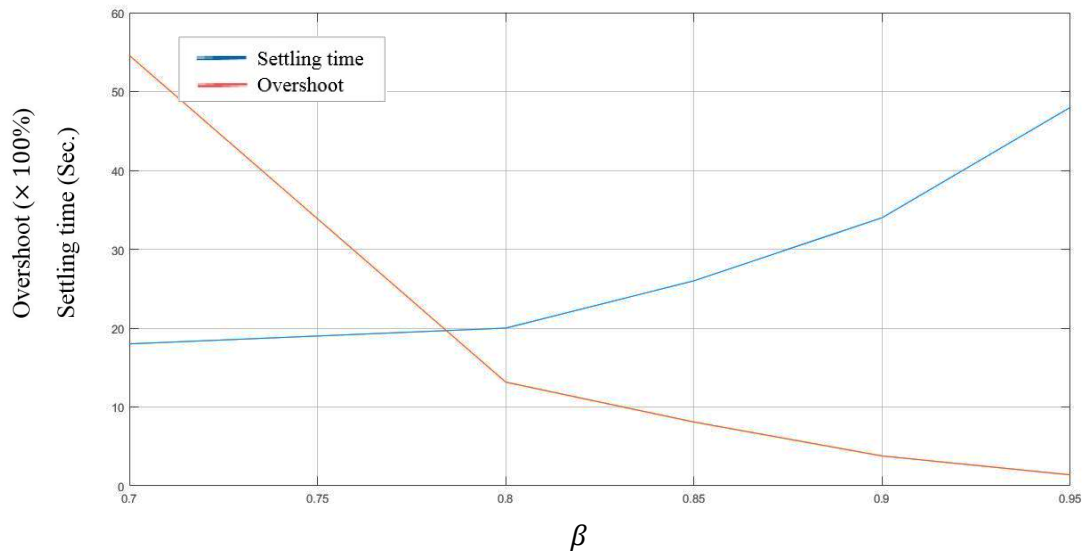


Fig. 3.19: Variation of settling time and maximum peak undershoot with β for condition $Q_0^+ = Q_1^-$ and $Q_0^- = Q_1^+$ with pole-zero cancellation at $z^2 = 0$

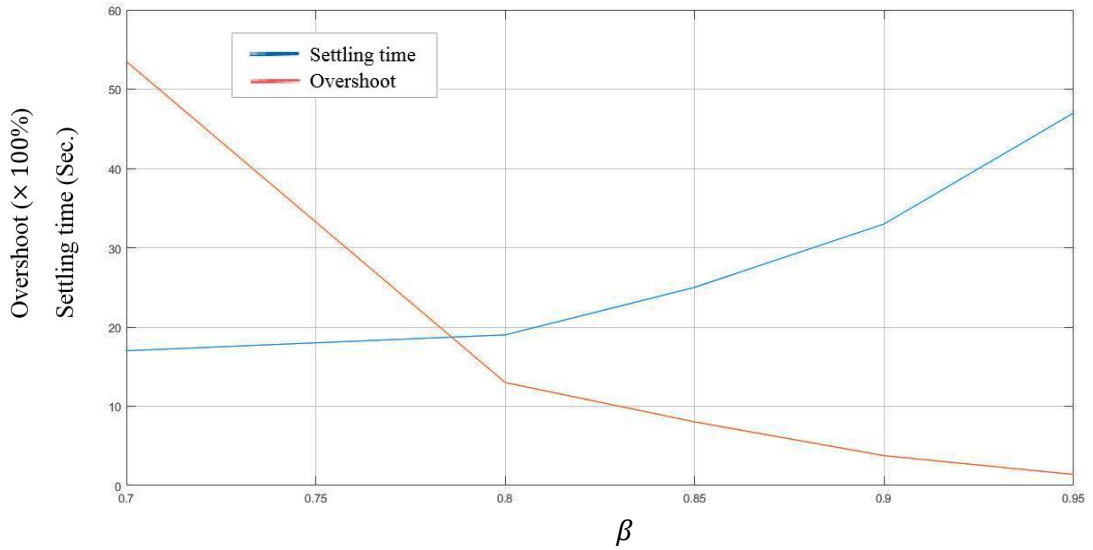


Fig. 3.20: Variation of settling time and maximum peak undershoot with β for condition $Q_0^+ = -Q_1^-$ and $Q_0^+ = -Q_1^+$ with pole-zero cancellation at $z^2 = 0$

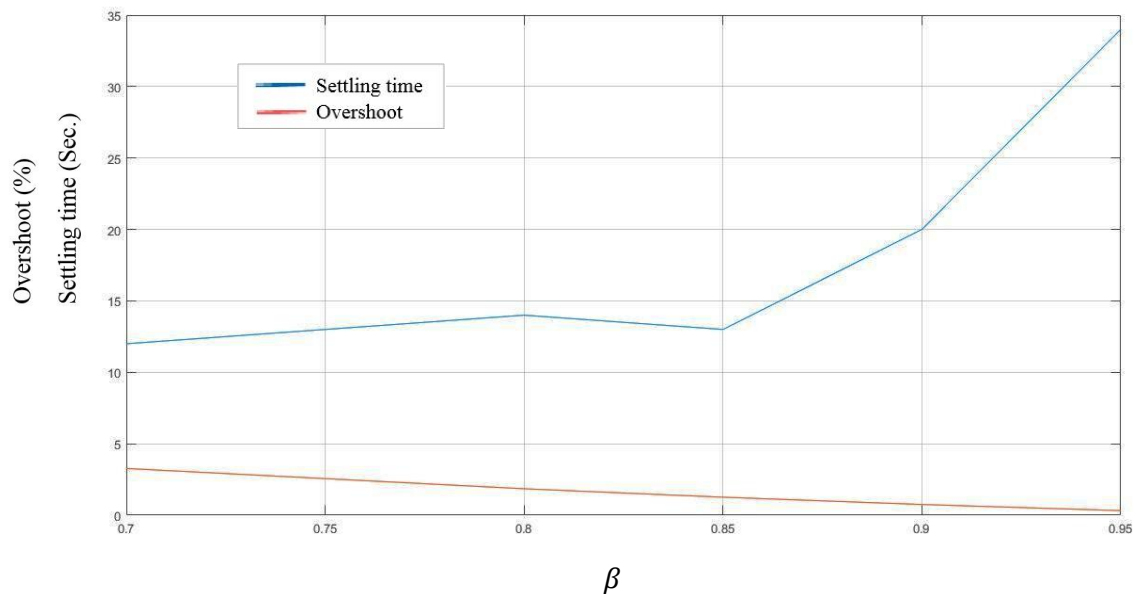


Fig. 3.21: Variation of settling time and maximum peak undershoot with β for condition $Q_0^+ = Q_1^-$ and $Q_0^+ = Q_1^+$ with pole-zero cancellation at $z^2 = 0.5$

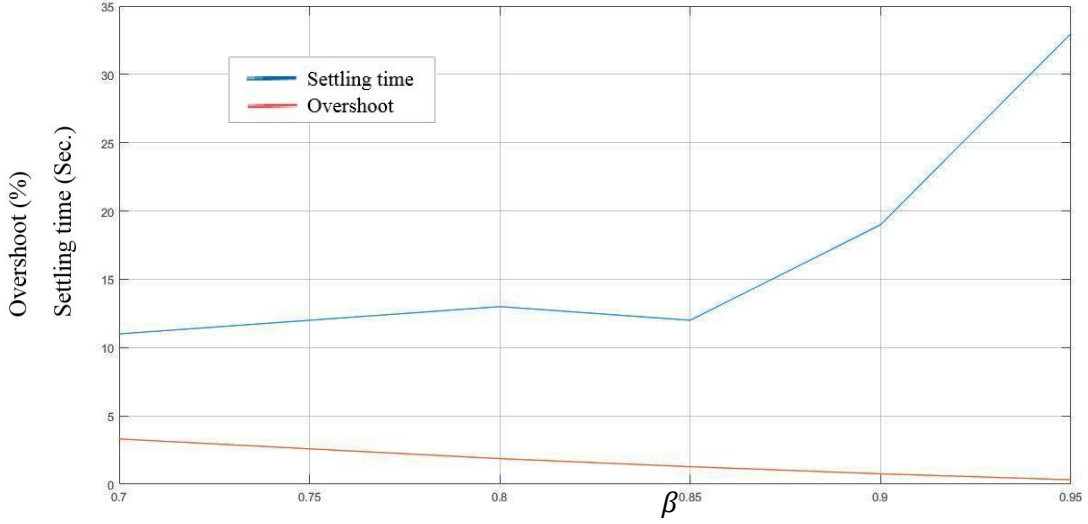


Fig. 3.22: Variation of settling time and maximum peak undershoot with β for condition $Q_0^+ = -Q_1^-$ and $Q_0^+ = -Q_1^+$ with pole-zero cancellation at $z^2 = 0.5$

Table 3.3: Comparison of settling time variation with 1-DOF and 2-DOF configuration with augmentation $\frac{z+1}{z}$ for conditions $Q_0^+ = Q_1^-$ and $Q_0^+ = -Q_1^-$

| Augmentation | Pole-zero cancellation at | α | Settling time (Sec.) | | | |
|-----------------|---------------------------|----------|----------------------|------------------|-----------------|------------------|
| | | | 1-DOF | | 2-DOF | |
| | | | $Q_0^+ = Q_1^-$ | $Q_0^+ = -Q_1^-$ | $Q_0^+ = Q_1^-$ | $Q_0^+ = -Q_1^-$ |
| $\frac{z+1}{z}$ | 0 | 0.1 | 28 | 29 | 26 | 25 |
| | | 0.15 | 38 | 39 | 37 | 35 |
| | | 0.2 | 44 | 45 | 39 | 37 |
| | | 0.3 | 72 | 73 | 65 | 63 |
| | | 0.4 | 180 | 185 | 173 | 171 |
| | 0.5 | 0.1 | 32 | 33 | 28 | 27 |
| | | 0.15 | 44 | 45 | 37 | 36 |
| | | 0.2 | 46 | 47 | 39 | 37 |
| | | 0.3 | 70 | 71 | 58 | 57 |
| | | 0.4 | 174 | 175 | 156 | 153 |

Table 3.4: Comparison of settling time variation with 1-DOF and 2-DOF configuration with augmentation $\frac{z+1}{z-1}$ for conditions $Q_0^+ = Q_1^-$ and $Q_0^+ = -Q_1^-$

| Augmentation | Pole-zero cancellation at | β | Settling time (Sec.) | | | |
|-------------------|---------------------------|---------|----------------------|------------------|-----------------|------------------|
| | | | 1-DOF | | 2-DOF | |
| | | | $Q_0^+ = Q_1^-$ | $Q_0^+ = -Q_1^-$ | $Q_0^+ = Q_1^-$ | $Q_0^+ = -Q_1^-$ |
| $\frac{z+1}{z-1}$ | 0 | 0.7 | 18 | 19 | 18 | 17 |
| | | 0.8 | 22 | 23 | 20 | 19 |
| | | 0.85 | 30 | 29 | 26 | 25 |
| | | 0.9 | 41 | 39 | 34 | 33 |
| | | 0.95 | 67 | 62 | 48 | 47 |
| | 0.5 | 0.7 | 24 | 29 | 18 | 16 |
| | | 0.8 | 28 | 33 | 20 | 19 |
| | | 0.85 | 32 | 37 | 22 | 21 |
| | | 0.9 | 40 | 45 | 27 | 26 |
| | | 0.95 | 60 | 63 | 39 | 38 |

3.6 Chapter Summary

This chapter discusses the synthesis of 2-DOF, 2-periodic controller and shows how the additional freedom can be utilized to tune the output response by cancelling undesired additional closed-loop poles. A numerical example, same as that used for 1-DOF case, is used illustrate the fact. The results indicate noticeable improvement in time response while the loop robustness properties remain the same.

CHAPTER 4

Stabilization of CIPS: A comparative study

4.1. Introduction

The stabilization of cart-inverted pendulum system (CIPS) is a benchmark problem of control system. It is a simple system consisting of a D.C. Motor, a pendant type pendulum, a cart, and a driving mechanism, shown in Fig.4.1. It is a single input multiple output (SIMO) system. Voltage is applied to the D.C. motor is taken as input signal while the angular position of the pendulum and position co-ordinate of the cart are the outputs.

There are several control challenges, like it is a non-linear, non-minimum phase, under-actuated system and the pendulum is highly unstable at the upright position. Track length and control voltage levels are the additional constraints on the system.

4.2. Mathematical model of cart-inverted pendulum system (CIPS)

The mechanical system has 2 Degrees of freedom, the linear motion of the cart in the X-axis, the rotational motion of the pendulum in the X-Y plane. Thus there will be two dynamic equations. The parametric representation of cart-inverted pendulum system is shown in figure 4.1.

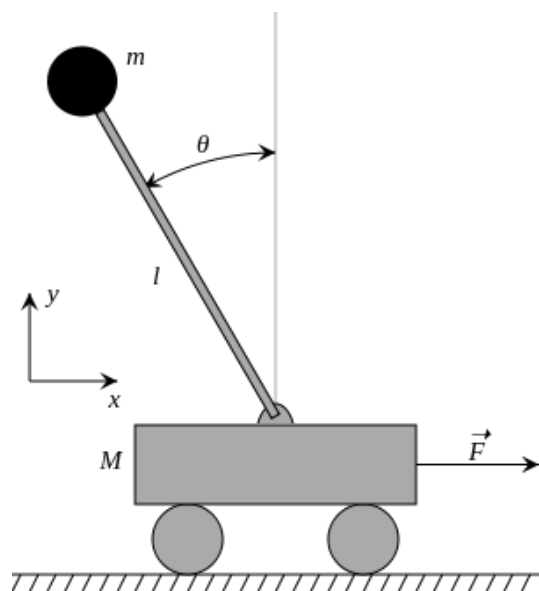


Fig. 4.1: Cart-inverted pendulum system

Let, M = Cart mass in kg

m = Pendulum mass in kg

l = Pendulum stick length in m

θ = Pendulum angle

x = Cart position co-ordinate

F = Force applied to the cart

And J = Pendulum inertia in $\text{kg}\cdot\text{m}^2$

g = Gravitational force in m/sec^2

H = Net horizontal force

V = Net vertical force

b = Damping constant in Ns/m

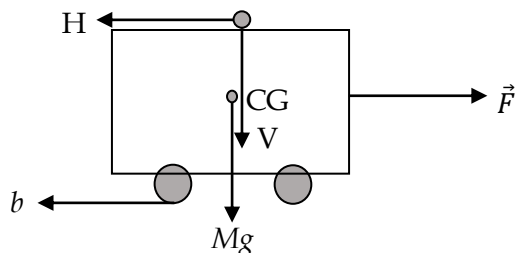


Fig. 4.2: Free body diagram of cart

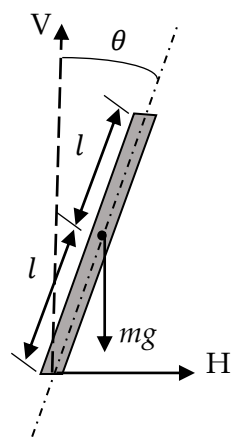


Fig. 4.3: Free body diagram of pendulum

From figure 4.2, force balance in the horizontal direction of the cart (M),

$$M \frac{d^2x}{dt^2} = F - H - b \frac{dx}{dt} \quad (4.1)$$

Now, force balance in the horizontal direction of the centre of gravity of the cart due to pendulum mass (m) yields

$$m \frac{d^2x}{dt^2} + ml \frac{d^2\theta}{dt^2} \cos \theta - ml \left(\frac{d\theta}{dt} \right)^2 \sin \theta = H \quad (4.2)$$

From figure 4.3, force balance in the vertical direction of the centre of gravity of the pendulum mass (m)

$$-(ml \frac{d^2\theta}{dt^2} \sin \theta + ml \left(\frac{d\theta}{dt} \right)^2 \cos \theta + mg) = V \quad (4.3)$$

Torque balance at the centre of gravity of the pendulum mass (m)

$$J \frac{d^2\theta}{dt^2} = Vl \sin \theta - Hl \cos \theta \quad (4.4)$$

Let us assume rail and air friction to be zero and considering $\theta \ll 1$ to linearize the system.

$$\therefore \sin \theta \cong \theta \quad \text{and} \quad \cos \theta \cong 1$$

Substituting V from equation (4.3) to (4.4) and H from (4.2) to (4.1) and using linearizing condition mentioned above, we get dynamic equations of the system as

$$(J + ml^2) \frac{d^2\theta}{dt^2} + mgl \sin \theta + ml \frac{d^2x}{dt^2} \sin \theta = 0 \quad (4.5)$$

$$(M + m) \frac{d^2x}{dt^2} + b \frac{dx}{dt} + ml \frac{d^2\theta}{dt^2} \cos \theta - ml \left(\frac{d\theta}{dt} \right)^2 \sin \theta = F \quad (4.6)$$

Performing Laplace Transform on equations (4.5) and (4.6) we get the transfer functions as

$$\frac{X(s)}{F(s)} = \frac{(J+ml^2)s^2-mgl}{s^2[J(M+m)+Mml^2}s^2-mgl(M+m)]} \quad (4.7)$$

$$\frac{\theta(s)}{F(s)} = \frac{-ml}{[J(M+m)+Mml^2}s^2-mgl(M+m)} \quad (4.8)$$

$$\frac{X(s)}{\theta(s)} = \frac{(J+ml^2)s^2-mgl}{mls^2} \quad (4.9)$$

Let, $x_1 = \theta$, $x_2 = \dot{\theta}$

and $x_3 = x$, $x_4 = \dot{x}$

Now, the equivalent non-linear state space model can be written as,

$$\begin{bmatrix} \dot{x}_1 \\ \dot{x}_2 \\ \dot{x}_3 \\ \dot{x}_4 \end{bmatrix} = \begin{bmatrix} 0 & 1 & 0 & 0 \\ \frac{g(m+M)ml}{J(M+m)+Mml^2} & 0 & 0 & 0 \\ 0 & 0 & 0 & 1 \\ \frac{-gm^2l^2}{J(M+m)+Mml^2} & 0 & 0 & 0 \end{bmatrix} \begin{bmatrix} x_1 \\ x_2 \\ x_3 \\ x_4 \end{bmatrix} + \begin{bmatrix} 0 \\ -\frac{ml}{J(M+m)+Mml^2} \\ 0 \\ \frac{J+ml^2}{J(M+m)+Mml^2} \end{bmatrix} F$$

and $\begin{bmatrix} y_1 \\ y_2 \end{bmatrix} = \begin{bmatrix} 1 & 0 & 0 & 0 \\ 0 & 0 & 1 & 0 \end{bmatrix} \begin{bmatrix} x_1 \\ x_2 \\ x_3 \\ x_4 \end{bmatrix}$ (4.10)

Values of plant parameters are taken from [40] and given in the following table.

Table 4.1: Inverted pendulum system parameters from [40]

| Parameter | Value |
|-----------------------------------|-----------------------|
| Cart mass (M) | 2.4 kg |
| Pendulum mass (m) | 0.23 kg |
| Pendulum stick length (l) | 0.36 m |
| Acceleration due to gravity (g) | 9.81 m/s ² |
| Pole moment of inertia (J) | 0.03 kgm ² |
| Cart friction coefficient (b) | 0.05 Ns/m |
| Motor voltage to force factor (k) | 8 N/V |

4.2.1 CIPS model in continuous-time domain

Substitution of parameters from Table 4.1 in the transfer functions of equations (4.7), (4.8), (4.9),

$$\frac{X(s)}{F(s)} = \frac{3.1047(s+2.511)(s-2.511)}{s^2(s+2.537)(s-2.537)} \quad (4.11)$$

$$\frac{\theta(s)}{F(s)} = \frac{-1.9957}{(s+2.537)(s-2.537)} \quad (4.12)$$

$$\frac{X(s)}{\theta(s)} = \frac{-1.5557(s+2.511)(s-2.511)}{s^2} \quad (4.13)$$

Substitution of parameters from Table 4.1 in the state space model of equation (4.10), we get,

$$\begin{bmatrix} \dot{x}_1 \\ \dot{x}_2 \\ \dot{x}_3 \\ \dot{x}_4 \end{bmatrix} = \begin{bmatrix} 0 & 1 & 0 & 0 \\ 14.2002 & 0 & 0 & 0 \\ 0 & 0 & 0 & 1 \\ -0.4471 & 0 & 0 & 0 \end{bmatrix} \begin{bmatrix} x_1 \\ x_2 \\ x_3 \\ x_4 \end{bmatrix} + \begin{bmatrix} 0 \\ -0.5504 \\ 0 \\ 0.3976 \end{bmatrix} F$$

and $\begin{bmatrix} y_1 \\ y_2 \end{bmatrix} = \begin{bmatrix} 1 & 0 & 0 & 0 \\ 0 & 0 & 1 & 0 \end{bmatrix} \begin{bmatrix} x_1 \\ x_2 \\ x_3 \\ x_4 \end{bmatrix}$ (4.14)

4.2.2 CIPS model in discrete-time domain

In practice, the pendulum angle and the cart position are measured as a function of continuous-time. But discrete-time periodic controller or LTI controllers work with discrete-time signals. So, the outputs of the plant should be sampled at suitable sample rate and fed to the discrete-time controller. The controller generates the signal in discrete-time domain. This signal is then passed through a hold device (generally zero order hold) to convert it to continuous-time domain and fed as input to the plant. In discrete-time domain plant dynamics depends on the choice of sampling time. A study on the choice of sampling time is presented in [42] and it is found that a choice of 25 msec. provides the best result.

So, discretizing the plant of equation (4.14) using a zero order hold device with sampling time 25 msec.

$$\begin{bmatrix} \dot{x}_1 \\ \dot{x}_2 \\ \dot{x}_3 \\ \dot{x}_4 \end{bmatrix} = \begin{bmatrix} 1.004 & 0.02504 & 0 & 0 \\ 0.3555 & 1.004 & 0 & 0 \\ -0.00014 & 0 & 1 & 0.025 \\ -0.01119 & -0.00014 & 0 & 1 \end{bmatrix} \begin{bmatrix} x_1 \\ x_2 \\ x_3 \\ x_4 \end{bmatrix} + \begin{bmatrix} -0.00017 \\ -0.01378 \\ 0.000124 \\ 0.00994 \end{bmatrix} F$$

and $\begin{bmatrix} y_1 \\ y_2 \end{bmatrix} = \begin{bmatrix} 1 & 0 & 0 & 0 \\ 0 & 0 & 1 & 0 \end{bmatrix} \begin{bmatrix} x_1 \\ x_2 \\ x_3 \\ x_4 \end{bmatrix}$ (4.15)

Discretizing transfer functions of equations (4.11), (4.12) and (4.13), we get,

$$\frac{X(z)}{F(z)} = \frac{0.00097023(z+1)(z-1.065)(z-0.9392)}{(z-1)^2(z-0.9385)(z-1.065)} \quad (4.16)$$

$$\frac{\theta(z)}{F(z)} = \frac{-0.00062387(z+1)}{(z-1.065)(z-0.9385)} \quad (4.17)$$

$$\frac{X(z)}{\theta(z)} = \frac{-1.5557(z-0.9382)(z-1.064)}{(z-1)^2} \quad (4.18)$$

4.3 Control Techniques for Cart-Inverted Pendulum System

Several methods have been described in literature for the stabilization of the cart-inverted pendulum system. These are classical control techniques, like frequency response method, the root locus method, PID control, Linear Quadratic Regulator (LQR) control etc. or intelligent control approaches, such as fuzzy logic control, neural network control, hybrid control etc. or linear time invariant control [35-39,42].

In this section, two types of control structures are considered for the stabilization of cart-inverted pendulum system,

- i. state-feedback control
- ii. 2-loop LTI control

To make the design practically implementable, the following constraints have been imposed on the design,

- i. Rail length limit: ± 0.5 m
- ii. Range of control signal: ± 2.5 V
- iii. The generated mechanical force range: ± 20 N.

And an initial condition of pendulum angle $\theta = 0.05$ rad. is taken for the design.

4.3.1 State-feedback Control

State-feedback control is a method where the controller is placed at the feedback path and system states are used to generate a control signal (shown in fig. 4.4). Among various state-feedback approaches linear quadratic regulator (LQR) method is selected to stabilize cart-inverted pendulum system. To derive the control signal by LQR algorithm, a cost function and weighting factors need to be considered. The algorithm finds the matrix K (fig 4.4) to find the minimum cost i.e. to optimize the controller.

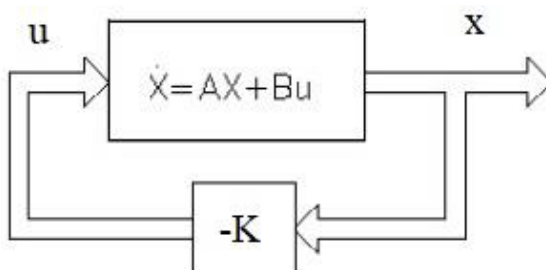


Fig. 4.4: State-feedback controller

From fig. 4.4, the LQR control signal can be determined by,

$$u = -(Kx) \quad (4.19)$$

And the cost function is,

$$J = -\frac{1}{2} \int_0^{\infty} (e^T Q e + u^T R u) dt \quad (4.20)$$

where, Q and R are the weighting matrices.

Considering, model of cart-inverted pendulum system of equation (4.15). To optimize the controller using the quadratic cost function of (4.20) with

$$Q = \begin{bmatrix} 1 & 0 & 0 & 0 \\ 0 & 1 & 0 & 0 \\ 0 & 0 & 1 & 0 \\ 0 & 0 & 0 & 1 \end{bmatrix} \quad \text{and} \quad R = 1$$

We obtain the gain vector $K = [-62.3848 \ -16.6566 \ -0.8991 \ -2.7412]$

Response of the optimized system is shown below (fig. 4.5)

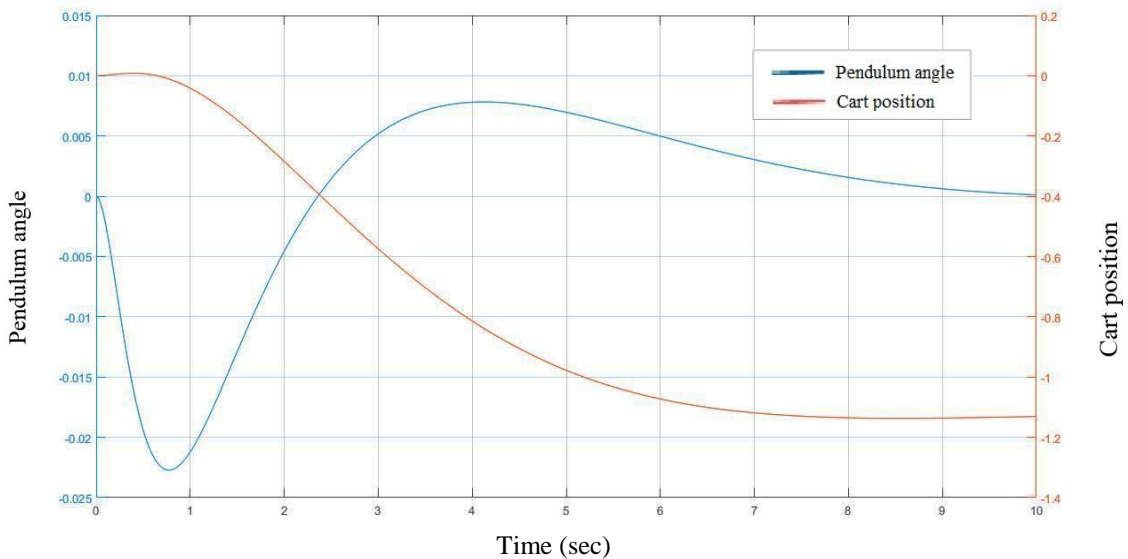


Fig. 4.5: Response of the optimized system showing pendulum angle and cart position

4.3.2 Two-loop LTI Control

The cascade representation of the cart-inverted pendulum system using 2-loop control structure is shown in figure 4.6. The system contains two loops for two control variables i.e. the pendulum angle (θ) and the cart position (x). These two variables are controlled using two different LDTI controllers placed in feedback path.

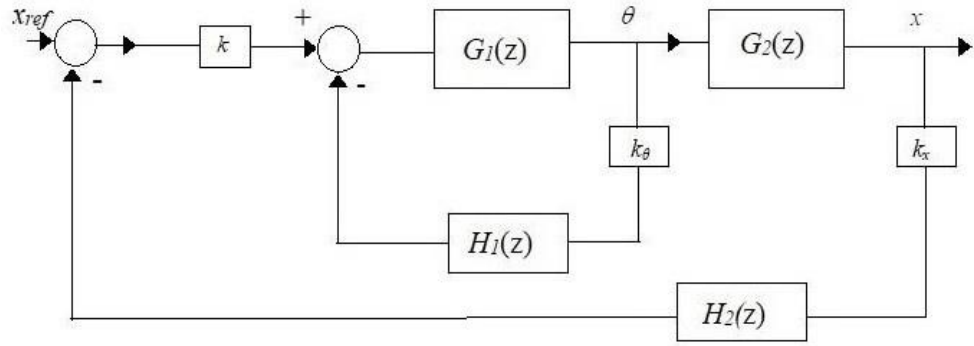


Fig. 4.6: 2-looop control structure for cart-inverted pendulum system

From figure 4.6 and equations (4.17), (4.18) we get,

$$G_1(z) = \frac{\theta(z)}{F(z)} = \frac{-0.00062387(z+1)}{(z-1.065)(z-0.9385)}$$

$$G_2(z) = \frac{X(z)}{\theta(z)} = \frac{-1.5557(z-0.9382)(z-1.064)}{(z-1)^2}$$

And k is the motor voltage to force factor, k_θ and k_x are sensor gains of θ -feedback and x -feedback paths respectively.

Let,

$$\text{the inner loop controller } H_1(z) = K_3 + \frac{K_4}{z} \quad (4.21)$$

$$\text{the inner loop controller } H_2(z) = K_1 + \frac{K_2}{z} \quad (4.22)$$

The parameters K_1 , K_2 , K_3 and K_4 are obtained by placing closed-loop poles in desired locations using root-locus technique. Based on the 2-loop control method, H_1 is designed first to make inner loop stable and then H_2 is evaluated to compensate the overall closed-loop system. The root locus plots and simulation results using different H_1 and H_2 are presented.

Case 1: The inner loop LDTI controller (H_1) is chosen as

$$H_1 = \frac{-378.3512(z-0.8507)}{z} \quad (4.23)$$

Gain margin (GM) is calculated as $GM = \frac{k_{max}}{k_{min}} = 73.53$

The root locus plots of the inner loop is shown in figure 4.7

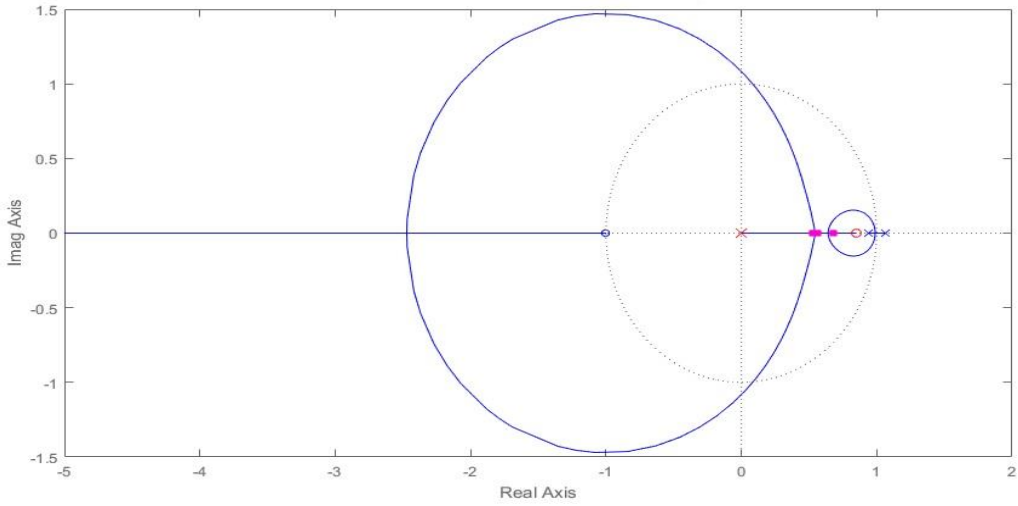


Fig. 4.7: Root locus of inner loop

Choosing H_2 as

$$H_2 = \frac{-170.81(z-0.9577)}{z} \quad (4.24)$$

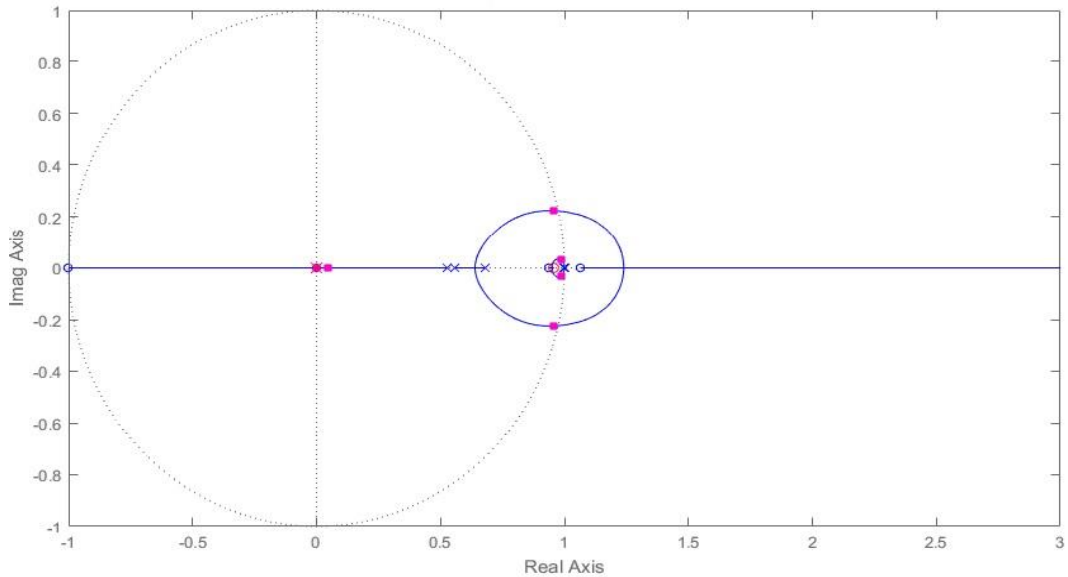


Fig. 4.8: Root locus of outer loop using controller H_2 of case 1.1

As k_{min} is not present in the root locus of figure 4.8, taking gain margin (GM) as

$$GM = \frac{k_{max}}{k_{opt}} = 1.093$$

Where, k_{opt} is the gain in which the system is operating.

Simulation results using LDTI controllers H_1 and H_2 of equations (4.23) and (4.24) are shown next.

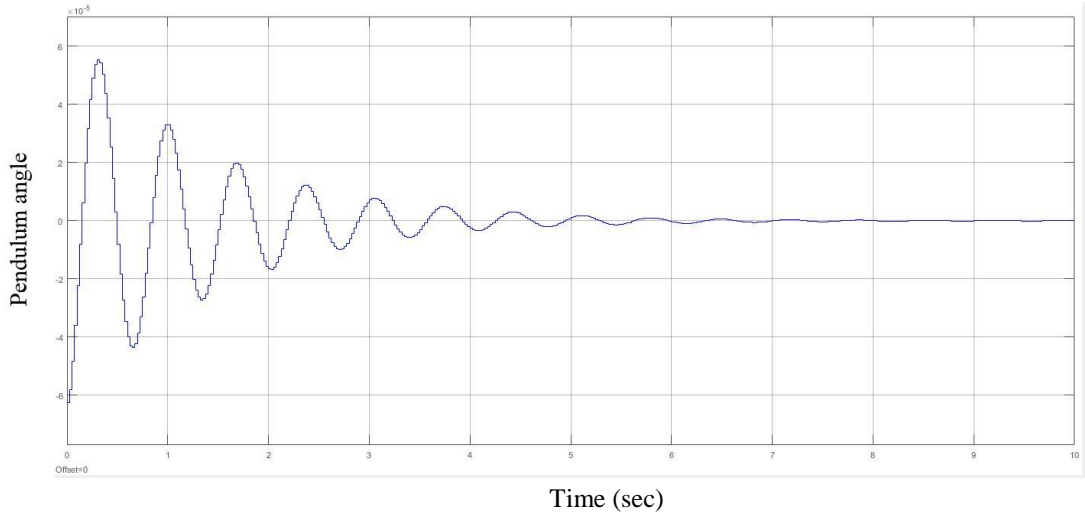


Fig. 4.9: Response of pendulum angle for case 1.1 using $k = k_\theta = k_x = 1$

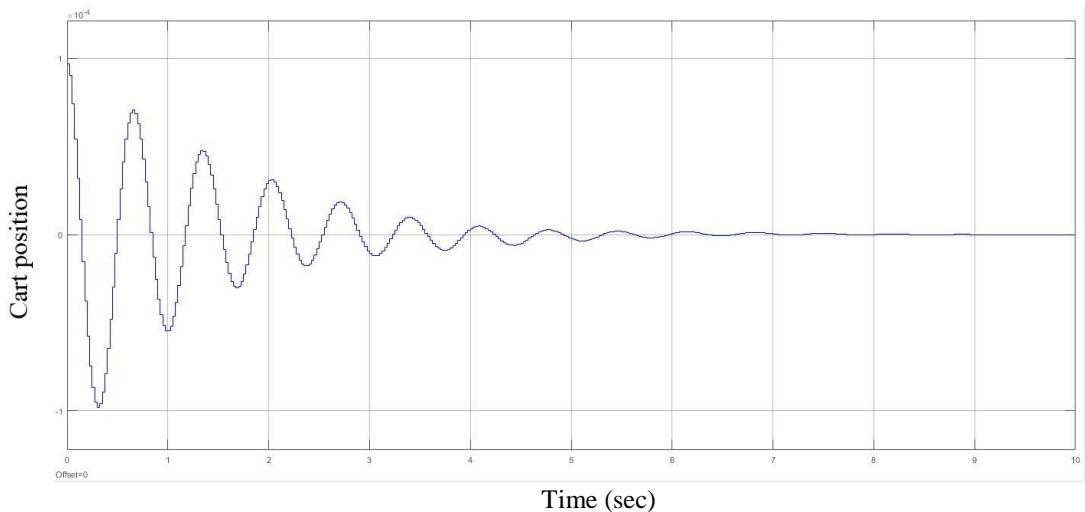


Fig. 4.10: Response of cart position for case 1.1 using $k = k_\theta = k_x = 1$

Case 2: The inner loop LDTI controller (H_1) is chosen as

$$H_1 = \frac{-292.47(z-0.9385)}{z} \quad (4.27)$$

Gain margin (GM) is calculated as $GM = \frac{k_{max}}{k_{min}} = 30.3568$

The root locus plots of the inner loop is shown in figure 4.11

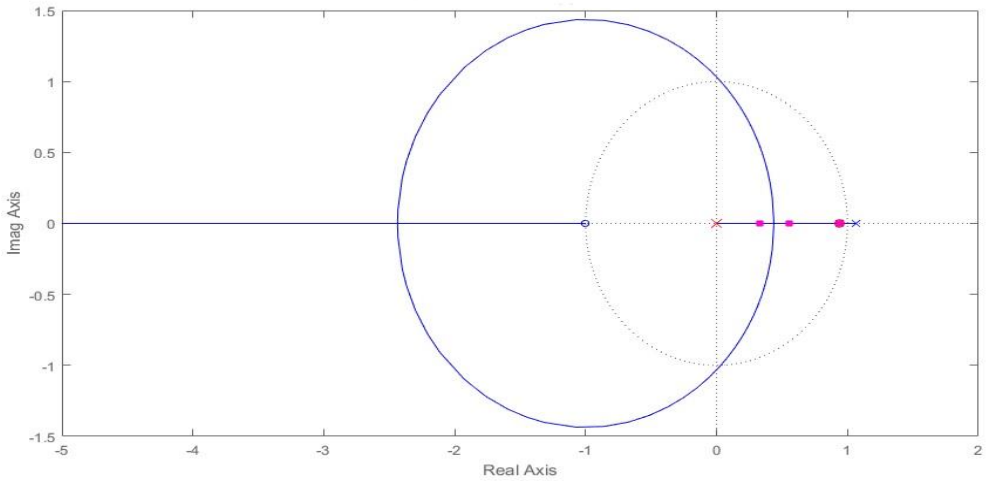


Fig. 4.11: Root locus of inner loop

Choosing H_2 as

$$H_2 = \frac{-110.02(z-0.9864)}{z} \quad (4.28)$$

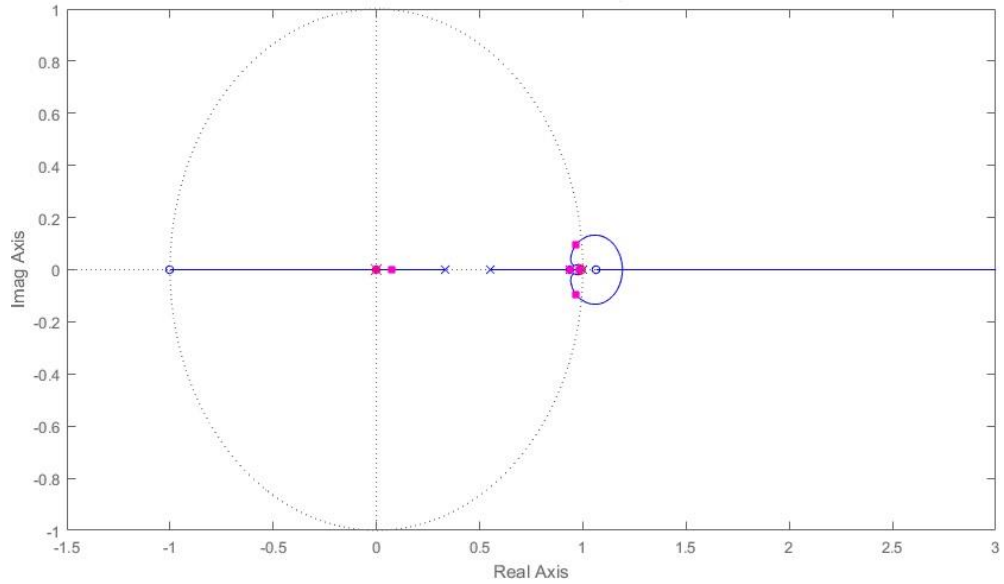


Fig. 4.12: Root locus of outer loop using controller H_2 of case 2.1

As k_{min} is not present in the root locus of figure 4.16, taking gain margin (GM) as

$$GM = \frac{k_{max}}{k_{opt}} = 1.2169$$

Where, k_{opt} is the gain in which the system is operating.

Simulation results using LDTI controllers H_1 and H_2 of equations (4.27) and (4.28) are shown below

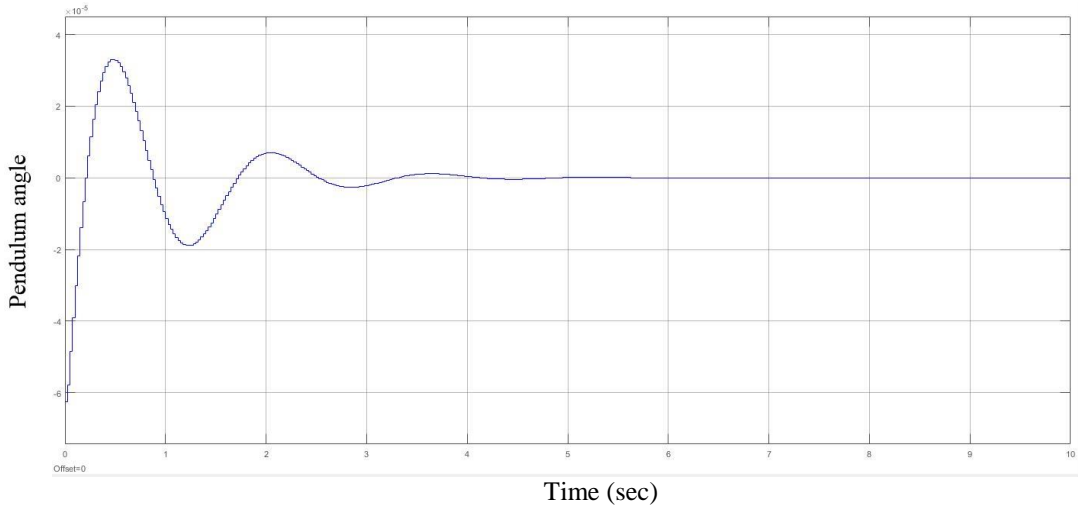


Fig. 4.13: Response of pendulum angle for case 2.1 using $k = k_\theta = k_x = 1$

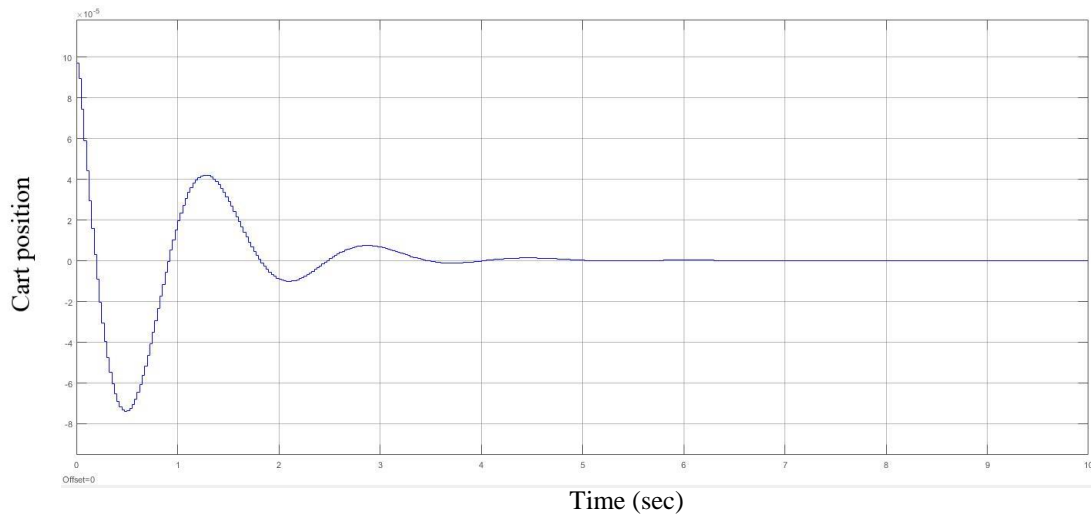


Fig. 4.14: Response of cart position for case 2.1 using $k = k_\theta = k_x = 1$

Table 4.2: Variation of settling time with the choice of the inner and the outer loop LDTI controller

| Inner loop LDTI controller (H_1) | Inner loop gain margin | Outer loop LDTI controller (H_2) | Outer loop gain margin | Settling time (sec.) | |
|--------------------------------------|------------------------|--------------------------------------|------------------------|----------------------|---------------|
| | | | | Pendulum angle | Cart position |
| $\frac{-378.3512(z - 0.8507)}{z}$ | 73.53 | $\frac{-170.81(z - 0.9577)}{z}$ | 1.093 | 5.6 | 6 |
| | | $\frac{-95.793(z - 0.9577)}{z}$ | 1.9488 | 1 | 7.5 |
| | | $\frac{-6.4568(z - 0.9577)}{z}$ | 28.912 | 0.4 | 170 |

| | | | | | |
|---------------------------------|---------|---------------------------------|---------|-----|------|
| $\frac{-292.47(z - 0.9385)}{z}$ | 30.3568 | $\frac{-110.02(z - 0.9864)}{z}$ | 1.2169 | 3.9 | 3.4 |
| | | $\frac{-34.594(z - 0.9864)}{z}$ | 3.9 | 4.2 | 10.8 |
| | | $\frac{-3.6976(z - 0.9864)}{z}$ | 36.5047 | 1.2 | 125 |

4.3.3 Design of a 2-periodic Controller

It can be observed from (4.17) and (4.18) that the outer loop transfer function of cart-inverted pendulum system contains a non-minimum phase zero and double pole at 1. As we know, LDTI controllers cannot relocate system zeros and it remains unaltered in closed loop transfer function. As a result, gain margin becomes very poor (can be observed from figures 4.8, 4.12 and 4.16). In this section, the outer loop of cart-inverted pendulum system is compensated using 2-periodic controller and thus gain margin is improved.

4.3.3.1 Design of a 1-DOF 2-periodic Controller

Following figure shows the block diagram of a cart-inverted pendulum system compensated by a 1-DOF 2-periodic controller in outer loop.

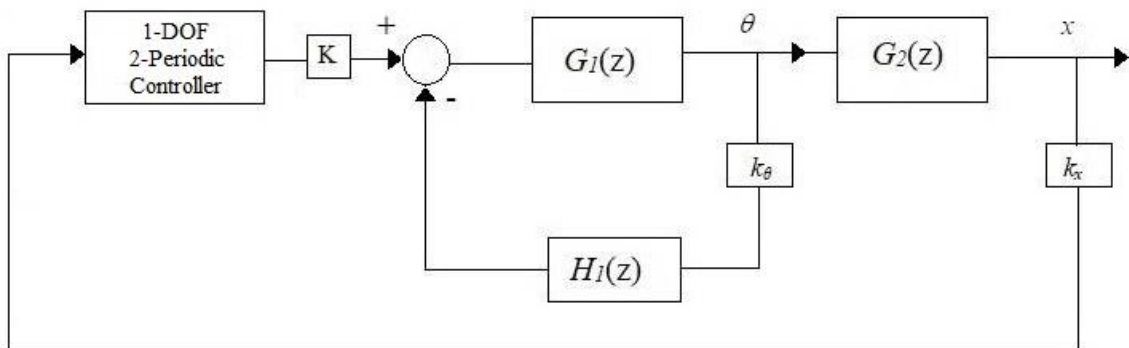


Fig. 4.15: 1-DOF 2-periodic controller in outer loop for cart-inverted pendulum system

From equations (4.17), (4.18), 2-loop structure of cart-inverted pendulum system are

$$G_1(z) = \frac{\theta(z)}{F(z)} = \frac{-0.00062387(z+1)}{(z-1.065)(z-0.9385)}$$

$$G_2(z) = \frac{X(z)}{\theta(z)} = \frac{-1.5557(z-0.9382)(z-1.064)}{(z-1)^2}$$

Case 1: Considering inner loop LDTI controller transfer function from equation (4.23)

$$H_1 = \frac{-378.35(z-0.85)}{z}$$

Now, after placing the compensated inner loop transfer function and $G_2(z)$ in series, the plant to be compensated using periodic controller becomes,

$$G_p(z) = \frac{0.00097006 z(z+1)(z-1.064)(z-0.9382)}{(z-1)^2(z-0.6809)(z-0.5592)(z-0.5274)} \quad (4.31)$$

From (3.23), the order of the periodic controller will be 4 and from (3.24) number of controller zeros will be 8.

$$\hat{A}(z^2) = (z^2 - 1)^2(z^2 - 0.4636)(z^2 - 0.3127)(z^2 - 0.2781)$$

Case 1.1: Taking controller poles at $z^2 = 0, 0.6, 0.7, 0.8$

$$\hat{P}(z^2) = z^2(z^2 - 0.6)(z^2 - 0.7)(z^2 - 0.8)$$

$$\begin{aligned} \hat{Z}(z^2) &= k_z z^2(z^2 - 0.4636)(z^2 - 0.3127)(z^2 - 0.2781)(z^2 - 0.6) \\ &\quad (z^2 - 0.7)(z^2 - 0.8)(z^2 - \beta) \end{aligned}$$

$$\begin{aligned} \check{D}(z^2) &= -z^2(z^2 - 0.4636)(z^2 - 0.3127)(z^2 - 0.2781)(z^2 - 0.6) \\ &\quad (z^2 - 0.7)(z^2 - 0.8) \end{aligned}$$

The transfer function of overall system is

$$G_{loop}(z) = \frac{(z^2 - \beta)}{(z^2 - 1)^2} \quad (4.32)$$

Controller is designed using different values of β (0.5 0.6 0.8) along with different gain margins and a comparison is presented table 4.3.

The root locus of system of (4.32) is shown below for different values of β (fig. 4.20),

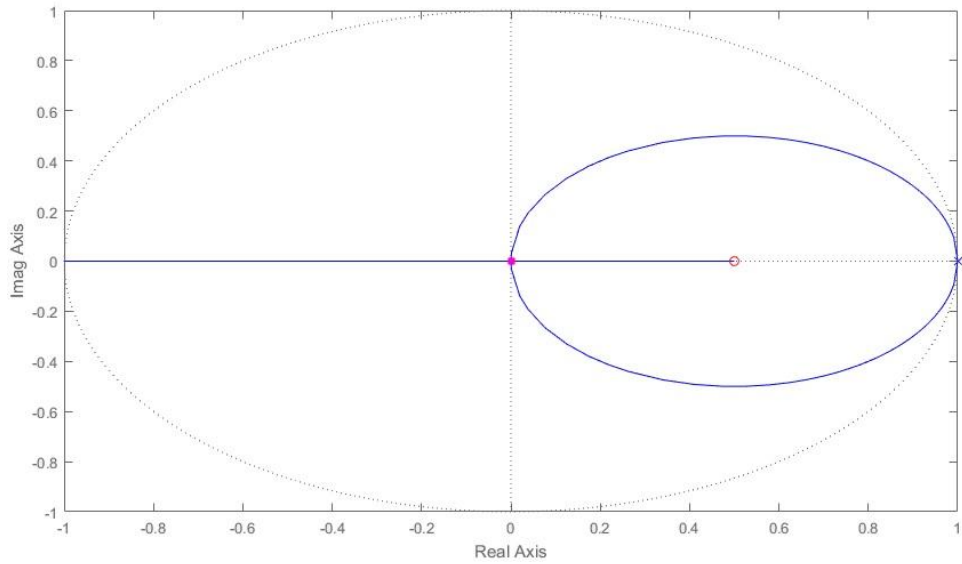


Fig. 4.16: Root locus of the system of (4.30) with $\beta = 0.5$

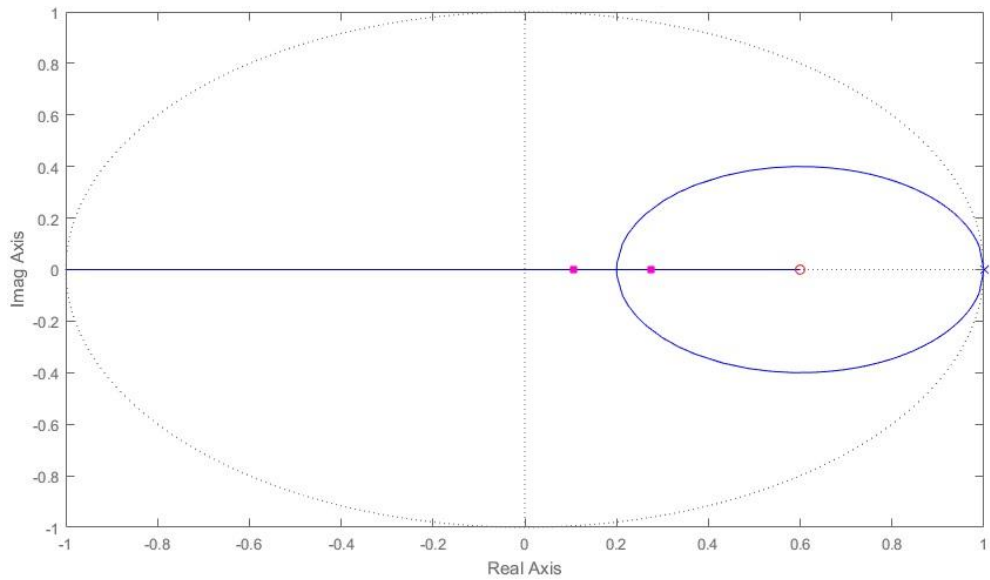


Fig. 4.17: Root locus of the system of (4.30) with $\beta = 0.6$

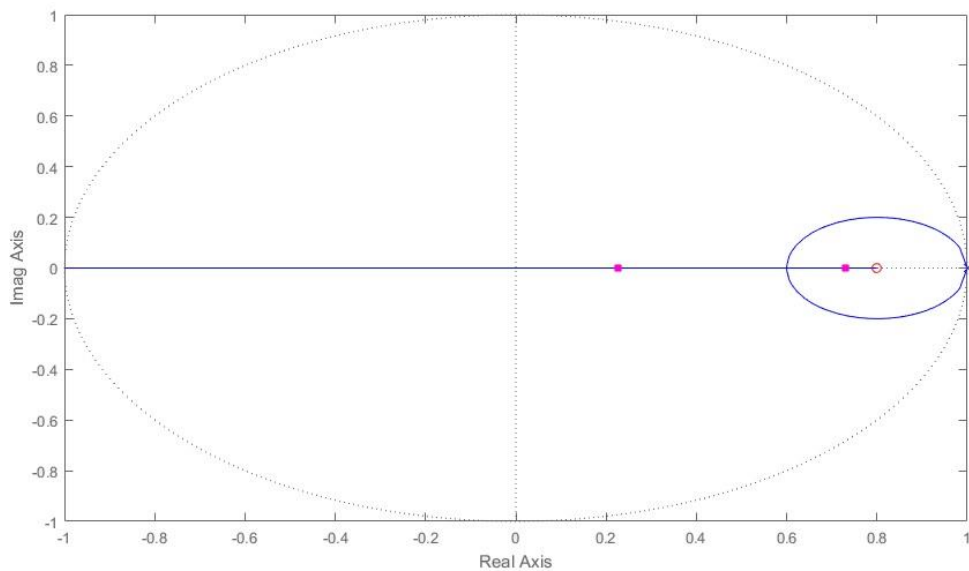


Fig. 4.18: Root locus of the system of (4.30) with $\beta = 0.8$

Now, considering $\beta = 0.6$ and taking

$$\tilde{\Delta} = (z^2 - 0.106)(z^2 - 0.276)$$

As k_{min} is not present in the root locus of figure 4.24, taking gain margin (GM) as

$$GM = \frac{k_{max}}{k_{opt}} = 1.545$$

Where, k_{opt} is the gain in which the system is operating.

Condition I: $Q_0^+ = Q_1^-$

Using techniques of section 3.3, controller parameters are obtained as follows

$$d_{0,0} = d_{0,1} = 0.00011788$$

$$d_{1,0} = -d_{1,1} = 0.00048244$$

$$d_{2,0} = d_{2,1} = 0.00039346$$

$$d_{3,0} = -d_{3,1} = 0.00051312$$

$$d_{4,0} = d_{4,1} = -62242$$

And $C_{0,0} = 0.4395$, $C_{1,0} = 86.9092$, $C_{2,0} = 177.7885$, $C_{3,0} = 92.4677$, $C_{0,1} = -0.4395$, $C_{1,1} = -85.1$, $C_{2,1} = 175.9002$, $C_{3,1} = -90.5129$

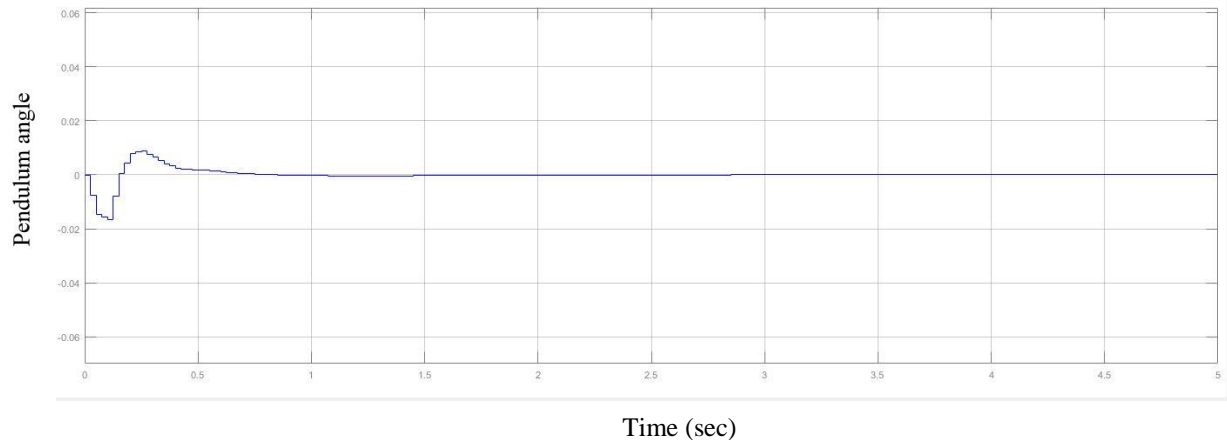


Fig. 4.19: Response of pendulum angle using 1-DOF periodic controller using case 1.1 for condition $Q_0^+ = Q_1^-$

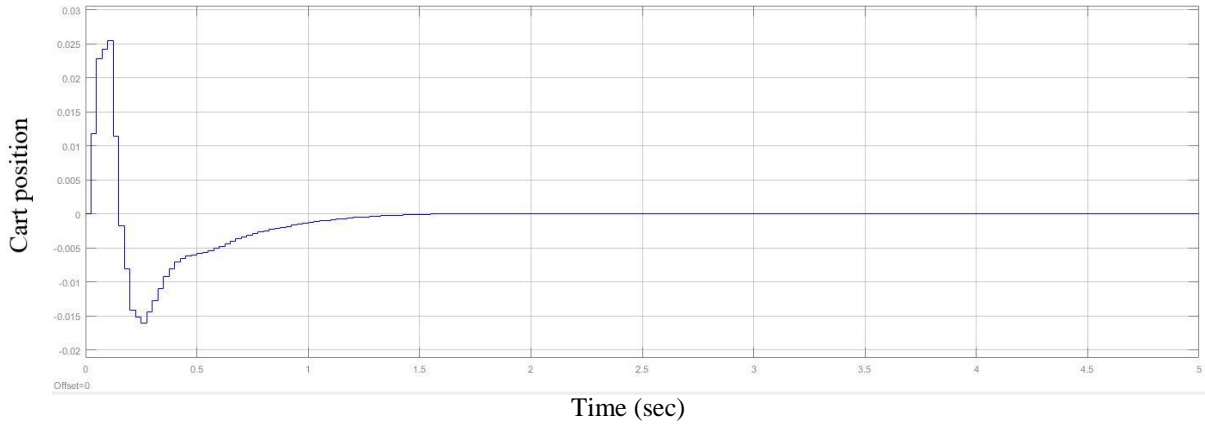


Fig. 4.20: Response of cart position using 1-DOF periodic controller using case 1.1 for condition

$$Q_0^+ = Q_1^-$$

Condition II: $Q_0^+ = -Q_1^-$

Using techniques of section 3.3, controller parameters are obtained as follows

$$d_{0,0} = -d_{0,1} = 0.00011788$$

$$d_{1,0} = d_{1,1} = 0.00048244$$

$$d_{2,0} = -d_{2,1} = 0.00039346$$

$$d_{3,0} = d_{3,1} = 0.00051312$$

$$d_{4,0} = -d_{4,1} = -62242$$

And $C_{0,0} = 0.4395$, $C_{1,0} = 86.9092$, $C_{2,0} = 177.7885$, $C_{3,0} = 92.4677$, $C_{0,1} = 0.4395$, $C_{1,1} = 85.1$, $C_{2,1} = -175.9002$, $C_{3,1} = 90.5129$

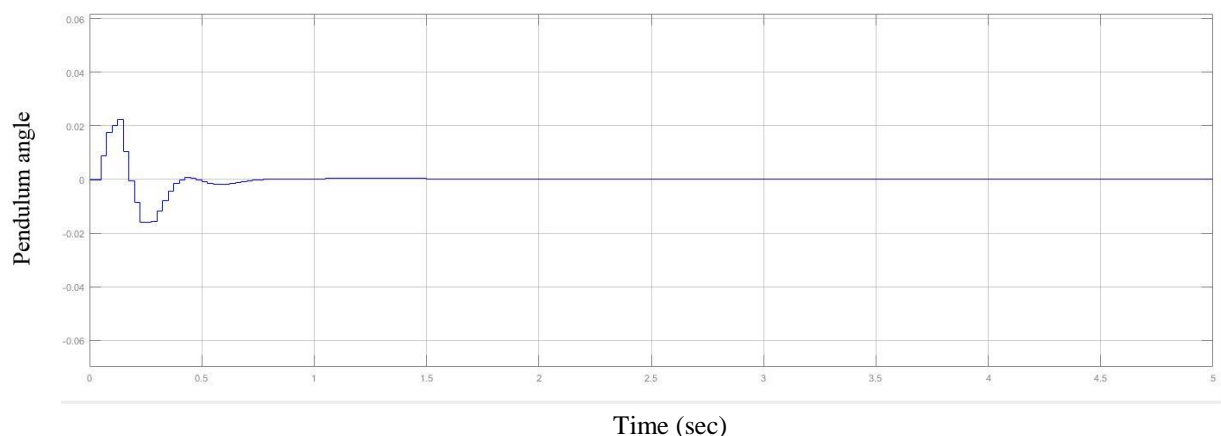


Fig. 4.21: Response of pendulum angle using 1-DOF periodic controller using case 1.1 for

$$\text{condition } Q_0^+ = -Q_1^-$$

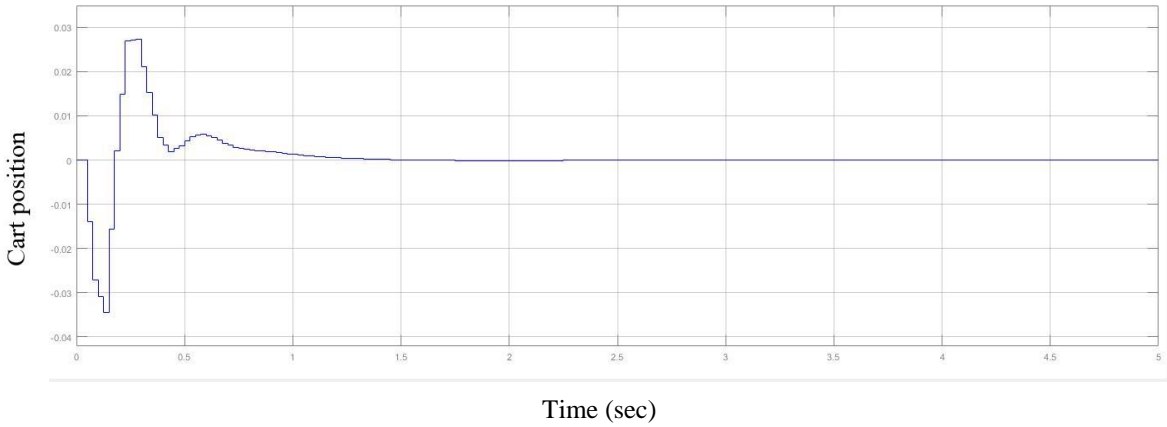


Fig. 4.22: Response of cart position using 1-DOF periodic controller using case 1.1 for condition

$$Q_0^+ = -Q_1^-$$

Condition III: $Q_0^+ = Q_1^+$

Using techniques of section 3.3, controller parameters obtained are equal to condition $Q_0^+ = Q_1^-$.

So the response curves are also same as figure 4.25 and 4.26.

Condition IV: $Q_0^+ = -Q_1^+$

Using techniques of section 3.3, controller parameters obtained are equal to condition $Q_0^+ = -Q_1^-$.

So the response curves are also same as figure 4.27 and 4.28

Case 1.2: Taking controller poles at $z^2 = 0, 0.4, 0.5, 0.6$

$$\begin{aligned}\hat{P}(z^2) &= z^2(z^2 - 0.4)(z^2 - 0.5)(z^2 - 0.6) \\ \hat{Z}(z^2) &= k_z z^2(z^2 - 0.4636)(z^2 - 0.3127)(z^2 - 0.2781)(z^2 - 0.4) \\ &\quad (z^2 - 0.5)(z^2 - 0.6)(z^2 - \beta) \\ \check{D}(z^2) &= -z^2(z^2 - 0.4636)(z^2 - 0.3127)(z^2 - 0.2781)(z^2 - 0.4) \\ &\quad (z^2 - 0.5)(z^2 - 0.6)\end{aligned}$$

The transfer function of overall system is

$$G_{loop}(z) = \frac{(z^2 - \beta)}{(z^2 - 1)^2} \quad (4.32)$$

Controller is designed using different values of β (0.5 0.6 0.8) along with different gain margins and a comparison is presented table 4.3.

The root locus of system of (4.32) for different values of β are shown in (fig. 4.20),

Now, considering $\beta = 0.6$ and taking

$$\tilde{\Delta} = (z^2 - 0.106)(z^2 - 0.276)$$

Gain margin (GM) is found as

$$GM = \frac{k_{max}}{k_{opt}} = 1.545$$

Condition I: $Q_0^+ = Q_1^-$

Using techniques of section 3.3, controller parameters are obtained and simulated using MATLAB. The response Plots are shown below.

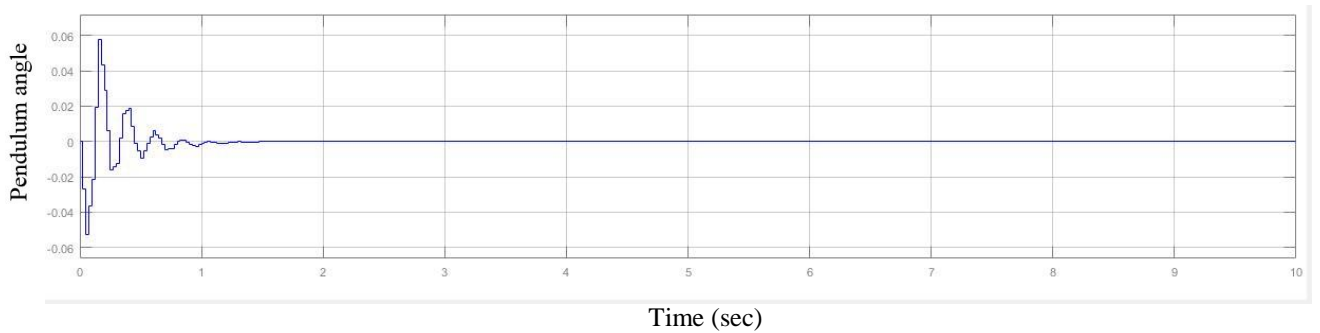


Fig. 4.23: Response of pendulum angle using 1-DOF periodic controller using case 1.2 for condition $Q_0^+ = Q_1^-$

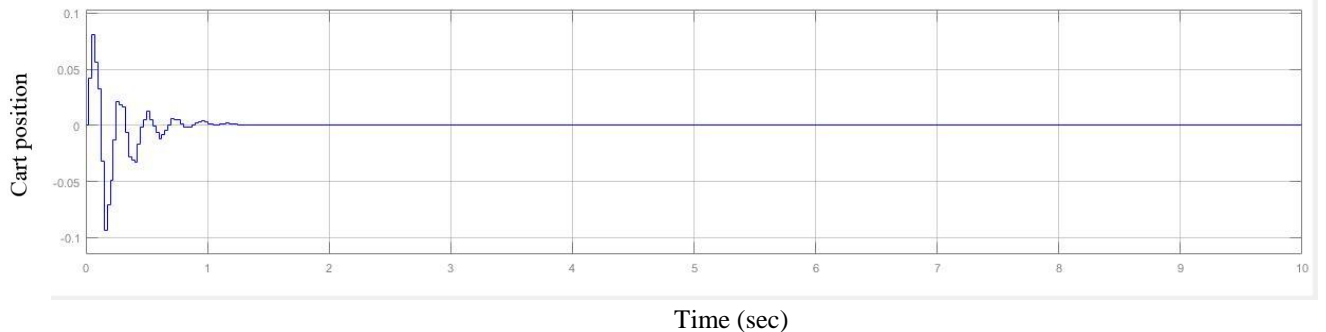


Fig. 4.24: Response of cart position using 1-DOF periodic controller using case 1.2 for condition $Q_0^+ = Q_1^-$

Condition II: $Q_0^+ = -Q_1^-$

Using techniques of section 3.3, controller parameters are obtained and simulated using MATLAB. The response Plots are shown next.

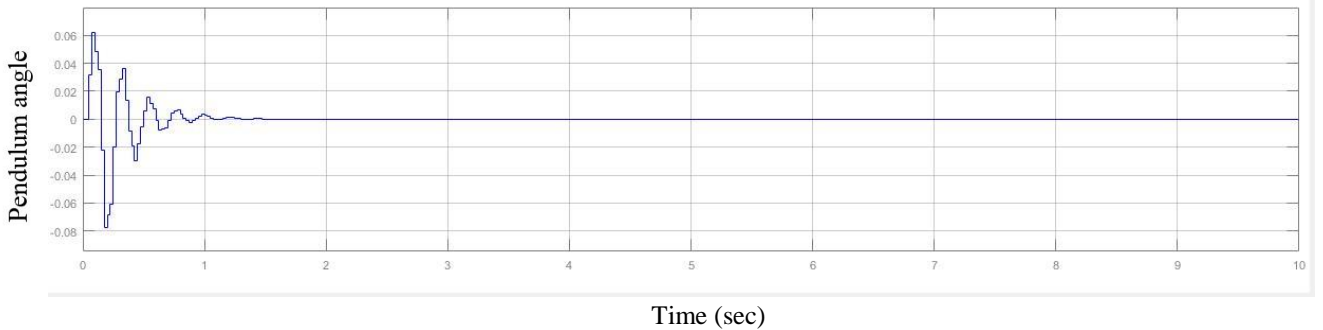


Fig. 4.25: Response of pendulum angle using 1-DOF periodic controller using case 1.2 for condition $Q_0^+ = -Q_1^-$

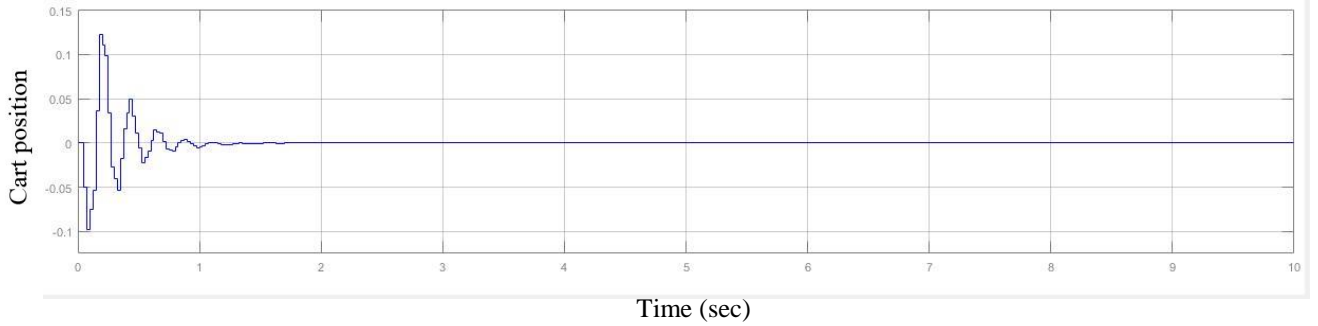


Fig. 4.26: Response of cart position using 1-DOF periodic controller using case 1.2 for condition $Q_0^+ = -Q_1^-$

Condition III: $Q_0^+ = Q_1^+$

Using techniques of section 3.3, controller parameters obtained are equal to condition $Q_0^+ = Q_1^-$. So the response curves are also same as figure 4.25 and 4.26.

Condition IV: $Q_0^+ = -Q_1^+$

Using techniques of section 3.3, controller parameters obtained are equal to condition $Q_0^+ = -Q_1^-$. So the response curves are also same as figure 4.27 and 4.28

Case 2: Considering inner loop LDTI controller transfer function from equation (4.23)

$$H_1 = \frac{-292.47(z-0.9385)}{z}$$

Now, after placing the compensated inner loop transfer function and $G_2(z)$ in series, the plant to be compensated using periodic controller becomes,

$$G_p(z) = \frac{0.00097006 z(z+1)(z-1.064)(z-0.9382)}{(z-1)^2(z-0.3306)(z-0.552)(z-0.9385)} \quad (4.31)$$

From (3.23), the order of the periodic controller will be 4 and from (3.24) number of controller zeros will be 8.

$$\hat{A}(z^2) = (z^2 - 1)^2(z^2 - 0.1093)(z^2 - 0.3047)(z^2 - 0.8808)$$

Case 2.1: Taking controller poles at $z^2 = 0, 0.6, 0.7, 0.8$

$$\hat{P}(z^2) = z^2(z^2 - 0.6)(z^2 - 0.7)(z^2 - 0.8)$$

$$\hat{Z}(z^2) = k_z z^2(z^2 - 0.1093)(z^2 - 0.3047)(z^2 - 0.8808)(z^2 - 0.6)$$

$$(z^2 - 0.7)(z^2 - 0.8)(z^2 - \beta)$$

$$\check{D}(z^2) = -z^2(z^2 - 0.1093)(z^2 - 0.3047)(z^2 - 0.8808)(z^2 - 0.6)(z^2 - 0.7)(z^2 - 0.8)$$

The transfer function of overall system is

$$G_{loop}(z) = \frac{(z^2 - \beta)}{(z^2 - 1)^2} \quad (4.32)$$

Controller is designed using different values of β (0.5 0.6 0.8) along with different gain margins and a comparison is presented table 4.3.

The root locus of system of (4.32) for different values of β are shown in (fig. 4.20),

Now, considering $\beta = 0.6$ and taking

$$\check{\Delta} = (z^2 - 0.106)(z^2 - 0.276)$$

Gain margin (GM) is found as

$$GM = \frac{k_{max}}{k_{opt}} = 1.545$$

Condition I: $Q_0^+ = Q_1^-$

Using techniques of section 3.3, controller parameters are obtained and simulated using MATLAB. The response Plots are shown next.

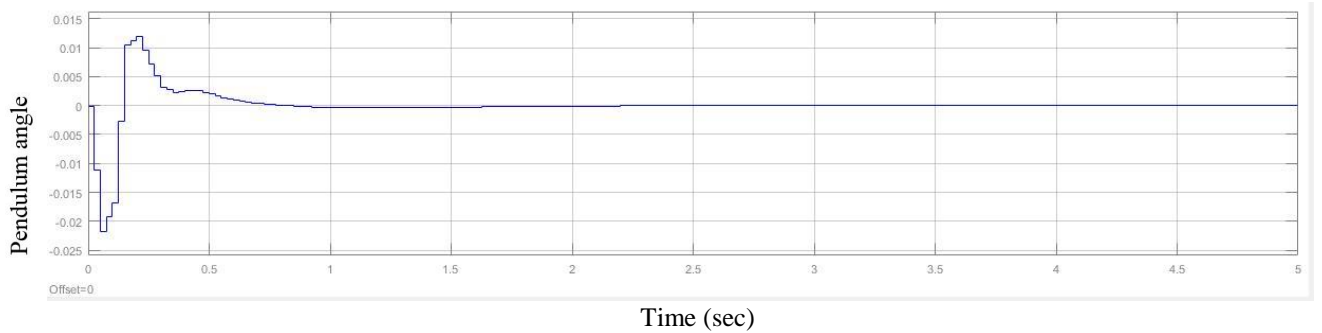


Fig. 4.27: Response of pendulum angle using 1-DOF periodic controller using case 1.2 for condition $Q_0^+ = Q_1^-$

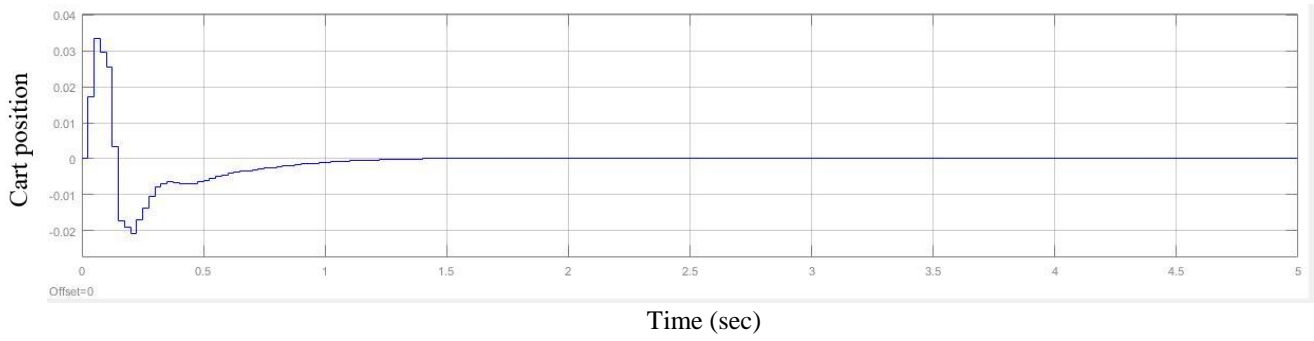


Fig. 4.28: Response of cart position using 1-DOF periodic controller using case 1.2 for condition

$$Q_0^+ = Q_1^-$$

Condition II: $Q_0^+ = -Q_1^-$

Using techniques of section 3.3, controller parameters are obtained and simulated using MATLAB. The response Plots are shown below.

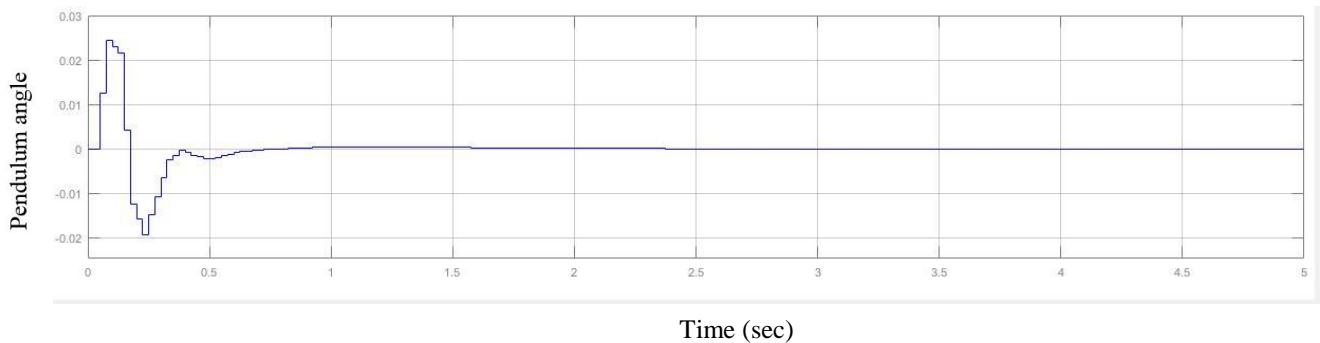


Fig. 4.29: Response of pendulum angle using 1-DOF periodic controller using case 1.2 for

$$\text{condition } Q_0^+ = -Q_1^-$$

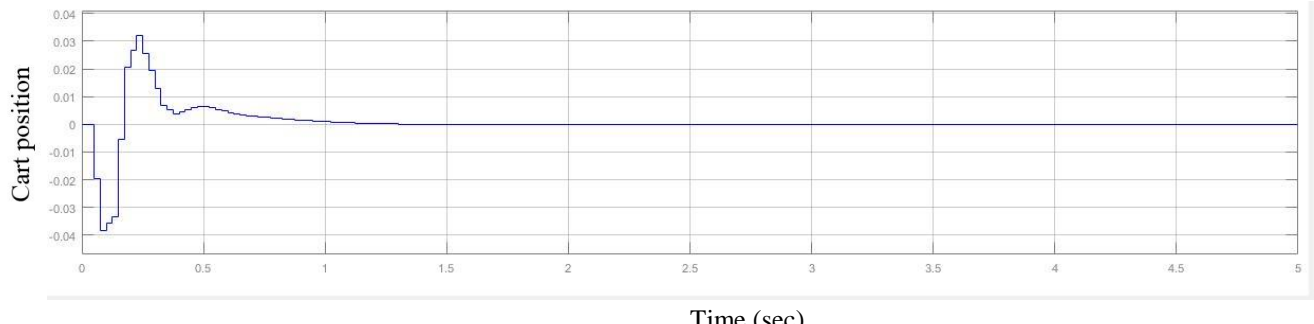


Fig. 4.30: Response of cart position using 1-DOF periodic controller using case 1.2 for condition

$$Q_0^+ = -Q_1^-$$

Condition III: $Q_0^+ = Q_1^+$

Using techniques of section 3.3, controller parameters obtained are equal to condition $Q_0^+ = Q_1^-$. So the response curves are also same as figure 4.25 and 4.26.

Condition IV: $Q_0^+ = -Q_1^+$

Using techniques of section 3.3, controller parameters obtained are equal to condition $Q_0^+ = -Q_1^-$. So the response curves are also same as figure 4.27 and 4.28

Case 2.2: Taking controller poles at $z^2 = 0, 0.4, 0.5, 0.6$

$$\begin{aligned}\hat{P}(z^2) &= z^2(z^2 - 0.4)(z^2 - 0.5)(z^2 - 0.6) \\ \hat{Z}(z^2) &= k_z z^2(z^2 - 0.1093)(z^2 - 0.3047)(z^2 - 0.8808)(z^2 - 0.4) \\ &\quad (z^2 - 0.5)(z^2 - 0.6)(z^2 - \beta) \\ \check{D}(z^2) &= -z^2(z^2 - 0.1093)(z^2 - 0.3047)(z^2 - 0.8808)(z^2 - 0.4) \\ &\quad (z^2 - 0.5)(z^2 - 0.6)\end{aligned}$$

The transfer function of overall system is

$$G_{loop}(z) = \frac{(z^2 - \beta)}{(z^2 - 1)^2} \quad (4.32)$$

Controller is designed using different values of β (0.5 0.6 0.8) along with different gain margins and a comparison is presented table 4.3.

The root locus of system of (4.32) for different values of β are shown in (fig. 4.20),

Now, considering $\beta = 0.6$ and taking

$$\bar{\Delta} = (z^2 - 0.106)(z^2 - 0.276)$$

Gain margin (GM) is found as

$$GM = \frac{k_{max}}{k_{opt}} = 1.545$$

Condition I: $Q_0^+ = Q_1^-$

Using techniques of section 3.3, controller parameters are obtained and simulated using MATLAB. The response Plots are shown next.

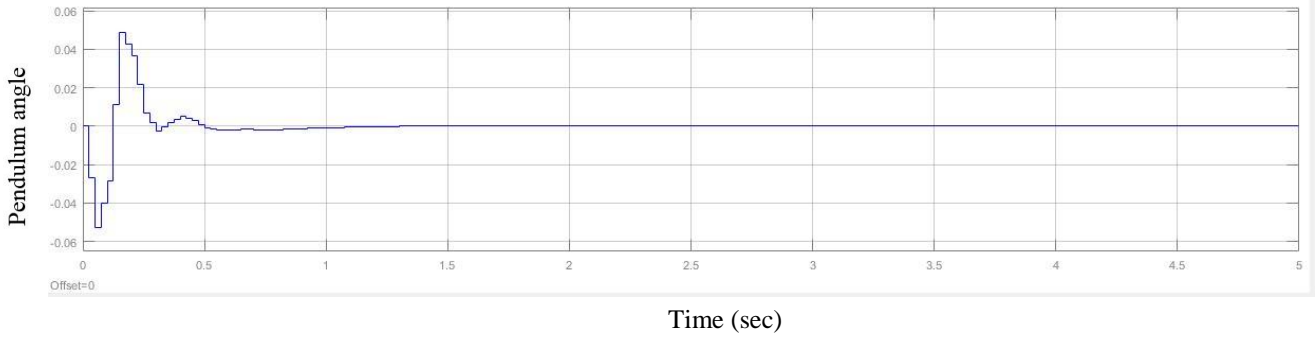


Fig. 4.31: Response of pendulum angle using 1-DOF periodic controller using case 1.2 for condition $Q_0^+ = Q_1^-$

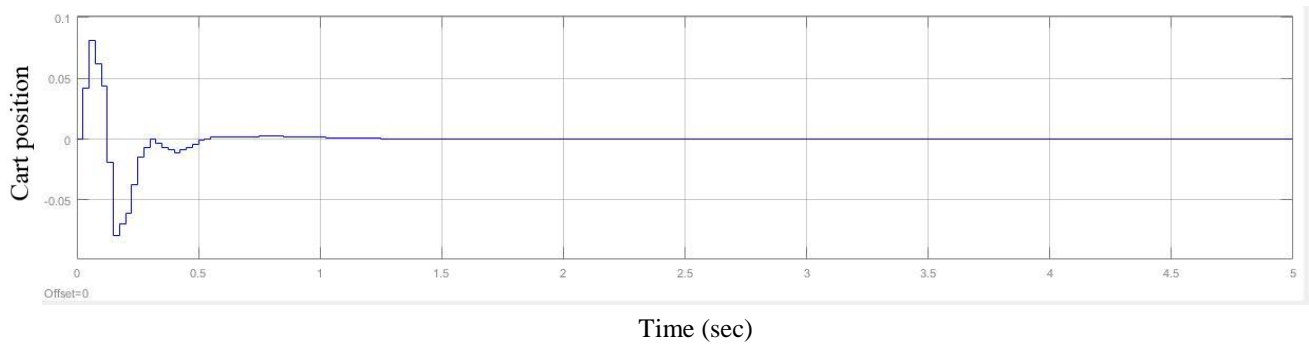


Fig. 4.32: Response of cart position using 1-DOF periodic controller using case 1.2 for condition $Q_0^+ = Q_1^-$

Condition II: $Q_0^+ = -Q_1^-$

Using techniques of section 3.3, controller parameters are obtained and simulated using MATLAB. The response Plots are shown below

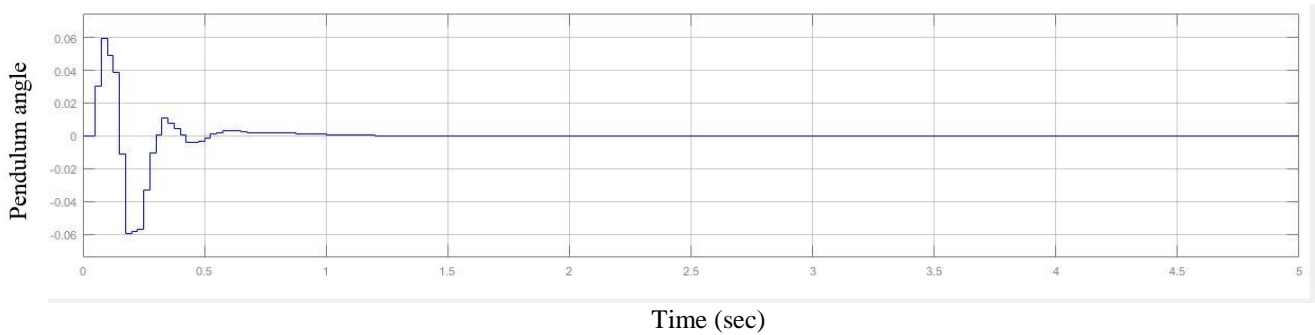


Fig. 4.33: Response of pendulum angle using 1-DOF periodic controller using case 1.2 for condition $Q_0^+ = -Q_1^-$

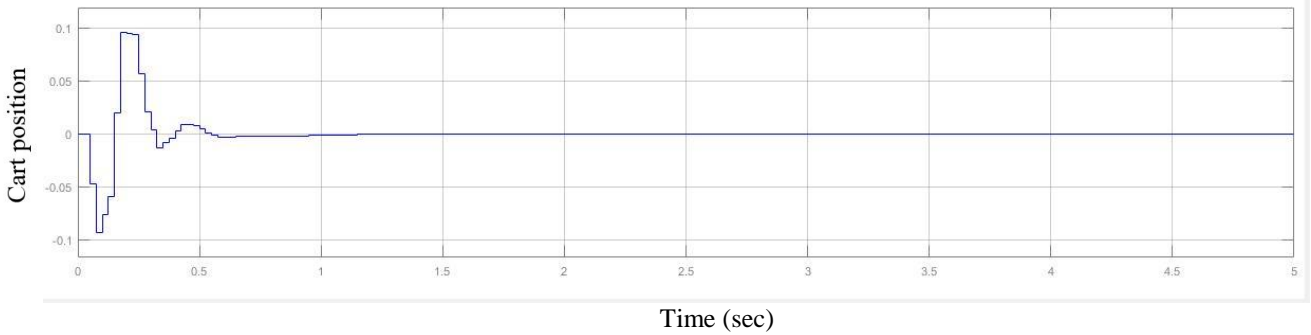


Fig. 4.34: Response of cart position using 1-DOF periodic controller using case 1.2 for condition

$$Q_0^+ = -Q_1^-$$

Condition III: $Q_0^+ = Q_1^+$

Using techniques of section 3.3, controller parameters obtained are equal to condition $Q_0^+ = Q_1^-$.

So the response curves are also same as figure 4.25 and 4.26.

Condition IV: $Q_0^+ = -Q_1^+$

Using techniques of section 3.3, controller parameters obtained are equal to condition $Q_0^+ = -Q_1^-$.

So the response curves are also same as figure 4.27 and 4.28

4.3.3.2 Design of a 2-DOF 2-periodic Controller

Now, the system order can be minimized by using a 2-degrees-of-freedom periodic controller. Additional controller gains are used to cancel out as many of additional closed-loop poles as possible. The following figure shows the block diagram of a cart-inverted pendulum system compensated by a 2-DOF 2-periodic controller in outer loop.

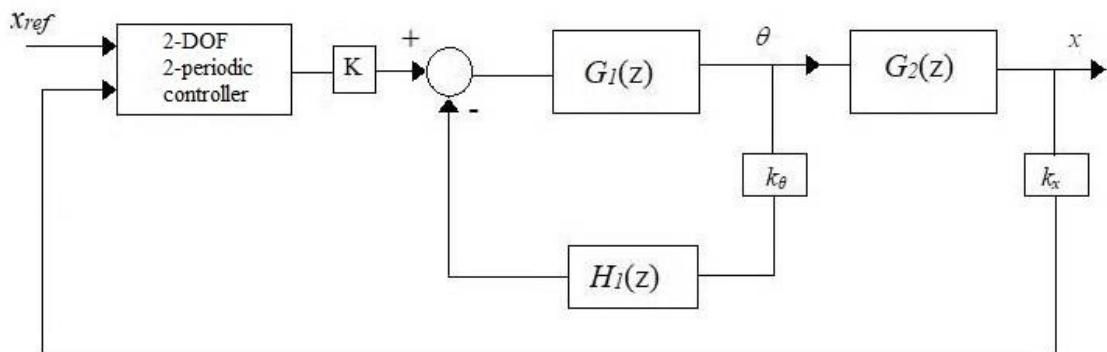


Fig. 4.35: Compensation of cart-inverted pendulum system by 2-DOF 2-periodic controller in outer loop

Case 1.1: Considering the conditions case 1.1 of section 4.3.3.1 C_i , d_i parameters obtained are same as in section 4.3.1. Using techniques of section 3.4, h_i parameters are obtained as follows

$$h_{1,0} = h_{3,0} = h_{1,1} = h_{3,1} = h_{4,1} = 0, h_{0,0} = 0.21, h_{2,0} = -1.05, h_{4,0} = 1, h_{0,1} = -0.21, h_{2,1} = 0.25$$

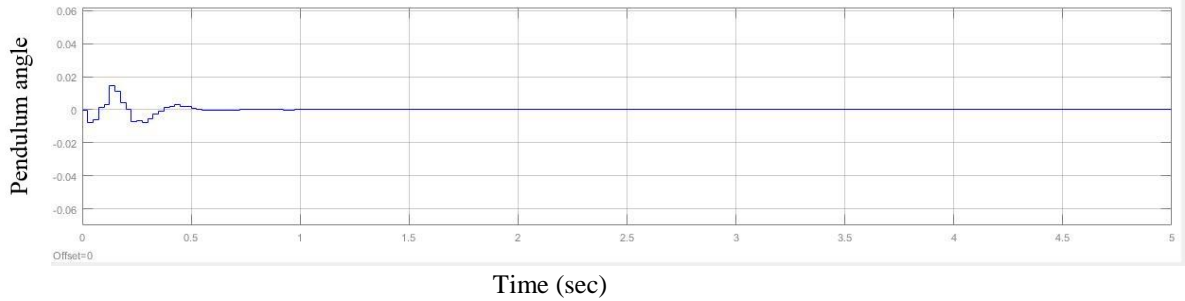


Fig. 4.36: Response of pendulum angle using 2-DOF periodic controller with $\beta = 0.6$ for conditions $Q_0^+ = Q_1^-$ and $Q_0^+ = Q_1^+$

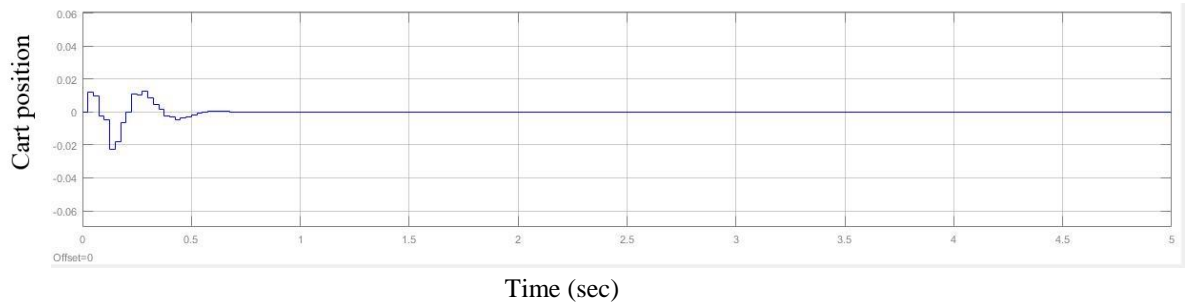


Fig. 4.37: Response of cart position using 2-DOF periodic controller with $\beta = 0.6$ for conditions $Q_0^+ = Q_1^-$ and $Q_0^+ = Q_1^+$

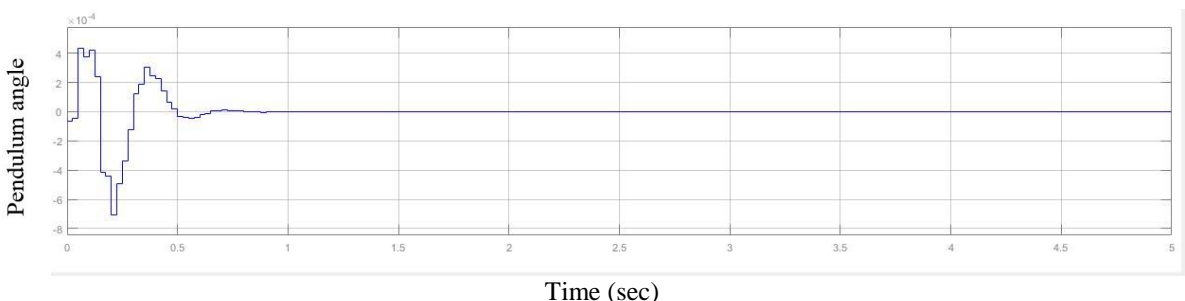


Fig. 4.38: Response of pendulum angle using 2-DOF periodic controller with $\beta = 0.6$ for conditions $Q_0^+ = -Q_1^-$ and $Q_0^+ = -Q_1^+$

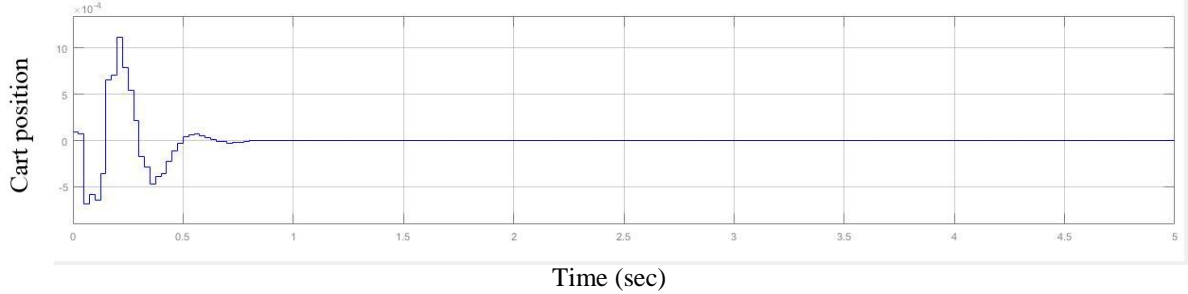


Fig. 4.39: Response of cart position using 2-DOF periodic controller with $\beta = 0.6$ for conditions

$$Q_0^+ = -Q_1^- \text{ and } Q_0^+ = -Q_1^+$$

Case 1.2: Considering the conditions case 1.2 of section 4.3.3.1. Using techniques of section 3.3 and 3.4, parameters of 2-DOF 2-periodic controller are calculated and response Plots are obtained using MATLAB, are shown below.

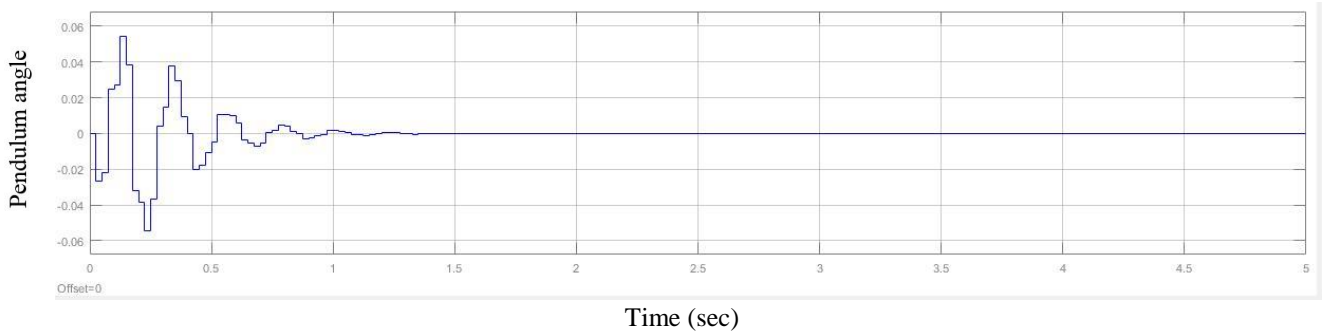


Fig. 4.40: Response of pendulum angle using 2-DOF periodic controller using case 1.2 for conditions $Q_0^+ = Q_1^-$ and $Q_0^+ = Q_1^+$

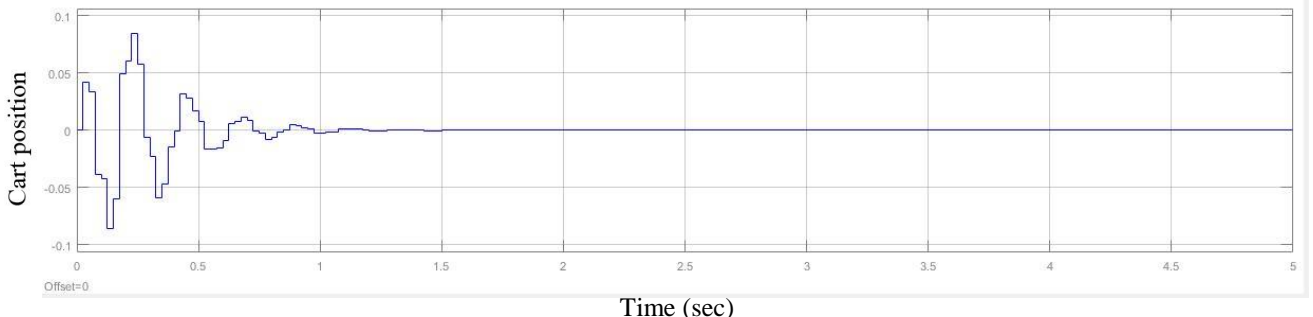


Fig. 4.41: Response of cart position using 2-DOF periodic controller using case 1.2 for conditions

$$Q_0^+ = Q_1^- \text{ and } Q_0^+ = Q_1^+$$

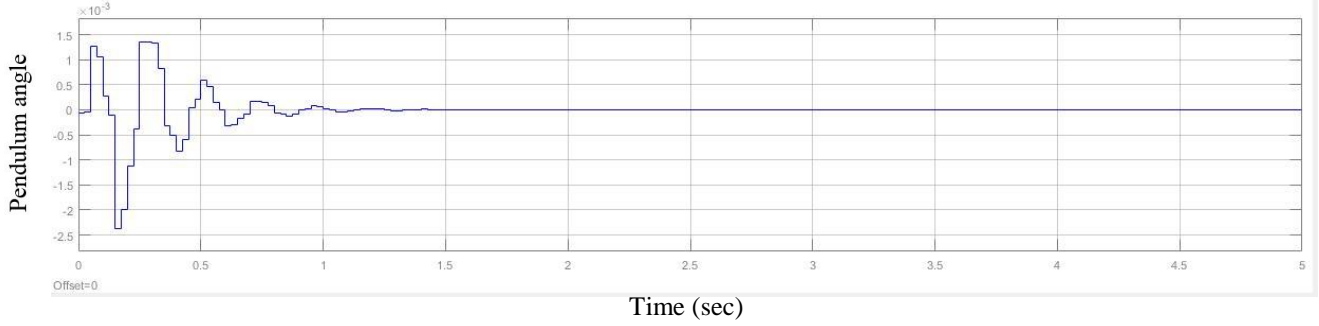


Fig. 4.42: Response of pendulum angle using 2-DOF periodic controller using case 1.2 for conditions $Q_0^+ = -Q_1^-$ and $Q_0^+ = -Q_1^+$

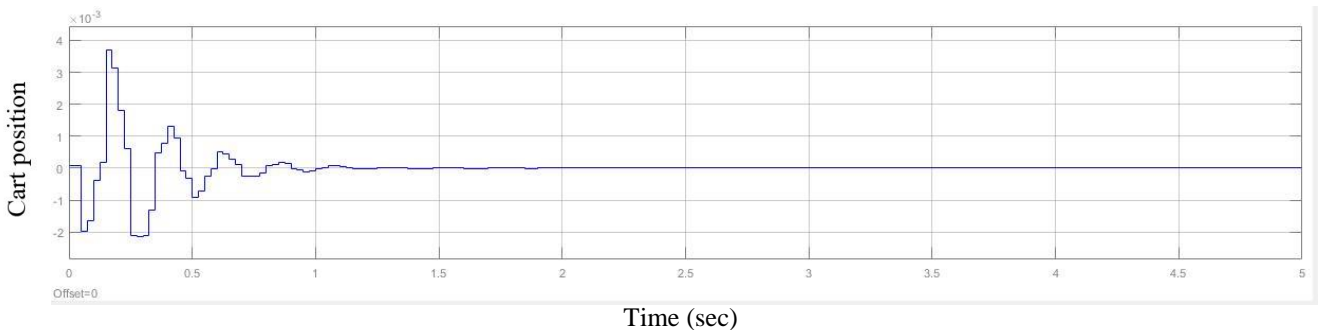


Fig. 4.43: Response of cart position using 2-DOF periodic controller using case 1.2 for conditions $Q_0^+ = -Q_1^-$ and $Q_0^+ = -Q_1^+$

Case 2.1: Considering the conditions case 2.1 of section 4.3.3.1. Using techniques of section 3.3 and 3.4, parameters of 2-DOF 2-periodic controller are calculated and response Plots are obtained using MATLAB, are shown below.

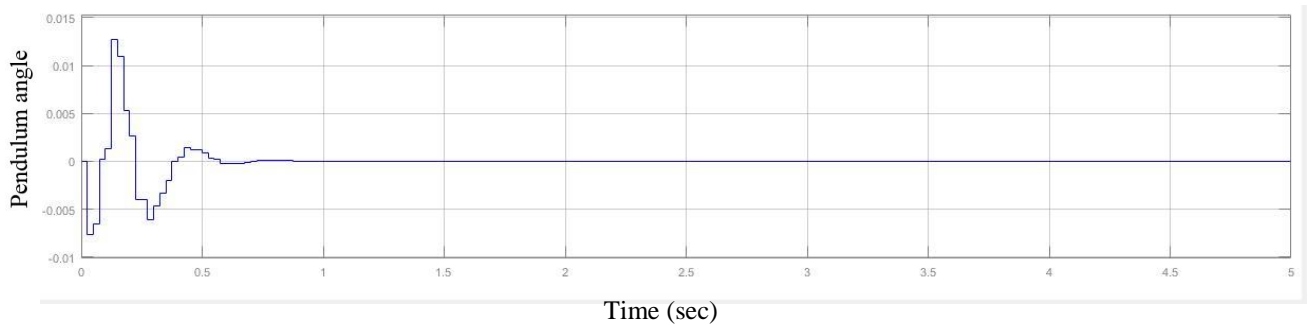


Fig. 4.44: Response of pendulum angle using 2-DOF periodic controller using case 2.1 for conditions $Q_0^+ = Q_1^-$ and $Q_0^+ = Q_1^+$

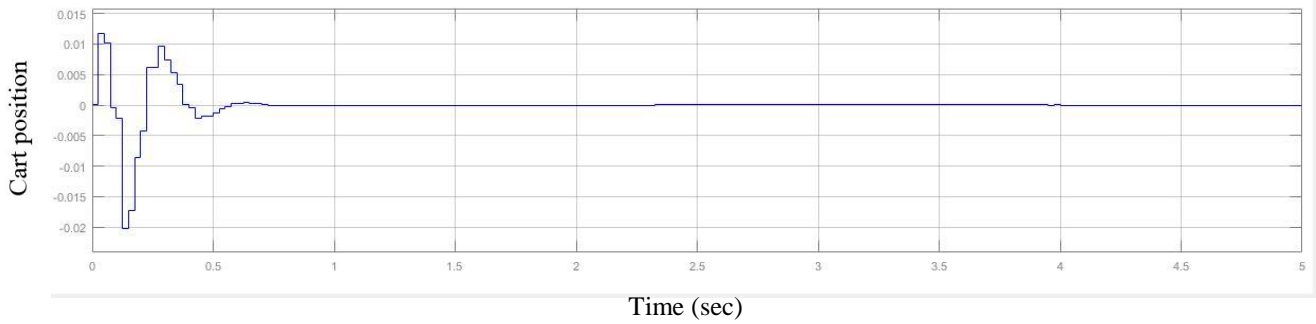


Fig. 4.45: Response of cart position using 2-DOF periodic controller using case 2.1 for conditions

$$Q_0^+ = Q_1^- \text{ and } Q_0^- = Q_1^+$$

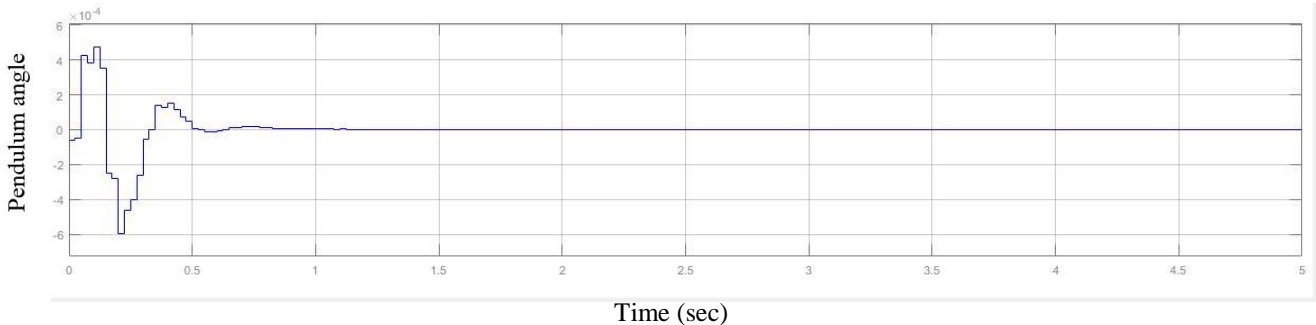


Fig. 4.46: Response of pendulum angle using 2-DOF periodic controller using case 2.1 for

$$\text{conditions } Q_0^+ = -Q_1^- \text{ and } Q_0^- = -Q_1^+$$

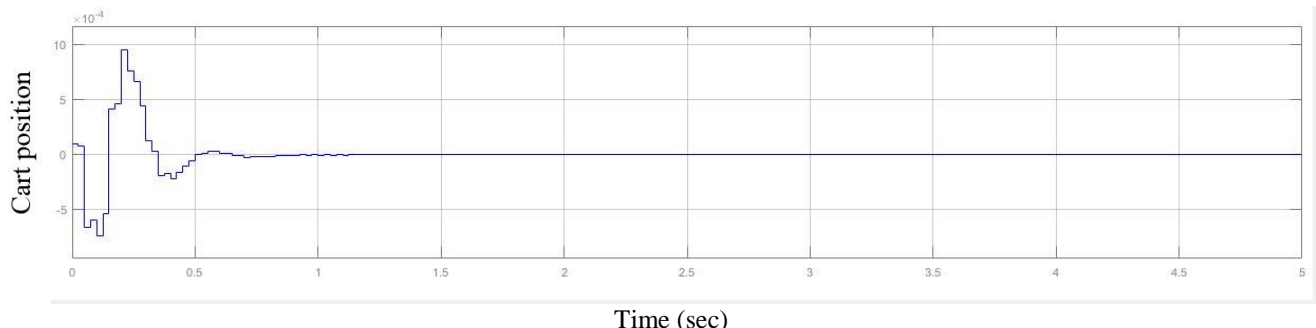


Fig. 4.47: Response of cart position using 2-DOF periodic controller using case 2.1 for conditions

$$Q_0^+ = -Q_1^- \text{ and } Q_0^- = -Q_1^+$$

Case 2.2: Considering the conditions case 2.2 of section 4.3.3.1. Using techniques of section 3.3 and 3.4, parameters of 2-DOF 2-periodic controller are calculated and response Plots are obtained using MATLAB, are shown below.

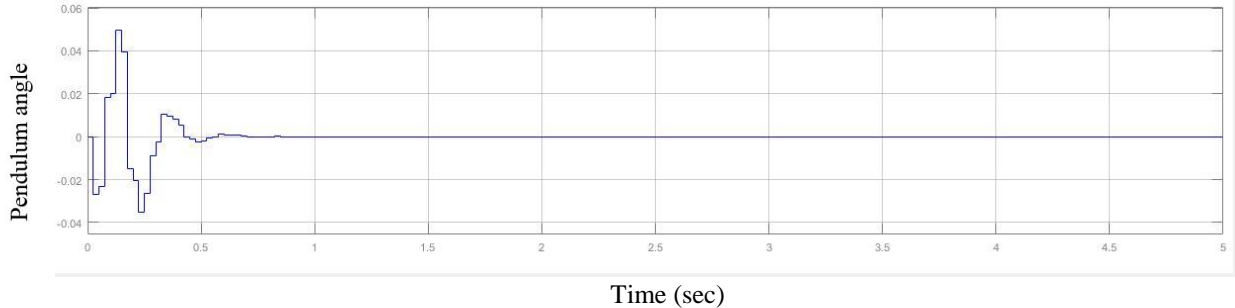


Fig. 4.48: Response of pendulum angle using 2-DOF periodic controller using case 2.2 for conditions $Q_0^+ = Q_1^-$ and $Q_0^+ = Q_1^+$

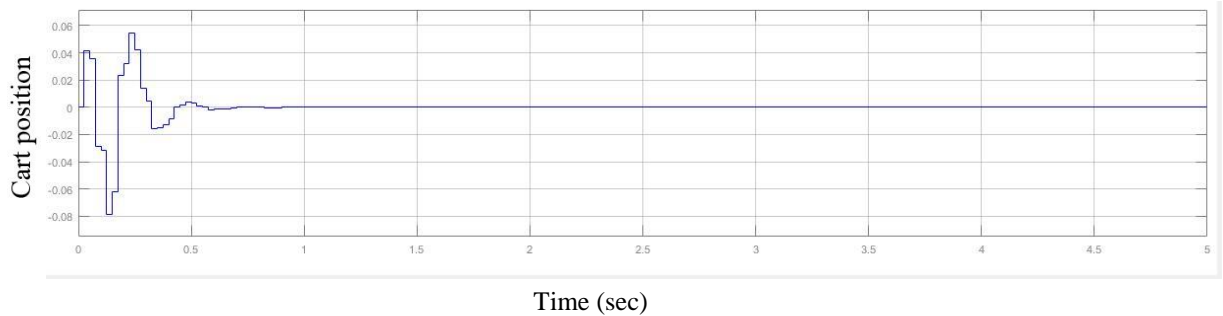


Fig. 4.49: Response of cart position using 2-DOF periodic controller using case 2.2 for conditions $Q_0^+ = Q_1^-$ and $Q_0^+ = Q_1^+$

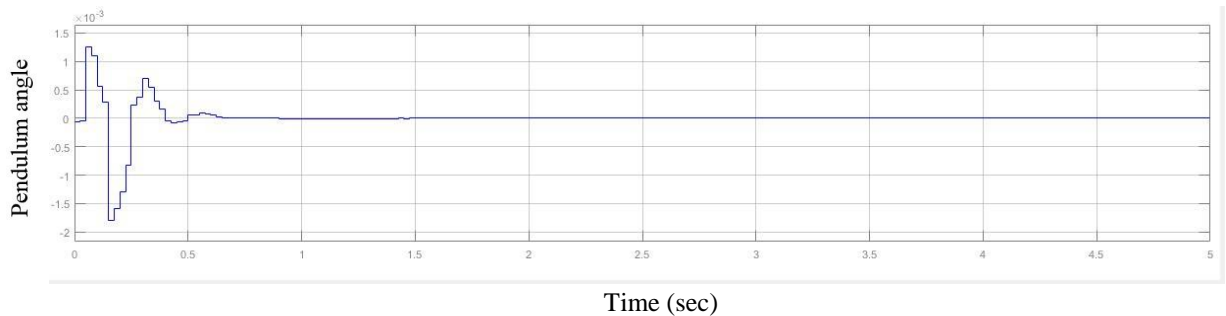


Fig. 4.50: Response of pendulum angle using 2-DOF periodic controller using case 2.2 for conditions $Q_0^+ = -Q_1^-$ and $Q_0^+ = -Q_1^+$

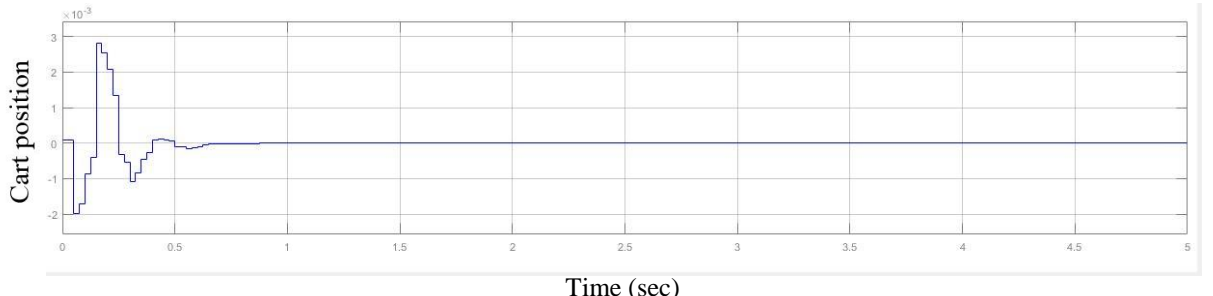


Fig. 4.51: Response of cart position using 2-DOF periodic controller using case 2.2 for conditions $Q_0^+ = -Q_1^-$ and $Q_0^+ = -Q_1^+$

Table 4.3: Comparison of performance of 1-DOF and 2-DOF 2-periodic controller for 2 different systems

| | Controller pole locations | β | Gain margin | Pendulum angle Settling time (sec.) | | | | Cart position Settling time (sec.) | | | |
|---------|---------------------------|---------|-------------|-------------------------------------|-----------------|-----------|------------------|------------------------------------|-----------------|-----------|------------------|
| | | | | 1-DOF | | 2-DOF | | 1-DOF | | 2-DOF | |
| | | | | Condition | $Q_0^+ = Q_1^-$ | Condition | $Q_0^+ = -Q_1^-$ | Condition | $Q_0^+ = Q_1^+$ | Condition | $Q_0^+ = -Q_1^-$ |
| Case I | $z^2 = 0, 0.6, 0.7, 0.8$ | 0.5 | 1.333 | 1.75 | 1.74 | 1.18 | 1.45 | 2.08 | 2.08 | 1.55 | 1.48 |
| | | 0.6 | 1.545 | 1.45 | 0.7 | 0.5 | 0.65 | 1.42 | 1.32 | 0.52 | 0.7 |
| | | 0.8 | 2.129 | 1.9 | 2.02 | 0.8 | 0.7 | 1.31 | 1.3 | 0.74 | 0.7 |
| | | 0.5 | 1.333 | 6.4 | 6.3 | 5.18 | 4.9 | 6.3 | 6.05 | 4.68 | 4.6 |
| | | 0.6 | 1.545 | 1.2 | 1.2 | 1.17 | 1.08 | 1.2 | 1.22 | 1.08 | 1 |
| | $z^2 = 0, 0.4, 0.5, 0.6$ | 0.8 | 2.129 | 5.1 | 5 | 3.8 | 4.45 | 5.4 | 5 | 3.42 | 4.05 |
| | | 0.5 | 1.333 | 1.62 | 1.57 | 0.57 | 0.6 | 1.2 | 1.12 | 0.58 | 0.6 |
| | | 0.6 | 1.545 | 1.74 | 1.58 | 0.68 | 0.77 | 1.2 | 1.21 | 0.7 | 0.7 |
| | | 0.8 | 2.129 | 1.93 | 1.83 | 0.82 | 0.97 | 1.35 | 1.26 | 0.72 | 1.05 |
| | | 0.5 | 1.333 | 1.8 | 1.77 | 1.8 | 1.78 | 1.67 | 1.68 | 1.7 | 1.8 |
| Case II | $z^2 = 0, 0.4, 0.5, 0.6$ | 0.6 | 1.545 | 1.07 | 1 | 0.68 | 0.62 | 1.02 | 0.95 | 0.68 | 0.62 |
| | | 0.8 | 2.129 | 1.45 | 1.4 | 0.8 | 0.75 | 1.48 | 0.9 | 0.76 | 0.75 |

4.4 Chapter Summary

In this chapter the cart-inverted pendulum system is compensated using LDTI, 1-DOF and 2-DOF 2-periodic controllers. A comparison of performances of the controllers are presented. It can be concluded that the 2-DOF 2-periodic controller can provide better performance in comparison to 1-DOF 2-periodic controller from the time response point of view.

CHAPTER 5

Conclusion

5.1 Contributions of the thesis

- i. Compensation of LDTI plants using 1-DOF 2-periodic controller has been studied in details and the controller synthesis steps are demonstrated with the help of a synthetic example.
- ii. A 2-DOF configuration of 2-periodic controller is considered and its synthesis algorithm is presented. The performances of 1-DOF and 2-DOF 2-periodic controllers are compared with respect to the compensation of the same synthetic plant. The results establish the fact that 2-DOF configuration improves the time response of the compensated system.
- iii. The cart-inverted pendulum system is stabilized using LDTI controller, 1-DOF and 2-DOF 2-periodic controller. Comparisons of the simulation results is presented to evaluate their performances. The results clearly show that the 2-DOF 2-periodic controller is superior to the others.

5.2 Scope of future work

- i. Several iterations are done in this work to find the suitable location of poles and zeros for 2-periodic controller. An algorithm for this purpose may be developed.
- ii. The proposed 2-DOF 2-periodic controller needs to be implemented on a real-time Cart-Inverted Pendulum System to study the possible merits and demerits of such controllers from a practical point of view.
- iii. A study on the synthesis of 3 or higher periodic controller may be carried out.
- iv. Sensitivity, disturbance rejection capabilities and robustness properties of 2-DOF, 2-periodic controllers are to be investigated.

References

- [1] K. Ogata, *Modern control engineering*, 1st ed. Delhi: Pearson, 2016.
- [2] K. Ogata, *Discrete-time control systems*, 1st ed. New Delhi: Prentice-Hall, 2007.
- [3] B. Kuo and F. Golnaraghi, *Automatic Control Systems*, 8th ed. New Delhi: Wiley India (P.) Ltd., 2012.
- [4] E. J. Jury, F. J. Mullin, “The analysis of sampled data control system with a periodically time varying sampling rate”, *IRE Transactions on Automatic Control*, vol. AC-5, pp. 15-21, May 1959.
- [5] S. Meerkov, “Principle of vibrational control: Theory and applications”, *IEEE Transactions on Automatic Control*, vol. 25, no. 4, pp. 755-762, Aug 1980.
- [6] I. P. Greschak and G. C. Verghese, “Periodically varying compensation of time invariant systems”, *Systems and Control Letters*, Vol. 2, pp. 88-93, August 1982.
- [7] P. T. Kabamba, “Control of Linear Systems using Generalized Sampled-Data Hold Functions”, *IEEE Transactions on Automatic Control*, Vol. 32, No. 9, pp. 772-783, Sept. 1987.
- [8] P. Khargonekar, K. Poolla and A. Tannenbaum, “Robust control of linear time invariant plants using periodic compensation”, *IEEE Transactions on Automatic Control*, vol. 30, no. 11, pp. 1088-1096, Nov 1985.
- [9] S. Bittanti, P. Colaneri, “Analysis of discrete-time linear periodic systems”, *Control Dynamic Systems*, vol. 78, pp. 313-339, 1996.
- [10] S. Bittanti, P. Colaneri, “Invariant representations of discrete-time periodic systems”, *Automatica*, vol. 36, pp. 1777-1793, 2000.
- [11] G. Lee, D. Jordan and M. Sohrwardy, “A multivariable compensation design algorithm using classical root locus methods”, *IEEE Conference on Decision and Control including the 17th Symposium on Adaptive Processes*, San Diego, CA, USA, pp. 789-794, 1978.
- [12] W. M. Hawk, “A Self-Tuning, Self-Contained PID Controller”, *American Control Conference*, San Francisco, CA, USA, pp. 838-842, 1983.
- [13] K. H. Ang, G. Chong and Yun Li, “PID control system analysis, design, and technology”, *IEEE Transactions on Control Systems Technology*, vol. 13, no. 4, pp. 559-576, July 2005.
- [14] J. B. Rawlings, “Tutorial overview of model predictive control”, *IEEE Transactions on Control Systems Technology*, vol. 20, no. 3, pp. 38-52, Jun 2000.
- [15] K. Zhou, J. C. Doyle, and K. Glover, *Robust and optimal control*, Vol. 40, New Jersey, 1996.

- [16] K. J. Astrom, P. Hagander and J. Sternby, “Zeros of sampled systems”, *19th IEEE Conference on Decision and Control including the Symposium on Adaptive Processes*, Albuquerque, NM, USA, pp. 1077-1081, 1980.
- [17] J. B. Hoagg and D. S. Bernstein, “Non-minimum-phase zeros - much to do about nothing - classical control - revisited part II”, *IEEE Control Systems*, vol. 27, no. 3, pp. 45-57, June 2007.
- [18] S. Lee, S. Meerkov and T. Runolfsson, “Vibrational feedback control: Zeros placement capabilities”, *IEEE Transactions on Automatic Control*, vol. 32, no. 7, pp. 604-611, Jul 1987.
- [19] R. Bellman, J. Bentsman, S. M. Meerkov, “Stability of fast periodic systems”, *IEEE Transactions on Automatic Control*, vol. AC-30, pp. 289-291, 1985.
- [20] B. A. Francis and T. T. Georgiou, “Stability theory for linear time-invariant plants with periodic digital controllers”, *IEEE Transactions on Automatic Control*, vol. 33, no. 9, pp. 820-832, Sept. 1988.
- [21] S. K. Das and P. K. Rajagopalan, “Periodic discrete-time systems: stability analysis and robust control using zero placement”, *IEEE Transactions on Automatic Control*, vol. 37, no. 3, pp. 374-378, Mar 1992.
- [22] S. K. Das and P. K. Rajagopalan, “Techniques of analysis and robust control via zero placement of periodically compensated discrete-time plants”, *Control and Dynamic Systems, Advances in Theory and Applications: Academic*, Vol.74, 1996.
- [23] A. Oppenheim, A. Willsky and S. Nawab, *Signal and Systems*, 2nd ed. Pearson India Education Services Pvt. Ltd., 2015.
- [24] B. Lehman, J. Bentsman, S. V. Lunel and E. I. Verriest, “Vibrational control of nonlinear time lag systems with bounded delay: averaging theory, stabilizability, and transient behaviour”, *IEEE Transactions on Automatic Control*, vol. 39, no. 5, pp. 898-912, May 1994.
- [25] K. Shujaee and B. Lehman, “Vibrational feedback control of time delay systems”, *IEEE Transactions on Automatic Control*, vol. 42, no. 11, pp. 1529-1545, Nov 1997.
- [26] A. Chakraborty, J. Dey, “Robust compensation of time delayed plant by continuous-time high frequency periodic controller with negligible output ripples”, *International Journal of Robust and Nonlinear Control*, 2015.
- [27] S. K. Das and J. Dey, “Periodic Compensation of Continuous-Time Plants”, *IEEE Transactions on Automatic Control*, vol. 52, no. 5, pp. 898-904, May 2007.

- [28] S. K. Das, “Simultaneous stabilization of two discrete-time plants using a 2-periodic controller”, *IEEE Transactions on Automatic Control*, vol. 46, no. 1, pp. 125-130, Jan. 2001.
- [29] S. K. Das, P. K. Kar, “Simultaneous pole placement of M discrete-time plants using a M-periodic controller”, *IEEE Transactions on Automatic Control*, vol. 48, no. 11, pp. 2045-2050, Nov. 2003.
- [30] J. Dey, “Periodic compensation of continuous-time plants”, Ph.D. dissertation, Indian Institute of Technology, Kharagpur, India, 2006.
- [31] S. Chakraborty, “2-periodic/2-rate compensation of discrete-time plants”, Ph.D. dissertation, Indian Institute of Technology, Kharagpur, India, 2015.
- [32] S. K. Das, S. Chakraborty, “Robust Compensation of Discrete-time Plant using 2-Periodic Controller”, *7th IFAC Symposium on Robust Control Design (ROCOND 2012)*, June 20-22, 2012.
- [33] G. Nayak, S. Chakraborty and S. K. Das, “2-Periodic compensation of SISO discrete-linear-time-invariant plants”, *Indian Control Conference (ICC)*, Guwahati, pp. 289-294, 2017
- [34] G. Nayak, S. Chakraborty and S. K. Das, “Robust compensation of discrete-time plants using 2-degrees-of-freedom 2-periodic controller”, *SICE International Symposium on Control Systems (SICE ISCS)*, Okayama, pp. 1-6, 2017.
- [35] S. K. Das and K. K. Paul, “Robust compensation of a Cart-Inverted Pendulum system using a periodic controller: Experimental results”, *Automatica*, Volume N47, Issue 11, pp. 2543-2547, Nov. 2011.
- [36] A. Chakraborty and J. Dey, “Real-time study of robustness aspects of periodic controller for cart-inverted pendulum system”, *IEEE International Conference on Industrial Technology (ICIT)*, Cape Town, pp. 169-174, 2013.
- [37] A. Chakraborty, J. Dey and T. K. Saha, “Robust stabilization of self-erecting cart pendulum system with periodic controller,” *IEEE International Conference on Industrial Technology (ICIT)*, Busan, pp. 35-40, 2014.
- [38] A. Chakraborty and J. Dey, “Performance comparison between sliding mode control and periodic controller for cart-inverted pendulum system”, *IEEE International Conference on Industrial Technology (ICIT)*, Seville, pp. 405-410, 2015.
- [39] A. Dey, S. Chakraborty and S. K. Das, “Stabilization of a Cart-Inverted Pendulum system using a 2-periodic controller: Simulation results”, *IEEE Conference on Systems, Process and Control (ICSPC)*, Kuala Lumpur, pp. 169-174, 2013.

- [40] “*Digital Pendulum: Control Experiments Manual*”, East Sussex, U K: Feedback Instruments Ltd., 2007.
- [41] J. Schaffer and R. Cannon, “On the control of unstable mechanical systems”, *Automatic and Remote Control III: Proceedings of the Third Congress of the IFAC*, 1966.
- [42] R. E. Hufnagel, "Analysis of cyclic-rate sampled-data feedback-control systems," in *Transactions of the American Institute of Electrical Engineers, Part II: Applications and Industry*, vol. 77, no. 5, pp. 421-425, Nov. 1958.
- [43] D. Chatterjee, A. Patra, and H. K. Joglekar, “Swing-up and stabilization of a cart-pendulum system under restricted cart track length,” *Systems and Control Letters*, vol. 47, no. 4, pp. 355–364, 2002.
- [44] Nirmal Murmu, “2-Periodic compensation of SISO discrete-time LTI plants”, M. E. dissertation, Jadavpur University, India, 2015.
- [45] Tashmita Saha, “2-periodic/2-rate compensation of discrete-time plants”, Ph.D. dissertation, Jadavpur University, India, 2015.
- [46] S. Bittanti, P. Colaneri, *Periodic Systems Filtering and Control*, Germany, Berlin: Springer, 2009.